UNIVERSITY OF OKLAHOMA

GRADUATE COLLEGE

HIGH RESOLUTION INTEGRATED VAIL-GALLOWAY SEQUENCE STRATIGRAPHY OF THE LEONARDIAN BONE SPRING FORMATION, N. DELAWARE BASIN, SOUTHEAST NEW MEXICO

A THESIS

SUBMITTED TO THE GRADUATE FACULTY

in partial fulfillment of the requirements for the

Degree of

MASTER OF SCIENCE

By

CYRIL S. FRAZIER
Norman, Oklahoma
2019

HIGH RESOLUTION INTEGRATED VAIL-GALLOWAY SEQUENCE STRATIGRAPHY OF THE LEONARDIAN BONE SPRING FORMATION, N. DELAWARE BASIN, SOUTHEAST NEW MEXICO

A THESIS APPROVED FOR THE
SCHOOL OF GEOSCIENCES

BY THE COMMITTEE CONSISTING OF

Dr. John D. Pigott, Chair

Dr. Heather Bedle

Dr. Brett Carpenter

I dedicate this thesis to my family, without whose constant support and encouragement I would surely have faltered and fallen short. To my parents, I offer my deepest gratitude for all you have done for me, and continue to do for me, as I transition at long last from the life of a student to the life of a working adult. To Dr. Pigott, many thanks for the opportunity to better myself under his tutelage and mentorship at the University of Oklahoma, it truly has been an unforgettable experience. Lastly, but most certainly not least, to my wife and my better half I cannot say this enough, “I love you, now and always!”

Acknowledgements

I would like to acknowledge Schlumberger for providing the 3D seismic survey that constitutes much of the foundational data utilized in this thesis. Further acknowledgement to the faculty and staff of the ConocoPhillips School of Geology and Geophysics at the University of Oklahoma, many of whom have offered much needed advice and direction over the course of my enrollment. I needs must also acknowledge the wonderful ladies of the 7th floor front office, those angels who are the glue to this department, and have ever been one of my greatest resources. Finally, a big shoutout to the friends who have studied, sweated, scuba-dived, and suffered with me over the past years; may we all remain forever close, in our hearts and minds if not in physical location.

Table of Contents

a

List of Figures

Abstract

This thesis investigation centers on high-resolution sequence stratigraphy derived from well logs via an adapted Galloway's gamma ray motif analysis in combination with 3D seismic sequence stratigraphy of the prolific Leonardian-aged Bone Spring Fm. of the Northern Delaware Basin. The integration of well log-derived sequence stratigraphy is an essential counter component to standalone 3D seismic stratigraphy analysis, as it offers much higher vertical resolution. While seismic data are universally constrained in vertical resolution according to Huygen-Fresnel principles (Thore, 1999), utilization of Galloway's motif analysis affords interpreters resolution capable of delineating 4th and even 5th order parasequence sets (Pigott and Bradley, 2014). Through the lens of well log sequence stratigraphy, the evolution of sedimentary processes over time are accessible to the interpreter and may be understood through gamma ray log signature proxies for depositional environments. Seismic stratigraphy, then, following the Vail approach, offers much greater lateral resolution and affords the interpreter an advanced array of tools and techniques for analyzing regional structure and its influence on depositional processes (Ibid). When integrated (Ibid), the resulting sequence stratigraphic framework provides a high degree of resolution into the sedimentary successions of interest, as well as the governing controls over their deposition, which in turn empowers the interpreter with insights on source and reservoir rock potential.

The following investigation is predicated upon just such an integrated Vail-Galloway sequence stratigraphic analysis, and as such provides a depositional history of the Bone Spring Fm. that has immediate pertinence to the ongoing exploration and

production of this premier producing interval. Indeed, the sequence stratigraphic model that constitutes the culmination of this investigation drew upon Galloway gamma motifs analysis, modified for carbonate systems and linked to defined lithologies through system process energy and sedimentological inference, to delineate 4^{th} and 5^{th} order parasequence sets within the Bone Spring Fm. The findings of this investigation, conducted inversely from small to large scale – that is to say proceeding from Galloway to Vail, well log to seismic respectively – directed the interpreter towards a more complete understanding of the depositional model of the Bone Spring Fm. and thusly, greater insights into the quality of reservoir and source rocks within.

Chapter 1: Introduction

West Texas and Southeast New Mexico host the Permian Basin, one of the world's premier oil and gas producing regions, with a history of hydrocarbon exploration and production that reaches back to the 1920's (Keller et al., 1980; Martin, 1955). Given this prolonged attention by the petroleum industry, the literature pertaining to the region's outcrop and subsurface geology is extensive, largely predicated upon the work of industry giants including P.B. King, E.R. Lloyd, N.D. Newell, J.E. Adams, J.F.R. Sarg, C. Kerans, S.W. Tinker, and others. Still, there persists a need for a more holistic understanding of the full array of depositional systems encompassed within the Leonardian strata, as historical exploration and production success in proximal settings led to targeted investigations that failed to include the full spectrum (Hart, 1997). With advances in technology and the ascendency of horizontal drilling and completion in the past decade, this need for investigation into the unconventional reservoirs more prevalent to distal depositional environments becomes paramount in order to inform oil and gas planning and development to the greatest degree possible.

The Permian Basin hosts several sub-basins, which includes the Delaware Basin that has seen a resurgence in recent years as horizontal drilling and hydraulic fracturing technologies rose to preeminence and provided unprecedented access to unconventional, reservoir-derived hydrocarbons. Evidence of this shift in focus from the conventional reservoirs of the more proximal depositional settings to the basinal unconventional reservoirs is manifest in recent trends in production history. Figure 1 highlights these trends, which oversaw production from Wolfcamp and Bone Spring Fms. surpass the

Bakken (Enverus (formerly DrillingInfo), 2018). Nor are these trends likely to be short-lived, as multiple studies have estimated the Delaware Basin in its entirety to host total recoverable reserves in excess of 45 BBO and 275 TCF within these two formations (USGS, 2018; Permian Scout, Enverus, 2019). Upon this backdrop, and with the impending push within the petroleum industry to establish means by which to exploit residual hydrocarbons in carrier beds, the investigation encompassed by this thesis gains heightened pertinence, validation, and value with respect to ongoing hydrocarbon exploration and production activities within the Delaware Basin.

The subject of this investigation, the Bone Spring Fm., encompassed a complex depositional history arising from the mixed siliciclastic-carbonate depositional history afforded by reciprocal sedimentation. Crosby (2015) outlines the governing control asserted by sea level fluctuation over alternating siliciclastic and carbonate deposition. This sedimentation model encompasses depositional processes capable of giving rise to both conventional and unconventional reservoirs as well as the potential for self-sourcing hydrocarbon generation (Bickley, 2019). Operating within such complex petroleum systems necessitates the highest degree of understanding of the subsurface geology down to the most fundamental level: depositional history and stratigraphic relationships. Building upon the previous works of Crosby (2015) and Bickley (2019) towards defining the sequence stratigraphy and reservoir quality of targets within the Bone Spring Fm. through cores, well logs, and seismic data, this investigation will expand that focus northward into New Mexico proper. Even more, the study area investigated over the course of this thesis affords addressment of subsurface geology encompassing both

proximal and basinal depositional environments, and will be empowered and informed by the integrated utilization of petrophysical and 3D seismic data.

The primary vehicles driving the investigation of this thesis are public domain well logs, digitized from TIFF to LAS format, professionally preconditioned PSTM (Post-stack Time Migrated) 3D seismic data, and synthetic seismic logs. These were used to delineate the complex depositional processes in high resolution towards construction of a sequence stratigraphic model that explains the observed geometries and stacking patterns of the depositional architecture hosted by the Bone Spring Fm. within the study area. At the culmination of this undertaking, the resulting refinement in understanding of the Bone Spring Fm.'s depositional history will prove valuable towards future endeavors at defining those petroleum systems elements, conventional and unconventional, encompassed therein.

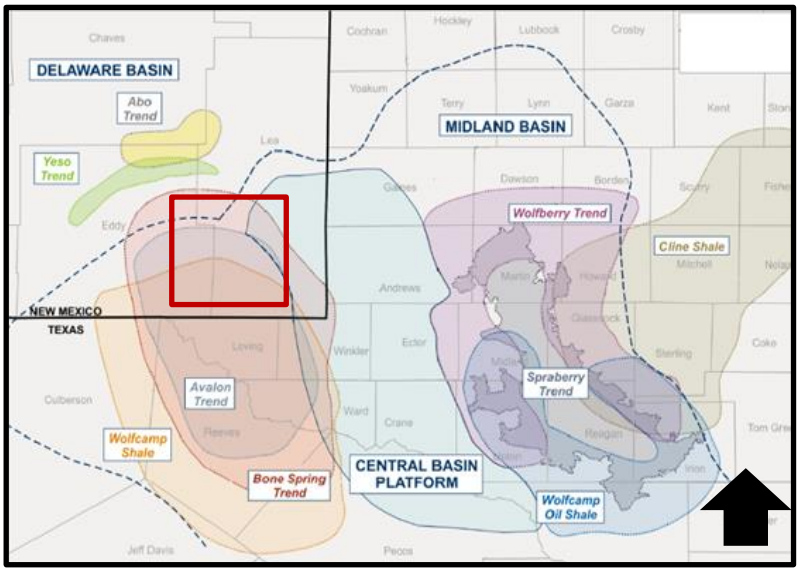

Figure 1: Overview of play trends in the Permian Basin. Highlights the overlapping Bone Spring, Wolfcamp, and Avalon trends in the Delaware Basin, modified from Bickley (2019) to show study area.

Study Location

Figure 1. provides an overview of the geometry of the Permian Basin, it's sub-basins, and the play trends of prominent producing intervals within the generalized study area shown. Given the proprietary nature of the seismic data provided by Schlumberger for this study, the exact locations of the 3D survey will not be provided. All of the wells used in this study are firmly situated within the boundaries defined by the 3D seismic survey, thus affording correlation via seismic well-tie, and were located using Enverus (formerly DrillingInfo) and obtained from the New Mexico Oil Conservation Division (NMOCD). Though the well logs utilized in this investigation are public domain, the exact well names and locations will be shielded in this thesis so as to preserve the confidentiality of Schlumberger's 3D seismic survey. The survey covers an area of approximately 100 square miles with a N-S length of ~10 miles and an E-W width of ~10 miles, and has a sample rate of 2ms, inline/crossline spacing of 110ft, datum elevation of 4,800 ft, and replacement velocity of 12,000 ft/second.

Within a geological context, the survey is situated in the Northern Delaware Basin and images the slope to basin transition of the Northwestern Shelf – Delaware Basin from the Wolfcampian onwards. As mentioned previously, the slope to basin transition captured within this survey offers a timely and unique opportunity to perform a high-resolution sequence stratigraphic investigation due to its envelopment of multiple potential energy surfaces across multiple depositional facies tracts as outlined by Pigott (2015). The close proximity of proximal and basinal depositional environments increases the likelihood of a preponderance of seismic reflection terminations.

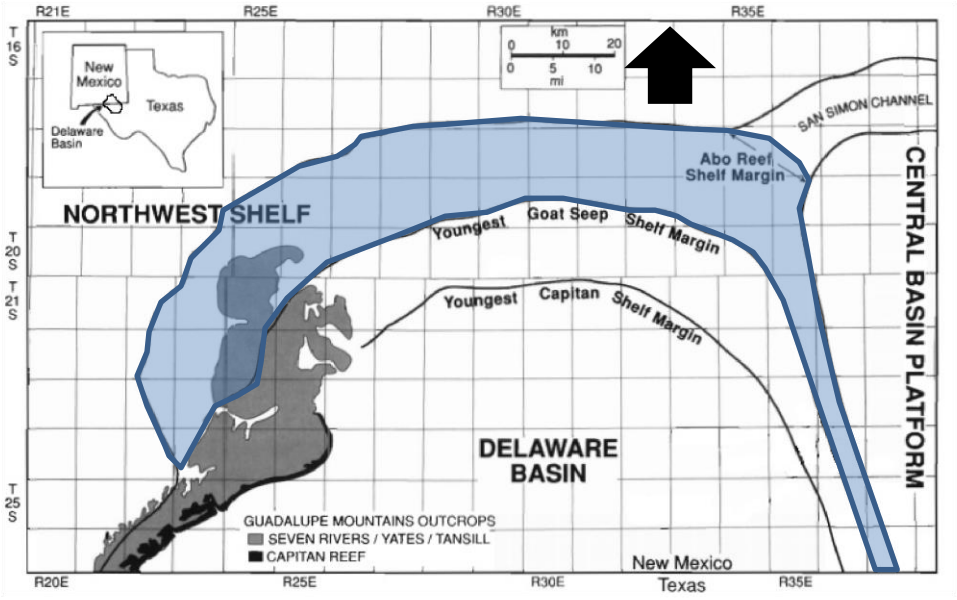

Figure 2: Generalized map of the Northwestern Shelf and Delaware Basin showing the evolution of the shelf margin from the Leonardian through the Guadalupian, as well as the San Simon Channel which plays an important role in moderating regional sea level fluctuation. Modified from P.M. Harris (2009) to highlight Abo Reef trend.

Previous Work

The robust array of literature pertaining to the geology of this area provides a solid conceptual understanding of the region's structural features as well as the overarching depositional processes that governed sedimentation along the Northwestern Shelf and in the Delaware Basin proper. This study is empowered by and builds upon that foundational work and will discuss it in further detail later on. Historically, the

primary focus of literature was concentrated on outcrop analogues and shallow well data, with only the past decade's advances in horizontal drilling and hydraulic fracturing technologies stimulating study of the basinal facies of the Delaware Basin like the Bone Spring Fm.

Of the pertinent literature available, the work conducted by Crosby (2015) and Bickly (2019) persist in their immediate relevancy in both subject matter and, to a certain extent, location area. As such, Crosby's "Depositional History and High Resolution Sequence Stratigraphy of the Leonardian Bone Spring Formation, Northern Delaware Basin, Eddy and Lea Counties, New Mexico," and Bickley's "High Resolution Sequence Stratigraphy and Seismic Stratigraphy of the Leonardian Bone Spring Formation, Delaware Basin, Southeast New Mexico," will be heavily drawn upon throughout this study, and supplemented when possible by other works. Through concurrent examination of well logs, cores, and through chemostratigraphic interpretation, Crosby (2015) constructed a depositional history and detailed sequence stratigraphic framework for the Bone Spring Fm. within the boundaries of his study area located within the Northern Delaware Basin, and came to the following conclusions:

- The degree of control over depositional history, and thus petroleum systems elements, occurs along the entire spectrum ranging from 1st to 5th order sea level cyclicity.
- Eight parasequences (i.e. 1st Bone Spring Carbonate) were distinguished from within previously identified 3rd order sequences of the Leonardian
- The dominant controls over sediment deposition included fluctuating sea levels, basin geometry and physiography, reciprocal sedimentation,

accommodation space and compensational sedimentary stacking patterns, and subaqueous erosional processes via mass transport deposits (i.e. sediment gravity debris flows)

- Within a sequence stratigraphic systems tract context, lowstands at 3rd order correlated with basinal siliciclastic deposits while 3rd order highstands correlated with predominantly carbonate deposits
- Within 3rd order sequences, higher frequency 4th order sequence stratigraphic cycles were readily delineated from both well logs and core data
- Lowstand intervals hosted the greatest concentration of terrigenous, detrital proxies, while highstands hosted higher carbonate concentrations
- Basinal anoxia correlated most with lowstand turbidites rather than highstand carbonates
- Anoxic events heightening TOC preservation suggests that many reservoirs within the Bone Spring Fm. may be self-sourced

Silver and Todd (1969) and Saller, Barton and Barton (1989) and Bickley (2019), expanded upon the overall understanding of the depositional processes that drove the cyclic deposition of the Bone Spring. Given the inherent quality and pertinence of Crosby's work to the study area under investigation, his 2015 thesis constitutes an ideal foundation upon which to build this investigation., as does the thesis work of Bickley (2019).

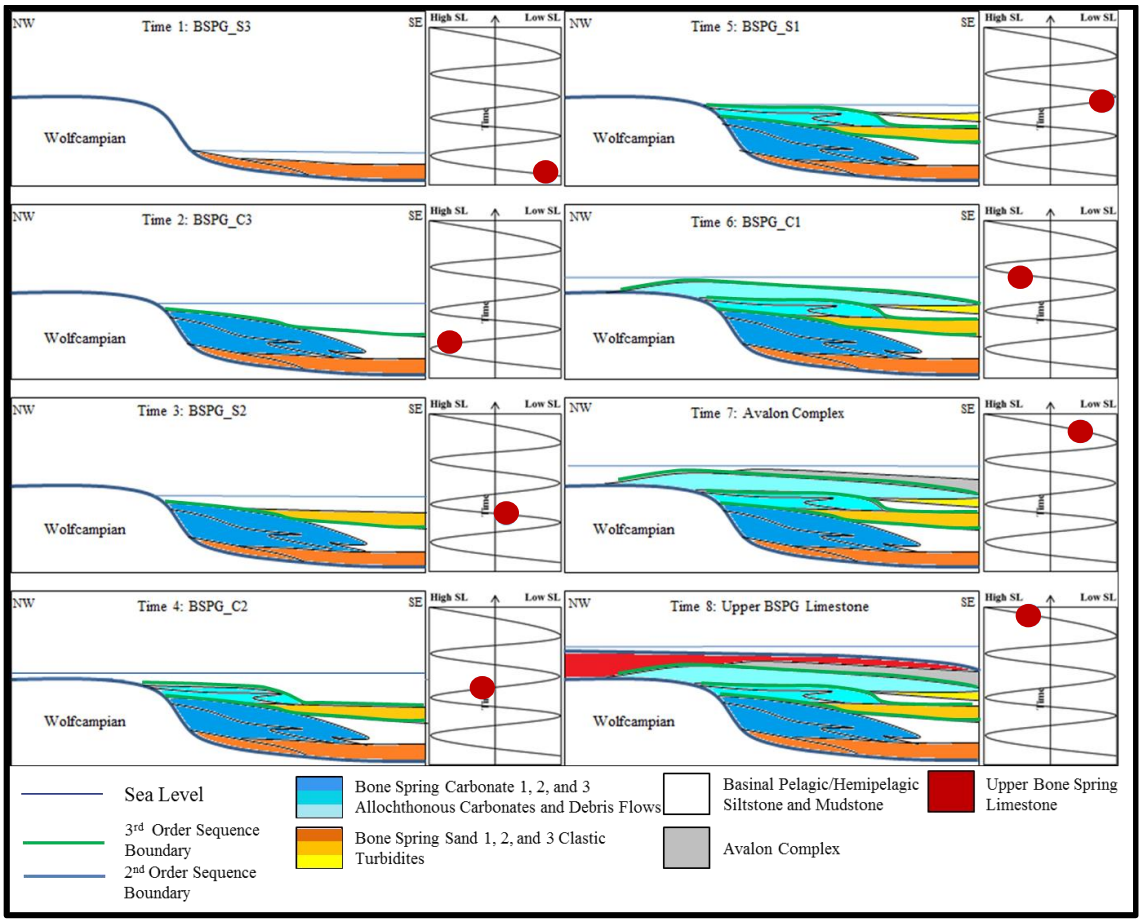

Figure 3: Illustration of the impact of 3rd order sea level fluctuations on Bone Spring deposition modified from (Crosby, 2015). 3rd Order highstands correlate with carbonate intervals while lowstands correlate with siliciclastic intervals.

Problem Definition

The overarching objective of this investigation is to provide further definition to the sequence stratigraphy of the Bone Spring Fm. and refinement to current understanding of its complete depositional history. Using public domain well logs, this study will expand on Crosby (2015) and Bickley (2019) sequence stratigraphic models of the Bone Spring Fm. as it occurs within the Northern Delaware Basin. The concentration of these historical studies in close proximity to the current study area will support direct

application of their inherent concepts to this investigation, which regrettably falls short of the robust array of primary data drawn upon by both Crosby and Bickley. Regardless, this investigation will attempt to expand upon their work through construction of an integrated Vail-Galloway sequence stratigraphic model of the Bone Spring Fm. through the approach outlined by Pigott and Bradley (2014). This endeavor will be aided by synthetic well ties, directly correlating the seismic reflection data to the high-resolution sequence stratigraphy evidenced in the well logs for subsequent validation via seismic sequence stratigraphy. The combined vertical resolution offered by well log sequence stratigraphy and the lateral resolution afforded by seismic sequence stratigraphy will hopefully empower this study to construct a more detailed and holistic depositional history of the Bone Spring Fm.

As concluded by Silver and Todd (1969), and further validated by Crosby (2015) and Bickley (2019), the Bone Spring Fm. is in places thousands of feet thick and enjoys a complex depositional history. Since the overall focus of this investigation is centered on the construction of a depositional history for the entire Bone Spring Fm. interval within the study area, detailed discussion of specific intervals will be done in a focused manner that supports the overarching broader context. The paucity of data utilized in this investigation relative to those conducted by Crosby and Bickley unfortunately constrains deeper analysis to some degree, though the 3D seismic data remains a robust source of data affording extensive analysis on multiple levels with respect to specific intervals, landing zones, and petroleum systems elements within the Bone Spring Fm. Therefore, a secondary objective for this study is to provide a first approximation interpretational gateway into the data encompassed within the 3D seismic survey, contextualized within

the framework of a broad sequence stratigraphic model and the intrinsic information it conveys on depositional settings in order to empower future, more detailed investigations. Much of the prerequisite work, basin modelling, petroleum generation and migration analysis, decline curve analysis, and statistical validation of reservoir quality via well logs and seismic attributes has already begun. Indeed, the ease of access, favorable cost to benefit ratio, and time effective nature of seismic attributes, all lend themselves to heightened utilization of attribute-driven seismic interpretation, which constitutes only a minor part of this study, but has the potential to provide multiple avenues towards validation of sequence stratigraphic and depositional models constructed through an integrated Vail-Galloway approach.

Chapter 2: Geologic Background

It is remains of paramount importance before committing to a focused geological study on a limited area, and on a formation with a limited period of deposition, to begin first from as comprehensive an understanding of the hosting region, in this case the Permian Basin, as may be afforded by the available repository of pertinent information. All of which means that it is necessary for the tectonic and depositional setting evolution of the Permian Basin over time to be considered through the lens of their impact on the Bone Spring Fm. In the geosciences, the past remains the key to the present, and in the context of this study, the "present," as it is fixed within the mind of the interpreter, is the Leonardian age, that time in which the Bone Spring Fm. was deposited. Through the marriage of the basinal history in its entirety and the insights gained by this study into the depositional history of the Bone Spring Fm., a more refined understanding of the

petroleum systems elements may arise, and in the future inform and optimize oil and gas exploration and production. The Leonardian-aged Bone Spring Fm. unconformably overlies Wolfcampian sediments and is bound on the top by the progradational, Guadalupian-aged Brushy Canyon Fm., meaning it was deposited over a relatively short period of time in comparison to other geologic units found within the Permian Basin.

The Delaware is a north-south elongate basin with an average length of about 200 miles and an average width of about 100 miles (Adams, 1965). The Permian Basin is made up of multiple smaller basins including the Delaware Basin and the Midland Basin. The Delaware and Midland basins are relatively isolated from each other with the Central Basin Platform creating a natural divide between the two. The Hovey Channel in the southwestern portion of the Delaware Basin historically connected the basin to the Panthalassic Ocean, while the Sheffield and San Simon Channels to the east connected the Delaware Basin to the Midland Basin (Figure 4). The bounding features of the Delaware Basin also include the Diablo Platform to the west, the Central Basin Platform to the east, the Northwest Shelf to the north, and the Marathon Ouachita thrust belt to the south (Yang and Dorobek, 1995).

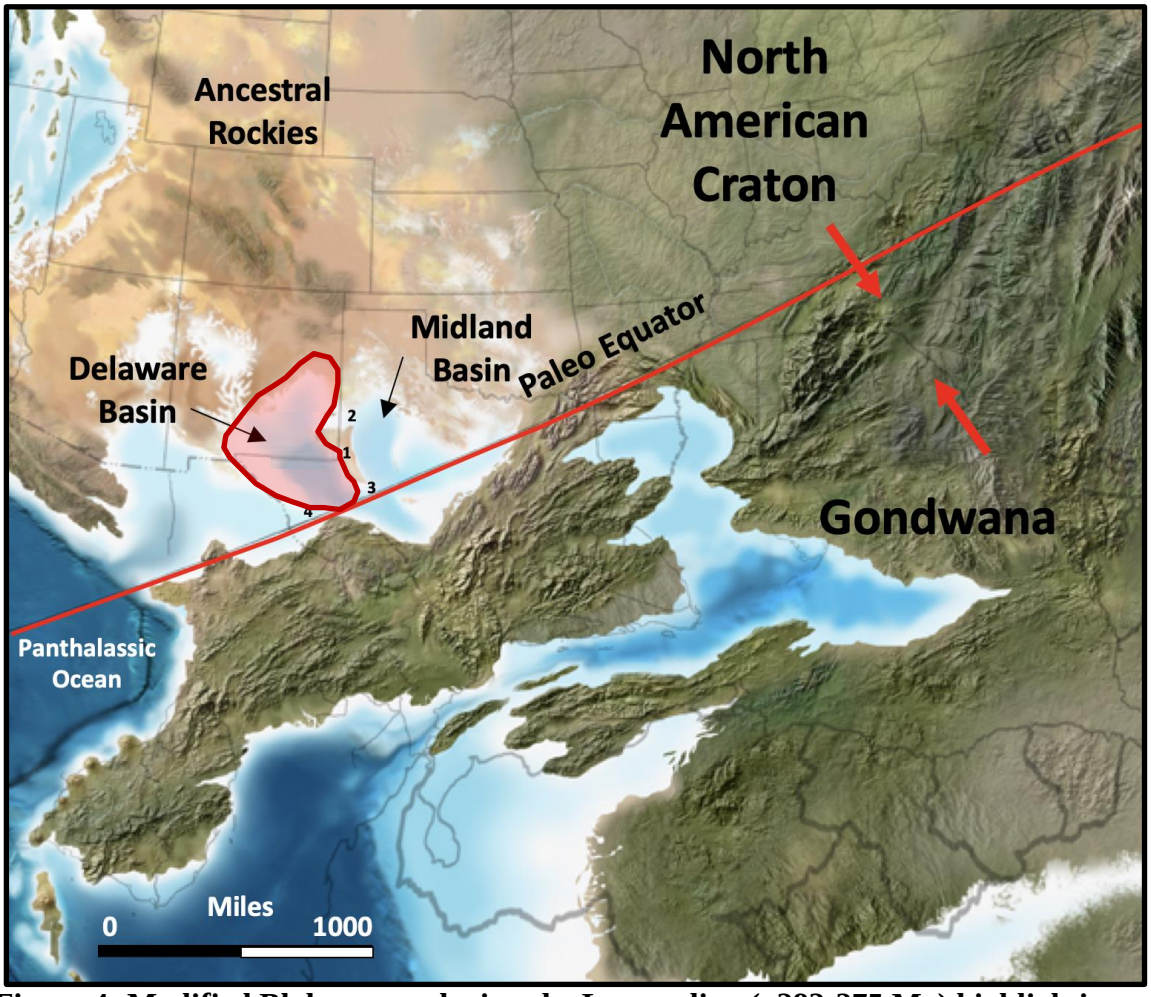

Figure 4: Modified Blakey map during the Leonardian (~282-275 Ma) highlighting the extent of the Delaware Basin, adapted from Bickley (2019). Also annotated are the major continental cratons colliding to during Pangea formation and the Ouachita Marathon thrust belt orogeny. 1 – Central Basin Platform, 2 – San Simon Channel, 3 – Sheffield Channel, 4 – Hovey Channel

Tectonic History

The origination and development of the Delaware Basin has been thoroughly discussed in literature (Galley, 1958; Hills, 1970, 1984; Walper, 1977; Shumaker, 1992; Yang and Dorobek, 1995, and others). Despite this attention, it is generally accepted that scant little is concretely known about the basin's Paleozoic evolution due to an ongoing lack of evidence, though it is widely held that the evolution may be traced back to the

formation and rifting of the supercontinents Rodinia and Pangaea in Earth's primordial past (Hills, 1984; Shumaker, 1992). Late Cambrian sediments (Dagger Flat Fm.), the earliest geologic record in the area, suggest the advancement of a sea over mature, granitic bedrock (Hills, 1984). Galley (1958) concludes that by the end of the Precambrian, the entire region sank alongside the southwestern portion of the craton as a welded accretion. This subsidence gave rise to the ancient Tobosa Basin (Figure 5), which he in turn posits as the parent basin to the Delaware Basin, a view generally accepted within literature (Hills, 1970, 1984; Adams, 1975; Walper, 1977; Shumaker, 1992). The establishment of the Tobosa basin coincided with diminishing subsidence and subsequent formation of a shallow sea that likely conjoined with the Tethys Sea (Hills, 1984).

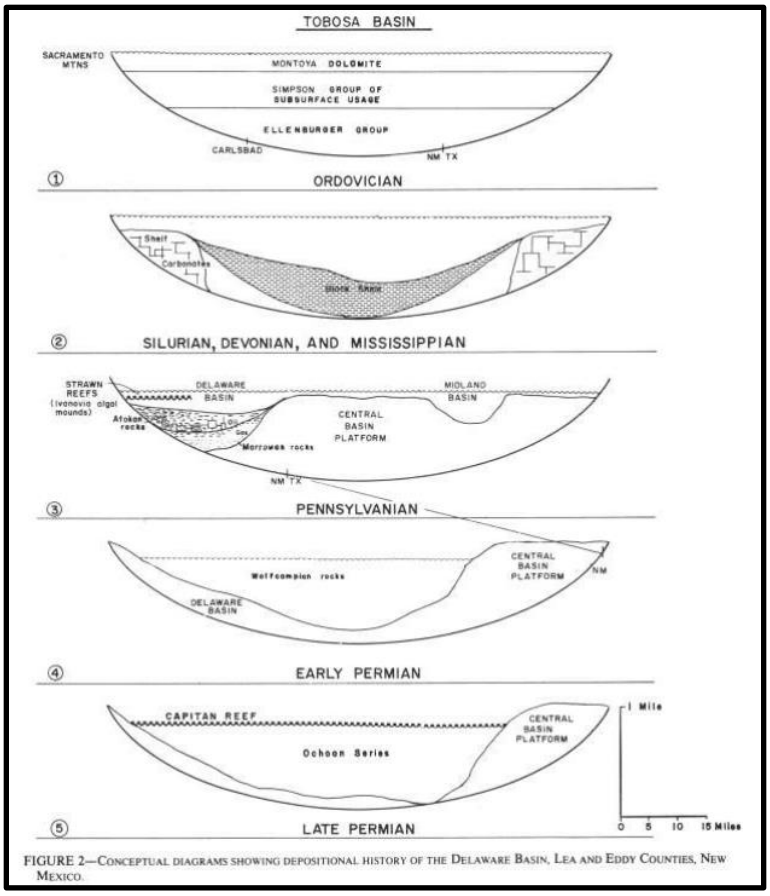

FIGURE 2—CONCEPTUAL DIAGRAMS SHOWING DEPOSITIONAL HISTORY OF THE DELAWARE BASIN, LEA AND EDDY COUNTIES, NEW MEXICO.

Figure 5. Diagrammatic cross-section showing the evolution of the parent Tobosa Basin into the subsequent sub-basins of the Permian, modified from Adams (1965).

The advent of the Cambrian continuing into the Early Ordovician coincides with large-scale deposition of shallow marine carbonates (Ellenburger Fm.) suggesting a prolonged period of tectonic quiescence and minimal, if any, significant basinal subsidence along the extent of the Ellenburger sea (Adams, 1965). The Middle Ordovician saw the transition to interlaminated shales and limestones (Simpson Fm.), shales in excess of 50% and accumulations exceeding 2000ft (600m), indicative of a drastic deepening and southward expansion of the Tobosa Basin driven by sediment loading, given the lack of tectonic activity (Hills, 1984). The return of platform carbonate deposition in the Late Ordovician is attributed to the inverse relationship between rates of subsidence (decreasing) and sea level rise (increasing) (Hills, 1984; Hardenbol et al., 1998; Haq and Schutter, 2008). This depositional regime persisted through the Silurian and well into the Devonian Period, which saw the introduction of more siliceous materials (Hills, 1970; 1984).

The transition from the Middle to Late Mississippian oversaw a profound shift in deposition such that carbonate production and deposition gave way to that of organic-rich shales. Within the Delaware Basin, this deposition is constituted by the 100-700ft (30-200m) Woodford Fm. evidencing a robust total organic content (TOC) in excess of 630mg/g (Zhang et al., 2012).

The expansive coverage of the Woodford Shale, which extends not only throughout the Delaware Basin area but also encompasses much of the Permian Basin and reaches through north Texas into Oklahoma and beyond, is indicative of the vastness of the Panthallassa sea that presided during this time (Ellison, 1950; Hills, 1984). Excluding the Woodford Shale, which deposited in areas well into the Early Mississippian, this Period marked a widespread transition from carbonate deposition throughout the Delaware Basin to the deposition of thick, organic-rich, basinal shales (Helms Fm.) with fine siliciclastic components (Adams, 1965; Hills, 1984).

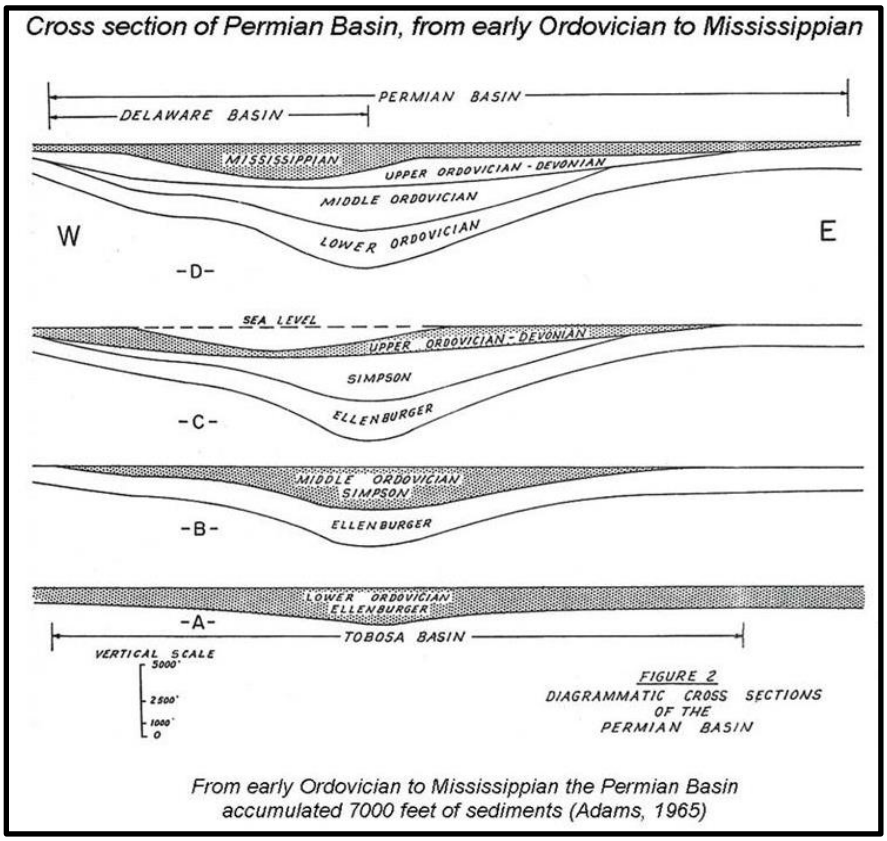

Figure 6: Diagrammatic cross-section of the Permian Basin, ranging in age from early Ordovician to Mississippian, modified from Adams (1965).

The provenance of these siliciclastic materials is generally considered to be what

would eventually become the Central Basin Platform and may be considered the earliest evidence of renewed tectonism, associated with the Variscan orogeny, in the Delaware Basin (Hills, 1984; Shumaker, 1992). Following Late Paleozoic lines of structural weakness, the compression-driven vertical movement of the Central Basin ridge rejuvenated steep reverse faults, initiating folding that apparently included the granitic basement, and coincided with widespread deformation of the Delaware Basin and subsequent deepening and tilting in the eastern margins (Figure 7). (Adams, 1965; Hills 1984).

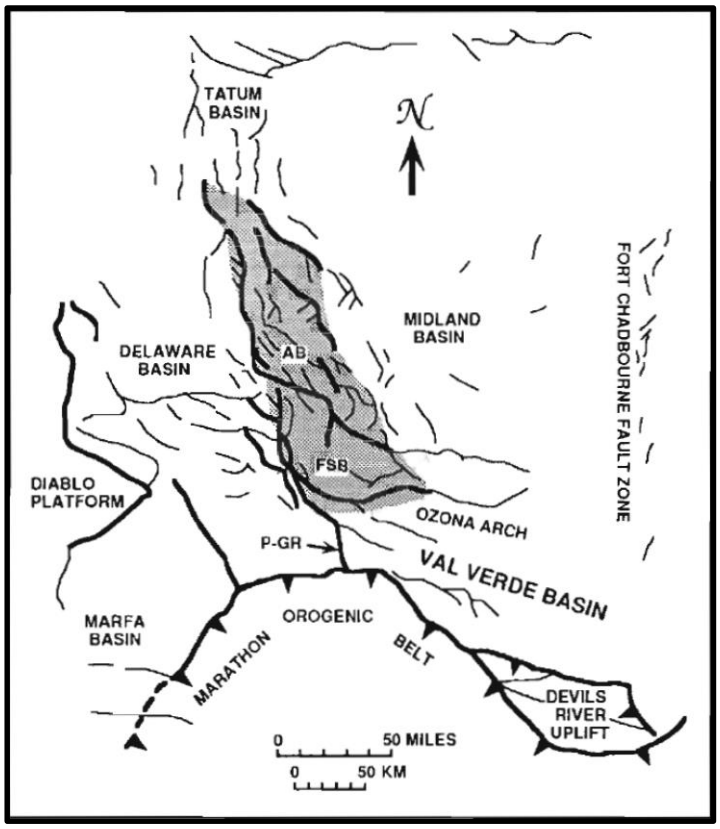

Figure 7: Schumaker's (1992) interpretation of the Central Basin Platform splitting in into two major uplift blocks showing clockwise rotation. Notice the Marathon Thrust Belt to the south which aided in the rapid subsidence of the Delaware Basin.

The Pennsylvanian saw the continued growth of the Delaware Basin as well as filling by deltaic sediments provenanced from central New Mexico (Hills, 1984). Tectonic activity during this Period associated with the Ouachita—Marathon fold-belt extended from modern day Oklahoma through West Texas and south into northern Mexico states of Coahuila and Chihuahua (Hickman, Varga, and Altany, 2009). Despite this tectonic activity, conditions within the Delaware Basin and along its margins remained insufficient to prevent carbonate deposition, which continued to establish broad carbonate shelves and ramps till the Period's conclusion (Mazzullo, 1981). As a result of these carbonate structures, clastic deposition into the basin gradually diminished and eventually ceased altogether, as clastic materials became trapped behind carbonate banks (Adams et al., 1951). Basinal sediments of this age exhibit notable compaction, almost certainly from overburden pressures exerted by basin-fill, with excellent fauna preservation indicative of dys- or anoxic conditions at depth in the Delaware Basin proper (Hills, 1984).

With the advent of the Permian, the final shudders of the Marathon orogeny drew to a lurching end, providing in culmination a renewed source of fine siliciclastics that progressively filled large swaths of the Delaware Basin's central and southern reaches (Hills, 1984). With the tectonic quiescence and diminishing introduction of siliciclastic materials, this fill manifested as thinly interlaminated siliciclastic and limestone beds (Adams, 1965). By Wolfcampian time, predominate carbonate deposition resulted in the accumulation of thick carbonate beds, which continue to enjoy considerable interest from the petroleum industry (Hamlin and Baumgardner, 2012). At the same time, the Delaware Basin's marginal shelf and platforms enjoyed ongoing carbonate deposition,

though accumulations were sufficient only for mild restriction of oceanic circulation such that normal salinities continued to prevail (Hills, 1984). Ongoing subsidence along historical lines of structural weakness (Figure 8) in the center of the basin allowed depths to remain in excess of 1000ft (300m), such that significant accumulations of organic-rich sediments were deposited (Hills, 1984).

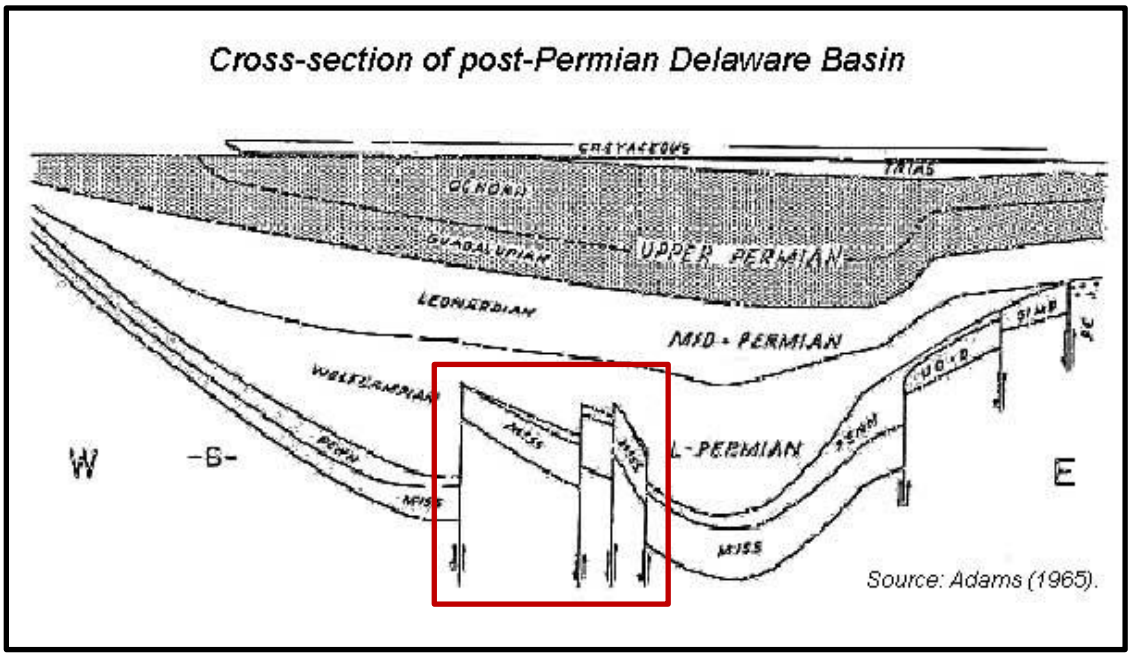

Figure 8: Diagrammatic cross-section of the Permian Basin, ranging in age from early Ordovician to Mississippian, modified from Adams (1965) to show the movement in the Proterozoic lines of structural weakness (red square).

By the end of the Early Permian, development of carbonate structures along the margins, especially the northern and southern, achieved sufficient stature to severely restrict oceanic circulation within the Delaware Basin (Adams, 1965). That circulation which persisted, through the Hovey Channel and Sheffield Channels to the southwest and southeast respectively (Figure 9) proved sufficient in keeping the surface of the seawater aerated and organically productive (Hills, 1984). Leonardian deposition of siliciclastic

thin-beds included periodic breaks for carbonate deposition, which formed numerous wedges along the basin margins. Compaction of the underlying Wolfcampian carbonate muds forced the upward migration of water into accommodating siliciclastic and carbonate intervals with the requisite permeability and porosity (Hamlin and Baumgardner, 2012). Gradually, burial of the Wolfcampian sediments reached depths greater than 3,000ft (900m), effectively entering those organic-rich intervals into the catagenic zone initiating kerogen production (Hills, 1984).

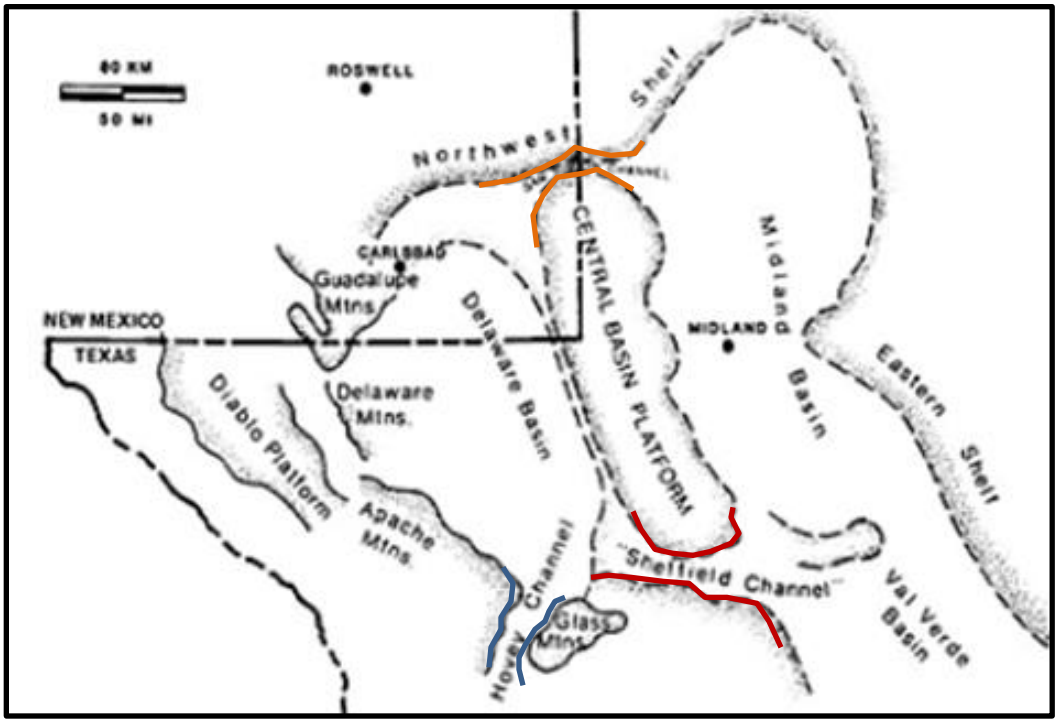

Figure 9. Map of the Permian Basin during the Early Permian, modified from Ward et al. (1986) to delineate the Hovey (blue) and Sheffield (red) channels responsible for establishing restricted oceanic circulation in the Delaware Basin.

Guadalupian deposition in the Middle Permian included fine siliciclastic basin-fill at depths up to 4,000ft (1,200m), encouraged by sediment loading-driven compaction and eastward basinal tilting approaching 5° (Adams, 1965). The resulting subsidence matched sedimentation for most of the Guadalupian, until the prolific carbonate structures (i.e. the Capitan reef complex) achieved enough stature to hinder sediment transport into the basin's central areas and further restrict oceanic circulation. Therefore, basinal deposition was constrained to thin, organic-rich carbonate muds in an increasingly dys- or even anoxic environment (Hills, 1984). By the end of this Period, thousands of feet of Guadalupian overburden drove the immediately underlying Permian strata into the catagenic zone resulting in the production of kerogen that subsequently matured into wet oil and gas, and the Wolfcampian strata into the lower extents of the catagenic zone where previously generated liquid hydrocarbons were overcooked into gas (Hills, 1984).

Increasing restriction of circulation within the Delaware Basin persisted into the Late Permian, leading to deposition of the world-renowned Castile and Salado evaporites (Adams, 1944) that blanketed the underlying sediments with 2000ft (600m) of impermeable sediments, effectively blocking any further upward migration of fluids, hydrocarbon or otherwise. As such, compaction driven fluid migration occurred laterally, eventually accumulating up-dip in stratigraphic traps along basin margins. The end of the Permian coincided with a large-scale fall in sea level and subsequent subaerial exposure that allowed significant erosion (Maley and Huffington, 1953) of the Dewey Lake and Rustler Fms., and initiated solution of the uppermost evaporite strata (Hills, 1984).

By the Mid-Triassic, deposition within the Delaware Basin had transitioned to the continental red-beds of the Dockum Group (McGowan et al., 1979). The lack of Jurassic and Early Cretaceous sediments (Figure 10) is explored by Adams (1940, 1965) who posits Delaware Basin-wide deposition of equivalents to the Paluxy sandstones and later Edwards limestones, though they are localized within the geologic record to northeastern Texas. Their deposition marks a profound shift in paleogeography as existed up through the Permian, for it includes no evidence of either the Delaware Basin or Central Basin platform (McGowan et al., 1979). Late Cretaceous tectonism, associated with the Laramide orogeny, resulted in subsidence-driven formation of numerous small-scale, relatively, basins in Winkler and Ward Counties, Texas, and Lea County, New Mexico (Hills, 1984), which filled over time with terrestrial siliciclastics.

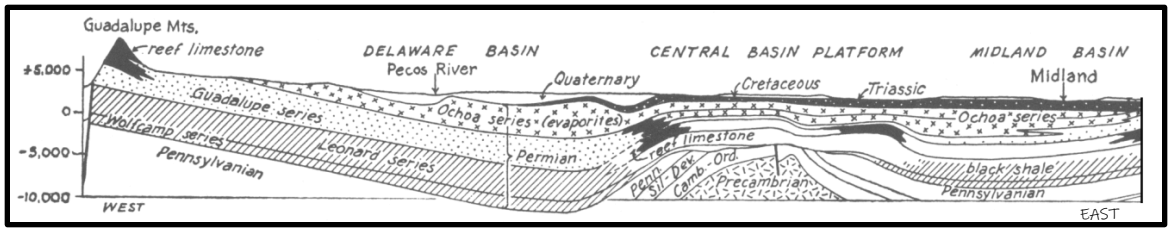

Figure 10. Diagrammatic cross-section of the Permian Basin up through the Cretaceous, modified from Adams (1965).

Depositional History

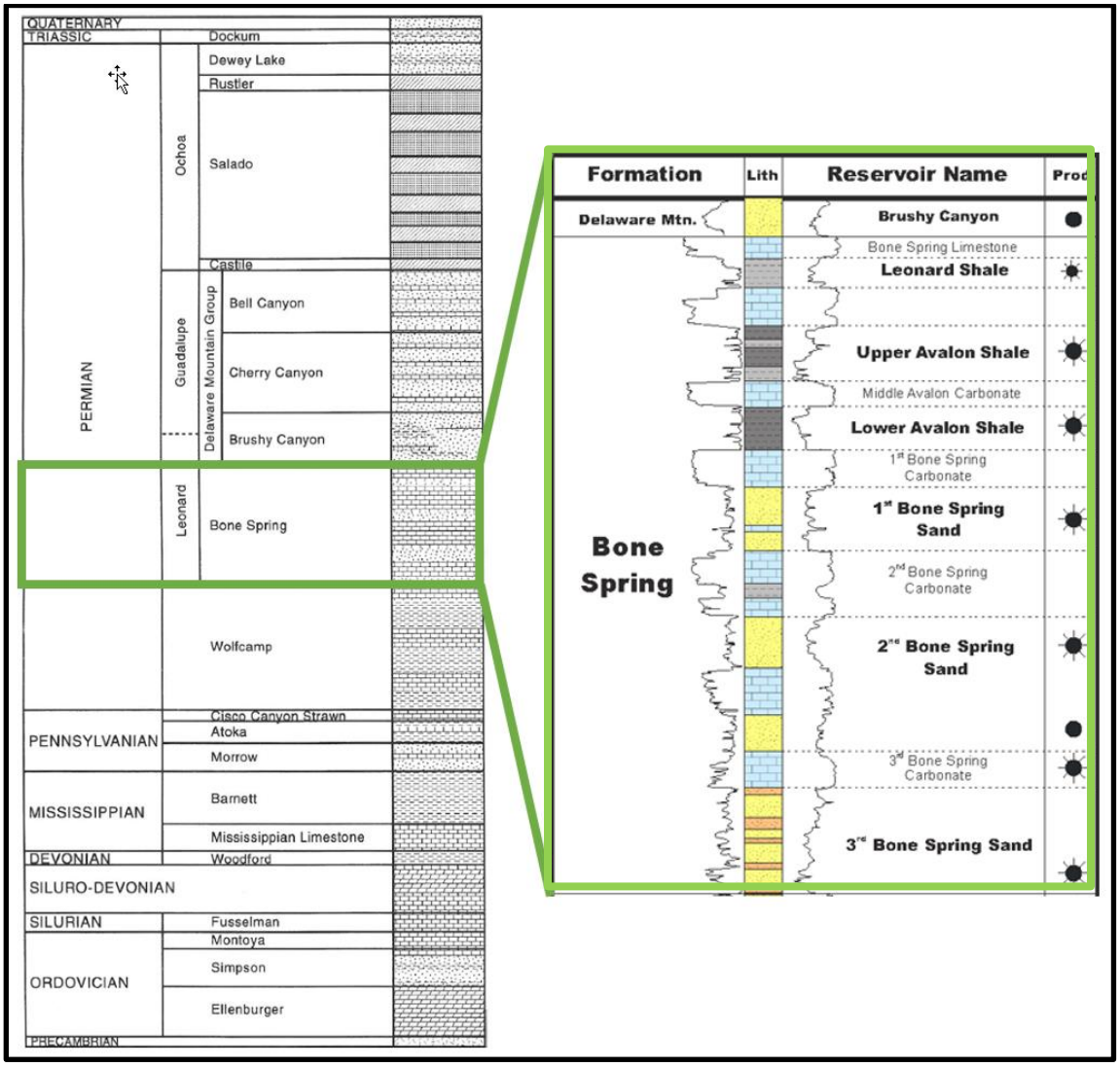

Figure 11: Stratigraphic column of the Delaware Basin modified from Hardage et al. (1998) and Bickley (2019). The Bone Spring formation is broken up into further detail showing the additional formations that exist within the Bone Spring and their variety of lithologies. Oil and gas producing targets are annotated to the right. (Core Laboratory, 2014)

Pre-Bone Spring Deposition

The earliest recorded strata within the Delaware Basin were Cambrian-aged sands shed during Precambrian uplifting of source terrains (Hills, 1984). These sands were deposited into the slight negative depression that existed even before the formal development of the Tobosa Basin, and which existed as a shallow coastal plain that afforded the laterally extensive deposition of the Ellenberger Fm. carbonates throughout Ordovician transgression (Adams, 1965). With the onset of the subsidence and subsequent formation of the Tobosa Basin, the interbedded limestones and shales of the Simpson Gp. deposited southward into a thickening wedge that pinches out to the north, east, and west (Hills, 1984).

Carbonate deposition remained persistent and dominant from the Ordovician to the Devonian – though the regular presence of thin-bed siliciclastics have been posited as relative sea level lowstand deposits – evidenced by the Thirtyone, Fusselman, and Montoya Fms. (Hills, 1984). Adams (1965), posits that this period of the Tobosa Basin was also marked by the formation of seaward prograding carbonate shelves.

The carbonate-dominant deposition of the Ordovician-Devonian drastically shifted to thick deposition of organic-rich, black shales through the Mississippian – the Woodford and Barnett Shales, which exhibit remarkable lateral continuity over large swaths of surface area, and remain world-class unconventional drilling targets – it is believed in response to the onset of the Marathon-Ouachita Orogeny (Hills, 1984). Reactivating relic zones of Proterozoic structural weakness, this orogenic event uplifted source terranes, including the Central Basin Platform, thereby increasing sourcing of siliciclastics into the Tobosa Basin (Hill, 1984).

Renewed tectonism within the region was marked by the advent of the Pennsylvanian, causing rapid subsidence in the basin proper and encouraging thick deposition of the predominately siliciclastic Atoka and Morrow Fms. (Adams, 1965). Adams (1965) references the Cisco Fm., which underlies the Wolfcamp Fm., as evidence that some carbonate shelf deposition occurred too in the Pennsylvania. Taken collectively, deposition into the Tobosa and later Delaware Basin from the Ordovician through to the Pennsylvanian remains characteristically thick, with trends of thickening in the direction of the Central Basin Platform, suggestive of Marathon-Ouachita Orogeny-driven flexural subsidence (Yang and Dorobek, 1995).

Deposition in earliest Wolfcampian is predominately clastic and often in the form of mass transport deposits (MTDs) shed off of the steep shelf slopes to the northwest, west, and southwest basin periphery (Hills, 1984). Carbonate deposition increased throughout Wolfcampian time as clastic influx decreased (Adams, 1965), likely due to rising relative sea level within the basin, which led to carbonate mud-dominated debris flows and turbidite deposits that characterize much of the Wolfcamp Fm. Pelagic- rain drapes, overlying many of the MTDs, are indicative of periods of tectonic quiescence within the basin, and these organic-rich deposits persist as quality unconventional drilling targets (Silver and Todd, 1969).

The Wolfcamp also encompassed the initial development of carbonate shelf build-ups around the rims of the Delaware Basin (Hills, 1984). These isolated algal mound deposits, comprised of skeletal hash and interbedded fine-grained shales, may have contributed in part to the further restriction of the basin proper, aiding in the preservation of TOC within the Wolfcamp Fm.'s organic-rich shales and lime muds as a result of

basinal dys- or anoxia (Silver and Todd, 1969; Hills, 1984). Adams (1965) came to a different conclusion, however, arguing that nutrients permeated the waters during the Wolfcampian, introduced into the water column by the frequent sediment reworking via debris flows and MTDs. Regardless, the Wolfcampian clearly oversaw a period of extensive deposition of organic-rich material in an environment favoring TOC preservation, as is evidenced in the ongoing and prolific horizontal drilling activities within.

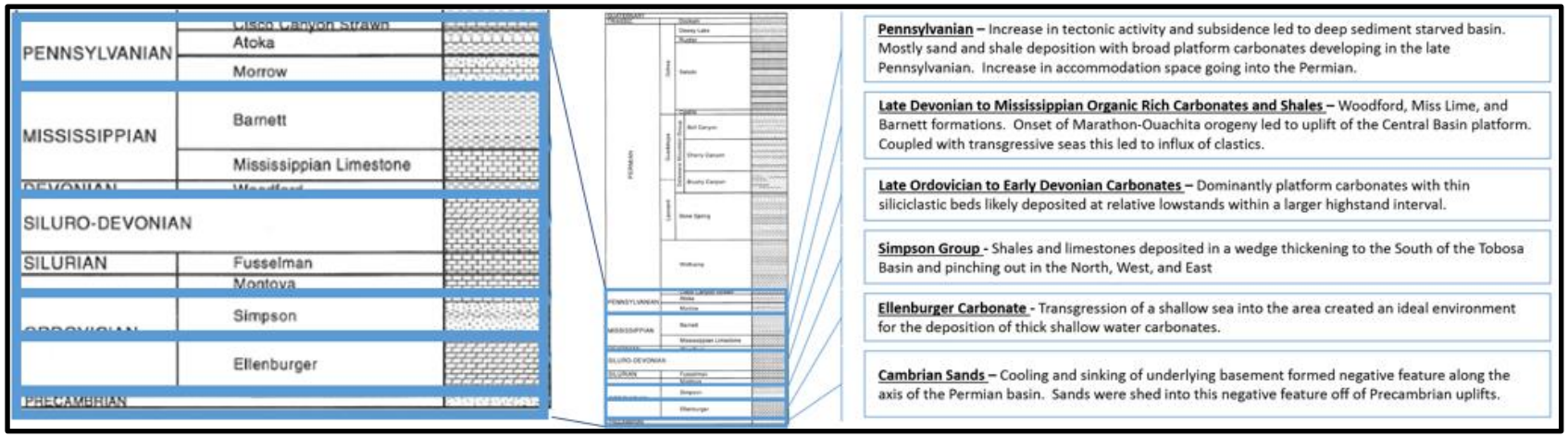

Figure 12: Summary of deposition prior to the Bone Spring in the Delaware Basin with formation locations on the stratigraphic column. Modified from Hardage et al., (1998) and later Bickley (2019).

Bone Spring Deposition

Henderson et al. (2012) proposes the Bone Spring Fm. to have occurred over the course of approximately ten million years, from ~282.5 – 272.3 Ma during the Leonardian age, Early-Middle Permian. Comprised of basinal, mixed carbonate and siliciclastic deposits, the Bone Spring Fm. may be characterized as amalgamated sediment gravity flows and mass transport complexes shed down the steepening slopes of the Northwestern Shelf.

To date, the Bone Spring has been subdivided most commonly into six stratigraphic units that cycle between carbonate and siliciclastic-dominated composition. This cyclic pattern of alternating carbonate-siliciclastic sedimentation is a hallmark of relative sea level-driven evolution of depositional settings and is associated with reciprocal sedimentation models (Montgomery, 1998; Crosby, 2015) Within this model, highstand sea levels afford prolific carbonate production on the shelf, with basinal carbonate deposition the result of highstand shedding of carbonate muds due to insufficient accommodation space along the shelf. Conversely, lowstand sea levels effectively shut down carbonate production, eliminating accommodation space on the shelf and affording sediment bypass of siliciclastics across the shelf and down the shelf slopes into the basin proper as sediment gravity flows or MTDs (Montgomery, 1998; Crosby, 2015). Hart (1997) arranges the six unique stratigraphic units, which measure a collective ~3000 – 4500 feet in thickness, into three major groups: the 1st, 2nd, and 3rd Bone Spring, so enumerated youngest to oldest in age (Bachman et al., 2014)

Several variables acting in concert are believed to have contributed significantly to the hydrocarbon potential enjoyed by the Bone Spring Fm. The establishment of restricted oceanic circulation within the Delaware Basin as the threshold of eustatic fluctuations capable of influencing relative sea level change within the basin rose accordingly with carbonate build-ups across the San Simon, Hovey, and Sheffield Channels. This, in turn, effected an environment in which basinal waters remained both nutrient rich due to ongoing carbonate activity, and steeply stratified in terms of oxygenation due to the restriction of water circulation to the uppermost portions of the water column (Hills, 1984; Crosby, 2005; Bickley, 2019). Figures 4 and 9 show the locations of these channels as they relate to the Delaware Basin. This environment encouraged TOC preservation during Bone Spring Fm. deposition, which in turn afforded intraformational self-sourcing of hydrocarbons. This taken in combination with the stacked pay intervals arising from reciprocal sedimentation contribute to the prolific production currently ongoing in the Bone Spring Fm. (Hills, 1984; Bickley, 2019).

Given the ongoing uplift of the Central Basin Platform during the deposition of the Bone Spring Fm., it may be reasonably inferred that tectonism, though slight in the study area so removed from the platform, persisted (Adams, 1965; Hart, 1998). Indeed, the amalgamated deep-water sediment gravity flows and MTDs characteristic of the Bone Spring Fm. offer a confirmation of such tectonism, if only by providing a mechanism by which they may have been initiated. Further confirmation of tectonism during Bone Spring Fm. deposition within the study may be found in the structure imaged by the seismic data, specifically a major fault zone trending NE-SW that persists through the strata comprising the Wolfcamp and the Bone Spring Fms. The pronounced

geomorphology of the Abo – Victorio Peak carbonate complex visible within the seismic is believed to be largely controlled by the inherited topography created by this faulting, which in turn governed to some degree the sedimentation pathways utilized during deposition of the Bone Spring Fm. and provided direction to the gravity flows and MTDs. This idea dates back to Hart's 1998 work that inherited topography, more specifically the presence of intrinsic paleo-bathymetric lows therein, acted as channels by which deep-water sediment gravity flows, turbidites, and to some degree MTDs were transported and directed, as evidenced by trends in depositional thickness and compensational stacking patterns.

On the basin rim during Bone Spring Fm. deposition, inherited topography encouraged the development of rimmed-shelf carbonate build-ups (Todd and Silver, 1969). These carbonate build-ups, within the context of the Northern Shelf, remain the topic of heated debate as to their true nature as rimmed-shelves or some other geomorphology. There remains consensus, however, that regardless of geomorphology, these carbonate structures did not impede basinal sedimentation, but rather afforded the creation and preservation of channels and incised valleys that acted as highways for the transport of siliciclastic sediments out into the basin (Adams, 1965). Crosby (2015) has also argued that these channels and incised valleys could have preferentially formed in the depressions inherent to carbonate spur and groove topography that developed on the shelf, a belief validated by the findings of this investigation.

The major formations of the Bone Spring (Figure 11) in order from bottom to top or oldest to youngest are the 3rd Bone Spring Sand, 3rd Bone Spring Carbonate, 2nd Bone Spring Sand, 2nd Bone Spring Carbonate, 1st Bone Spring Sand, Lower 1st Bone Spring

Carbonate, Avalon Sand/Shale, and the Upper 1st Bone Spring Carbonate (Crosby, 2015). As mentioned above, this alternation of lithologies may be explained through a reciprocal sedimentation model wherein depositional environment evolution is driven by fluctuations in relative sea level. When viewed through this lens of reciprocal sedimentation, it becomes apparent that basinal carbonate deposition in the Bone Spring Fm. occurred at relative highstand and siliciclastic deposition occurred at relative lowstand (Hart, 1998; Crosby, 2015; Bickley, 2019). Crosby (2015) and Bickley (2019) posit that carbonate debris flows transporting reworked sediment into the basin may be constrained to subaqueous erosion during highstands. It is the belief of this author that this view it too narrow in scope, and that such debris flows and MTDs likely occurred too during regressive (falling) stands as a result of decreasing pore pressure and the lag between carbonate sedimentation rates on the shelf and sea level fall which created a window in which there existed increased overburden along the shelf-margin. At relative lowstands, classic channel/turbidite systems establish within the basin with siliciclastic sediments observed moving into the basin through channels and incised valleys that pass through the established shelf reefs (Montgomery, 1998). Studies tend to agree that the slope to basin floor transition zone of the Bone Spring is dominated by four major facies: meggabreccias (debris flows), allochthonous packstones, fine to very fine-grained sandstone turbidites, and dark laminated mudstones (Saller et al., 1989) as in Figure 13.

In his 2019 work, Bickley shows a one-dimensional basin model created with one of the wells within the study area as a means by which to verify subsidence history and determine thermal maturity windows for hydrocarbon generation.

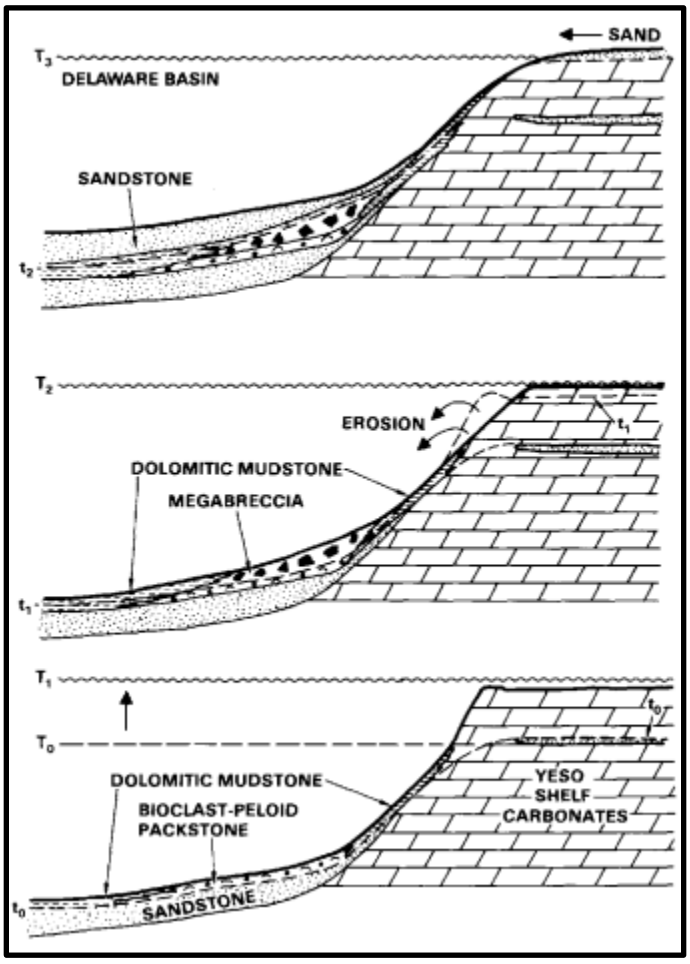

Figure 13: Depositional model constructed by Saller, Barton and Barton (1989) providing mechanism for observed trends in turbidite, megabreccia, and laminated strata proximal to toe-slope.

The model he utilized included, depths, thicknesses, porosity, TOC, and temperatures determined from either logs or core data, with facies, organofacies, and paleobathymetry estimated based upon depositional environment inference. A temperature log was used to calculate a current heat flow that was found to agree with regional heat flow maps. The model (Figure 14) shows the subsidence profile for the portion of the Delaware Basin studied by Bickley (2019) and highlights the change from slow subsidence of the Tobosa Basin to the rapid subsidence experienced by the

Delaware Basin during the Permian. Of note, the entire Bone Spring Fm. is found to lie within the oil maturity windows offering validation to the idea that some of the hydrocarbons therein may have been self-sourced. However, it must also be considered that oil generation from underlying sources, i.e. the Woodford and Barnett Fms. could have migrated upwards and been trapped within the Bone Spring (Bickley, 2019).

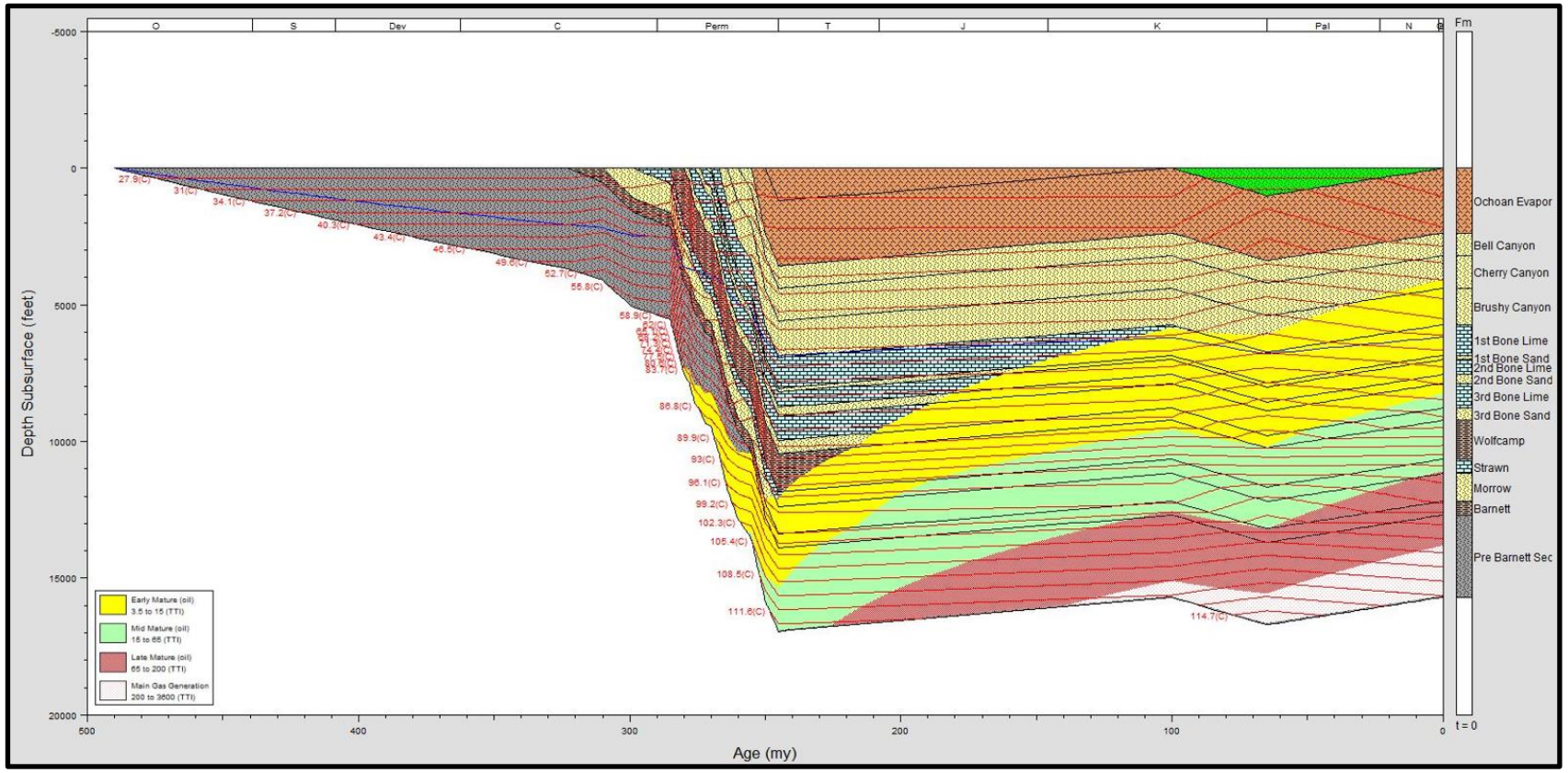

Figure 14: One dimensional basin model showing Bickley (2019) study area's subsidence profile highlighting the rapid subsidence occurring during the Permian. The entire Bone Spring is in the oil maturity window and could be self-sourcing.

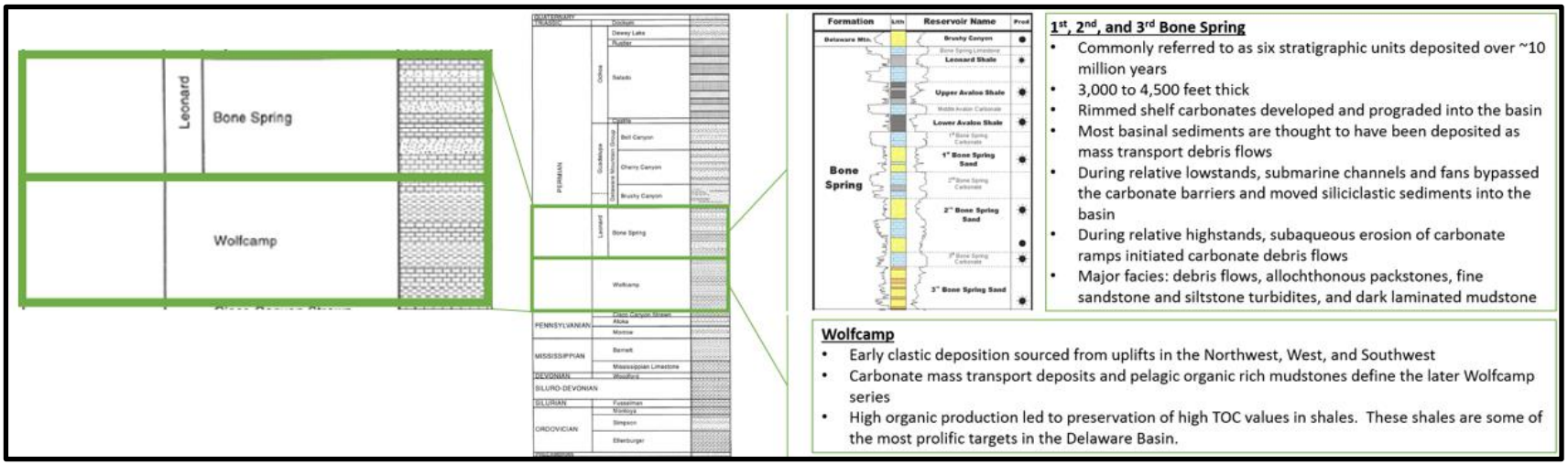

Figure 15: Summary of Wolfcamp and Bone Spring deposition and their position in the stratigraphic column. Modified from Hardage et al, 1998, Bicley, 2019, and Core Laboratory, 2014.

Post-Bone Spring Deposition

Deposition immediately following that of the Bone Spring Fm. with the onset of the Guadalupia consisted of the Delaware Mountain Grp., comprised in order of oldest to youngest of the Brushy Canyon, Cherry Canyon, and Bell Canyon Fms. (Silver and Todd, 1969). These formations unconformably overlie the Bone Spring Fm. in the study area, and highlight the marked shift away from cyclic, reciprocal carbonate and siliciclastic deposition of the Bone Spring Fm. in the Delaware Basin to a predominately siliciclastic system (Harms, 1974; Ross and Ross, 1995). Carbonate development during this time is much more confined to the shelf margin with more pronounced reef development than at any other time during the Permian, development which eventually resulted in a completely restricted basin coinciding with the end of the Guadalupian series (Adams, 1965, Hills, 1984).

The Ochoan issued in a period of dominant evaporitic deposition within the Delaware Basin forming the Rustler, Salado, and world-renowned Castile Fms. (Adams, 1965). The thickness and lateral extent of these units, along with the nature of their evaporitic mineralogy, provided a capping seal to the multiple underlying petroleum systems, and provided for many shallow conventional targets that initially attracted the attention of petroleum industry to this area (Bickley, 2019). The end of the Ochoan marks the near complete cessation of sedimentation into the Delaware Basin, that by this point has little accommodation space left to it. Though pulses of sedimentation occurred towards the end of the Permian and Late Triassic, depositing prograding red-beds, the

remainder of the Delaware Basin's geologic history is dominated by erosion of Permian sediments and subsequent deposition of Pliocene-Pleistocene alluvium (Hills, 1984).

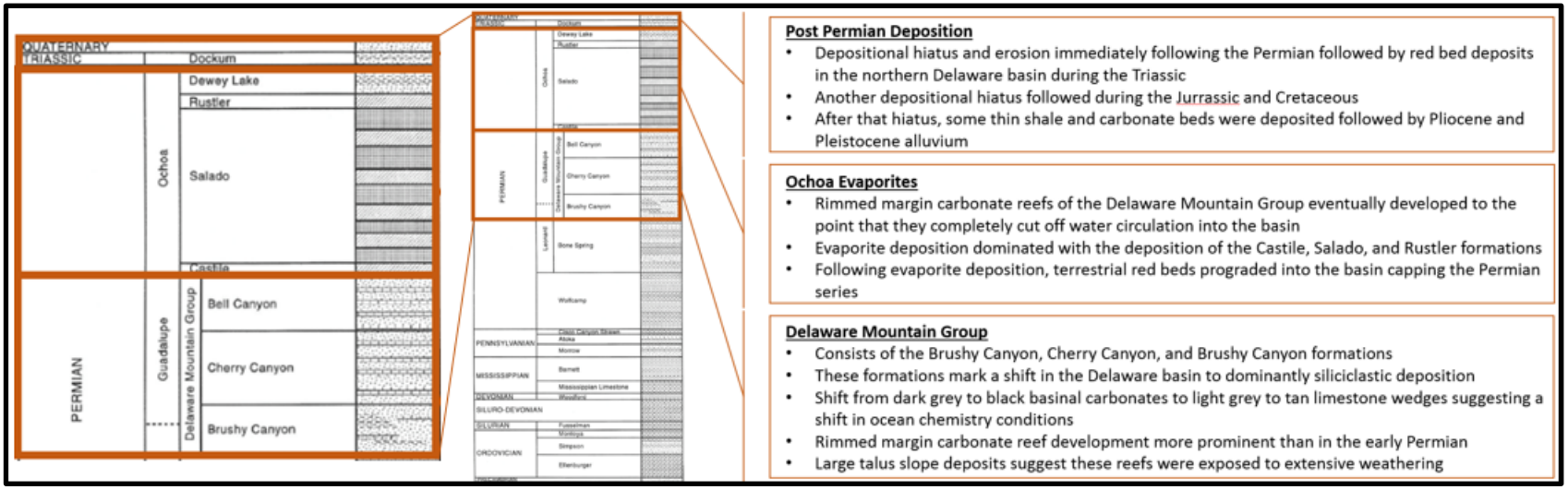

Figure 16: Summary of post Bone Spring deposition. Modified from Hardage et al. (1998) and Bickley (2019).

Chapter 3: Stratigraphy Introduction

The integration of both well log sequence stratigraphic elements and seismic stratigraphy within this investigation makes it necessary to introduce those concepts that will empower the process, drive the ensuing discussion, and provide the foundation upon which subsequent assumptions and inferences are built. As the nomenclature for stratigraphic models varies geographically, between discipline subsets, and even between enclosed systems of training for those subsets, this author will establish a unified lexicon of terms and their definitions.

The overarching purpose of sequence stratigraphy is to provide a mechanism by which the hierarchy of interconnected and multifaceted processes governing over sedimentation may be succinctly understood. Primary controls may be understood to include relative sea level fluctuations, tectonic subsidence, and sedimentation rate, though many other variables of lesser prominence play a role in sedimentation processes, and these in turn vary depending on the nature of the sediment being deposited, i.e. carbonates or siliciclastics.

Sequence stratigraphy may be understood as the study of genetically related facies within a framework of chrono-stratigraphically significant surfaces (Van Wagoner et al., 1998). A sequence, the fundamental stratal unit for sequence stratigraphy, is defined as a relatively conformable, genetically related succession of strata bonded by unconformities or their correlative conformities (Mitchum, 1977). Sequence boundaries arise according to change in relative sea level and the control it exerts over sedimentation. A

parasequence is defined as a relatively conformable, genetically related succession of beds or bedsets bounded by flooding surfaces or their correlative surfaces (Van Wagoner et al., 1998). In turn, a parasequence set is defined as a succession of genetically related parasequences that manifest a distinctive stacking pattern, often bounded by significant surfaces (i.e. flooding, erosional), and comprised of bedsets, beds, laminasets and laminae (Van Wagoner et al., 1998).

Slatt (2006), offers a more succinct definition and more easily accessible definition: sequence stratigraphy involves the tracking of regionally correlatable time surfaces or unconformities, namely sequence boundaries (SB) and maximum flooding surfaces (mfs), through the rock record. These surfaces essentially delineate sedimentary packages, parasequences and sequences, from within a stratigraphic column, affording the interpreter the ability to make inferences regarding their depositional environments according to their interrelation (Slatt, 2006). Correlation of these surfaces and identification of the sedimentary packages that they bound empower more accurate depositional interpretations and better lateral prediction of facies (Slatt, 2006).

Below are definitions of some key stratigraphic terms as they will be used in this study, as previously compiled in Bickley's 2019 thesis (Crosby, 2015; Catuneanu et al., 2011; McCullough, 2014; Zhou, 2014):

- Parasequence – A genetically related, conformable succession of beds or bedsets bounded by sub-regional correlative surfaces
- Sequence – A succession of genetically related strata during a full cycle of change in accommodation or sediment supply bounded by sequence boundaries

- Sequence Boundary – A regional surface that denotes the transition from one sequence to another. Vail and Galloway define sequence boundaries differently based on what is easily correlated on seismic or well logs respectively. This study compares well log and seismic stratigraphy and it is therefore essential to use a common definition of the sequence boundary. This investigation adopts the Vail sequence boundary which places sequence boundaries on the top of highstand systems tracts (Vail, 1987; Galloway, 1989).
- Maximum Flooding Surface – Interpretation of highest relative sea level. Marked by widespread silt/shale deposition in clastic sediments and can also be marked by blocky carbonate deposition in carbonates (May, 2018).
- Lowstand Systems Tract (LST) – A systems tract deposited at a relative lowstand in sea level usually associated with increased process energy and progradation of coarser grained sediments into the basin. In the Bone Spring, 3rd order LSTs correlate with the dominantly siliciclastic 1st, 2nd, and 3rd Bone Spring Sands as well as the Avalon Sand/Shale.
- Highstand Systems Tract (HST) – A systems tract associated with a relative highstand in sea level usually marked by progradation onto the maximum flooding surface. The HST is capped by the Vail sequence boundary (Vail, 1987). In the Bone Spring, HSTs are associated with the dominantly carbonate deposition of the 1st, 2nd, and 3rd Bone Spring carbonates.

- Transgressive Systems Tract (TST) – Sediments deposited during the onset of sea level rise usually following an LST. The TST is then caped by the maximum flooding surface.
- Falling Stage Systems Tract (FSST or RST) – Sediments associated with the onset of a fall in sea level deposited on top of the HST. In the Bone Spring this is associated with incision and erosion and the beginning of siliciclastic sediments being transported into the basin. At a higher order within relative LSTs, FSSTs can also be associated with carbonate erosion and slumping moving more carbonate sediment into the basin (Li, 2015; Pigott and Bradley, 2014).

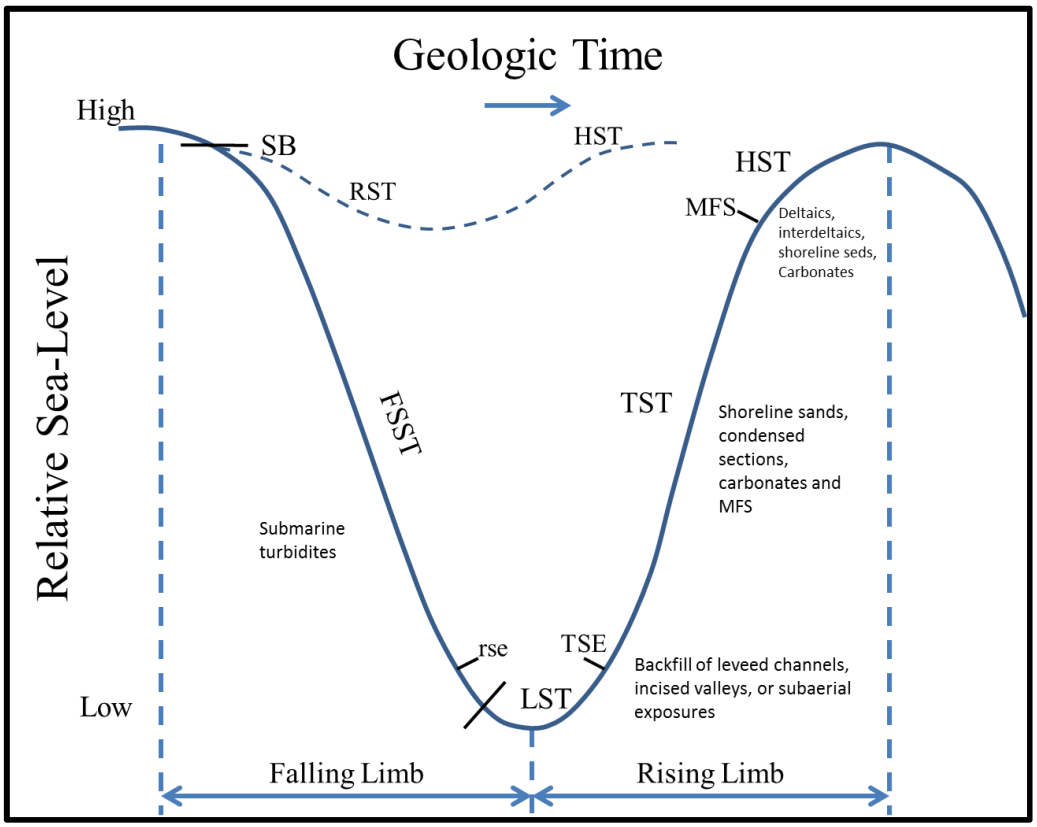

Figure 17: One full relative sea level cycle highlighting the positions of important sequence stratigraphic systems tracts and markers within the falling limb and rising limb of sea level change (Slatt, 2006, 2013; Crosby, 2015; Bickley, 2019).

A visual representation of these terms over one full cycle of sea level change may be seen in Figure 17, which presents the sea level curve annotated with the various systems tracts according to the position they occupy as well as some characteristic facies deposited during those systems tracts. In a mixed carbonate/siliciclastic basin like the Delaware Basin, eustatic and relative sea level changes seem to have a great impact on the makeup of sediments and depositional processes occurring within the Bone Spring. It is important to note that other factors such as subsidence, tectonics, climate, depositional process energy, and basin paleo bathymetry also impact the deposition of sediments. However, with all these controls in mind, it is possible to map out high order changes in sea level within the Bone Spring which seem to have a very strong impact on reservoir and source quality in the formation.

Reciprocal Sedimentation Model

Reciprocal sedimentation is predicated upon the idea that mixed carbonate and siliciclastic depositional environments cycle over time according to sea level fluctuation (Catuneanu et al., 2009; Crosby, 2015; Bickley, 2019). Within the Bone Spring Fm., this reciprocal sedimentation manifests through signature sedimentation trends including carbonate fan deposition, sediment gravity, and mass transport deposits during highstand and falling stand systems tracts, and classic turbidite sand deposition during lowstand systems tracts (Mullins and Cook, 1986; Saller, Barton and Barton, 1989), wherein carbonate flows are characteristically deposited as carbonate aprons according to Mullins and Cook (1986). As observed in this study area, carbonate flows are comprised of mud supported debris flows and allochthonous detrital packstones and as such may be

interpreted as being inner apron deposits of these carbonate fans. This study area, being situated overtop the shelf-margin with shelf, shelf slope, and basin deposits in close proximity of one another, portrays these carbonate fans as having wedge-like geometries. Nevertheless, the deposition of carbonate fan wedges is interrupted during relative lowstands, as the fall in sea level precipitates a shutdown in the carbonate factory on the shelf and initiates siliciclastic migration across the shelf and into the basin. This migration of siliciclastic sediment is marked by textbook incised channels and valleys cut through the underlying carbonate build-up, which act as avenues of transport out into the basinal setting. In this study area, as in Crosby (2015) and Bickely (2019), siliciclastic sediments are comprised of at least fine grained to silt sized sand, according to gamma ray response, and likely exhibit Bouma sequence patterns (Slatt, 2006). The reciprocal sedimentation model with specific context for the Bone Spring is shown in Figure 18.

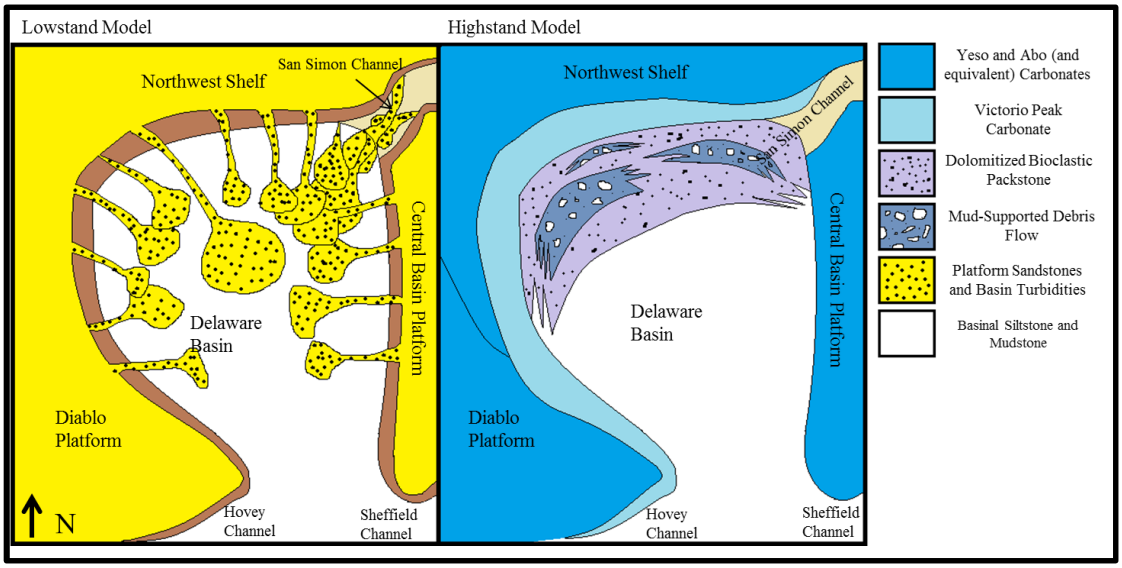

Figure 18: Idealized model of reciprocal sedimentation of the Bone Spring highlighting the deposition of siliciclastic turbidite fans and channel systems at relative lowstands and carbonate apron deposition at relative highstands (Scholle, 2002; Crosby, 2015; Bickley 2019).

Carbonate-Adapted Galloway Motif Sequence Stratigraphy

Well log sequence stratigraphy relies on the assumption that the gamma ray curve acts as a proxy for both intra-depositional system energy and grain size, and therefore can infer that coarser siliciclastic sediments have deposited at lowstand times under higher process energy and finer grained sediments during highstand times with lower process energy (Pigott, 2018). The arrows below the GR curve (left) in Figure 19 show classic Galloway sequence stratigraphic motifs, assuming siliciclastic system, with increasing gamma representing transgression and highstand deposits and decreasing gamma representing regression and lowstand intervals (Galloway, 1989; Pigott, 2018). This model persists as an effective tool by which to predict sequence stratigraphic-driven evolution of deposition environments, and thus sedimentation processes, within siliciclastic environments.

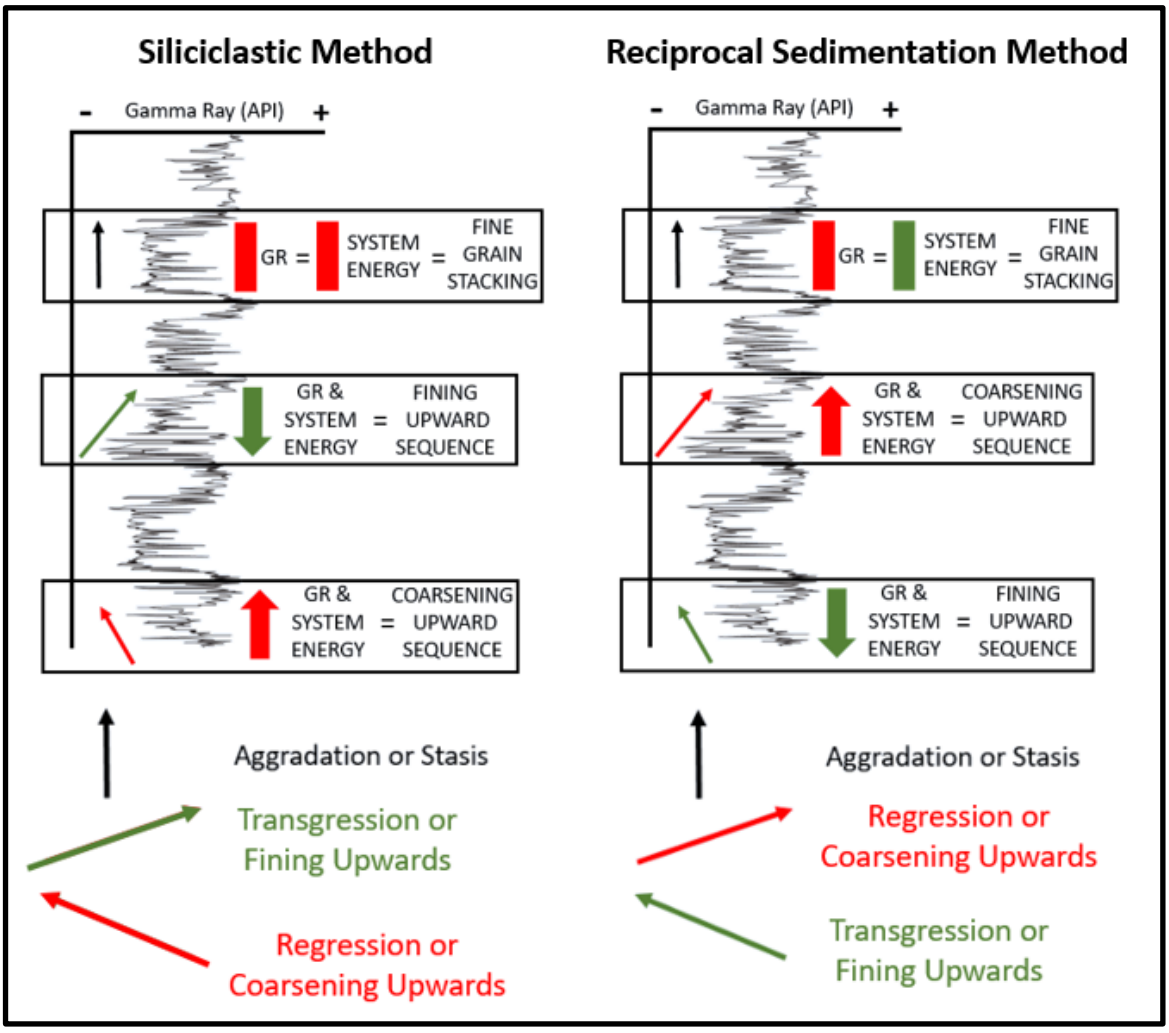

Figure 19: Classic Galloway based sequence stratigraphic motifs contrasted with modified, Reciprocal Sedimentation Model Galloway based sequence stratigraphic motifs. Though the former works well in the lowstand 3rd Bone Spring Sand with highstands consisting of finer grained siltstones and lowstands consisting of coarser grained sandstones, it breaks down in the highstand carbonates with the suggestion that these facies were deposited during a relative lowstand when they are known to be deposited during relative highstands, precipitating the need for the latter model.

However, the underlying principles that empower this tool do not remain valid for depositional settings hosting mixed siliciclastic – carbonate sedimentation as may be found in a reciprocal sedimentation model. The analysis breaks down due to the fundamental differences in the depositional processes that govern between siliciclastic

and carbonate depositional environments, as is highlighted in Figure 19 (right) which shows how the process may be adapted to account for reciprocal sedimentation.

Consequently, it becomes necessary to offer some background into the differences in those depositional processes and depositional environments that exist between carbonate and siliciclastic systems of sedimentation. While finer grained siliciclastic muds and shales are deposited at relative highstands in distal basinal settings, high gamma carbonates are in turn associated with carbonate mud that is more abundant at relative lowstand times and likely to be mixed with siliciclastic material in the Bone Spring (Pigott, 2018). Inversely, while lower gamma ray clean sands are expected at relative lowstands while in a siliciclastic system, low gamma ray readings within a carbonate system are indicative of cleaner, "blocky" carbonates that more closely resemble highstand carbonate growth (Pigott, 2018).

Therefore, this study has adopted the modified Galloway approach of Pigott (2018) which accounts for the integration of these differing sedimentation styles into one depositional system so as to more accurately capture the cyclical relative sea level changes responsible for the reciprocal sedimentation observed in the Bone Spring Fm. As is shown in Figure 20, the adapted Galloway approach is essentially an inverse operation in the interpretation of classic Galloway gamma ray motifs during carbonate dominated intervals. This approach allows for representation of the sedimentation processes inherent to carbonate systems that make blocky carbonate deposition more widespread during relative highstand times. Increasing gamma response, then, may be tied to relative sea level regression in carbonate intervals while decreasing gamma response is tied to relative sea level transgression and highstand, and the accompanying

increase in production (and subsequent transport to the basin) of cleaner, low gamma carbonate intervals via highstand shedding as a function of decreasing accommodation space on the shelf. Even more, within the context of reciprocal sedimentation, this adapted method better accounts for the fact that relative high frequency 4th order lowstands intrinsic to 3rd order highstands may precipitate increased siliciclastic deposition.

Figure 21 shows the adapted Galloway technique as applied to the 3rd Bone Spring. The adapted motifs tell a more coherent story and better represent the changes in relative sea level that occurred over the course of Bone Spring Fm. deposition. As was stated before, this study also diverges from classical Galloway interpretation in the fact that sequence boundaries are defined at the top of HSTs rather than at maximum flooding surfaces (Galloway, 1989). While this technique works very well for delineating general trends, the presence of shale dominated maximum flooding surfaces within carbonate intervals must also be noted during times when sea level is high enough to flood the reef and blanket underlying sediments in a shale drape.

The adapted Galloway method draws upon lithologic inference when determining sequence stratigraphic trends. In a formation such as the Bone Spring, where reciprocal sedimentation leads to a complex intermingling of carbonates and clastics, this method of analysis is essential to reasonably account for changes in lithology rather than blindly relying on trends in the gamma ray curve.

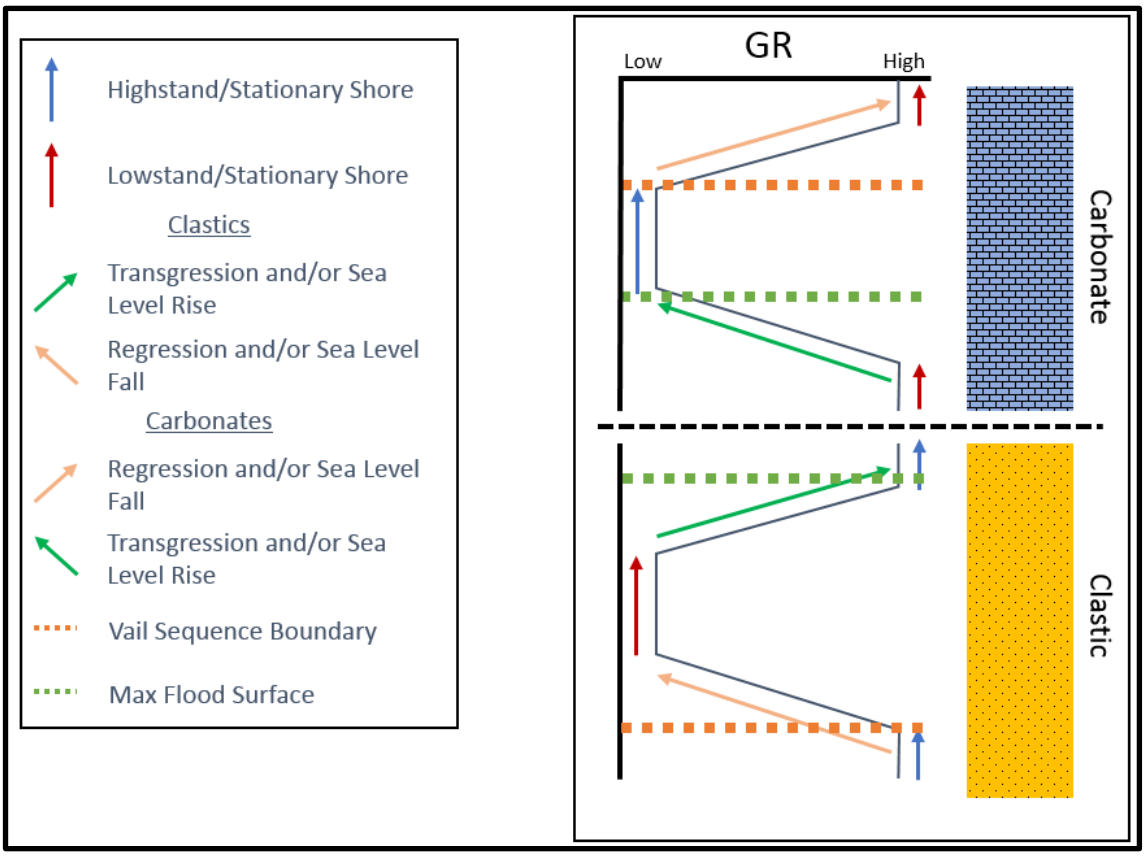

Figure 20: Idealized representation of the proposed adapted Galloway sequence stratigraphic motifs. The clastic model agrees with the conventional Galloway school of thought other than in the placing sequence boundaries at the top of HSTs as is done in the Vail approach. In carbonates, the motifs are reversed to better represent deposition of clean, blocky carbonates at highstand times (Galloway, 1989; Pigott, 2017; Bickley, 2019).

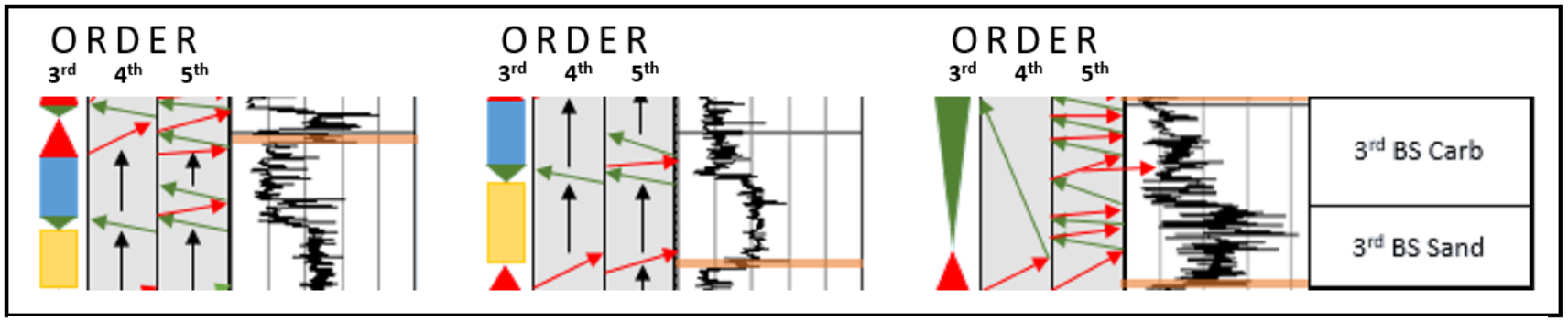

Figure 21: The adapted Galloway motif model applied to the 3rd Bone Spring interval gamma ray log from within a well utilized in this investigation.

Seismic Stratigraphy

The seismic stratigraphic approach utilized in this investigation draws directly upon the original model proposed by Vail in 1987. Seismic stratigraphy is based on the fundamental assumption that the reflectors observed in a seismic volume represent bedding planes and can therefore be interpreted as time surfaces that are chrono-stratigraphically significant (Pigott, 2018). As such, the pattern of reflector terminations into other reflectors may represent the intersection of sedimentary strata into operational sequence boundaries, which then may be interpreted as unconformities or correlative conformities. The primary termination types within Vail's model include erosional truncation and toplap at upper boundaries and onlap and downlap at basal boundaries. Figure 22 adapted from Vail (1987) illustrates how this study represents these terminations and sequence boundaries.

According to Vail (1987), sequence boundaries occur at the top of HSTs. So as to encourage integration of the Vail method with the adapted Galloway method discussed above, this study interprets well log sequence boundaries, too, at the top of HSTs. By performing seismic well-tie through the construction and correlation of synthetic seismic logs using petrophysical data (i.e. velocity and density curve crossplots), this study essentially opened an avenue through which the high vertical-resolution stratigraphic data contained within the well logs might be directly attributed to the 3D seismic reflection data. Even more, in the opposite direction, the lateral resolution afforded by the 3D seismic data may be attributed to the well logs. In such a way, this investigation will attempt to construct a dynamic, integrated Vail-Galloway-derived sequence stratigraphic

framework that affords the highest possible resolution, both vertically and laterally. In the complex Bone Spring Fm. interval, wherein the nature of individual reflectors can be hard to determine due to their chaotic manifestation that arises from the characteristic entropy of sediment gravity flows and MTDs, such a stratigraphic framework with optimized vertical and lateral resolution is truly a high-value tool.

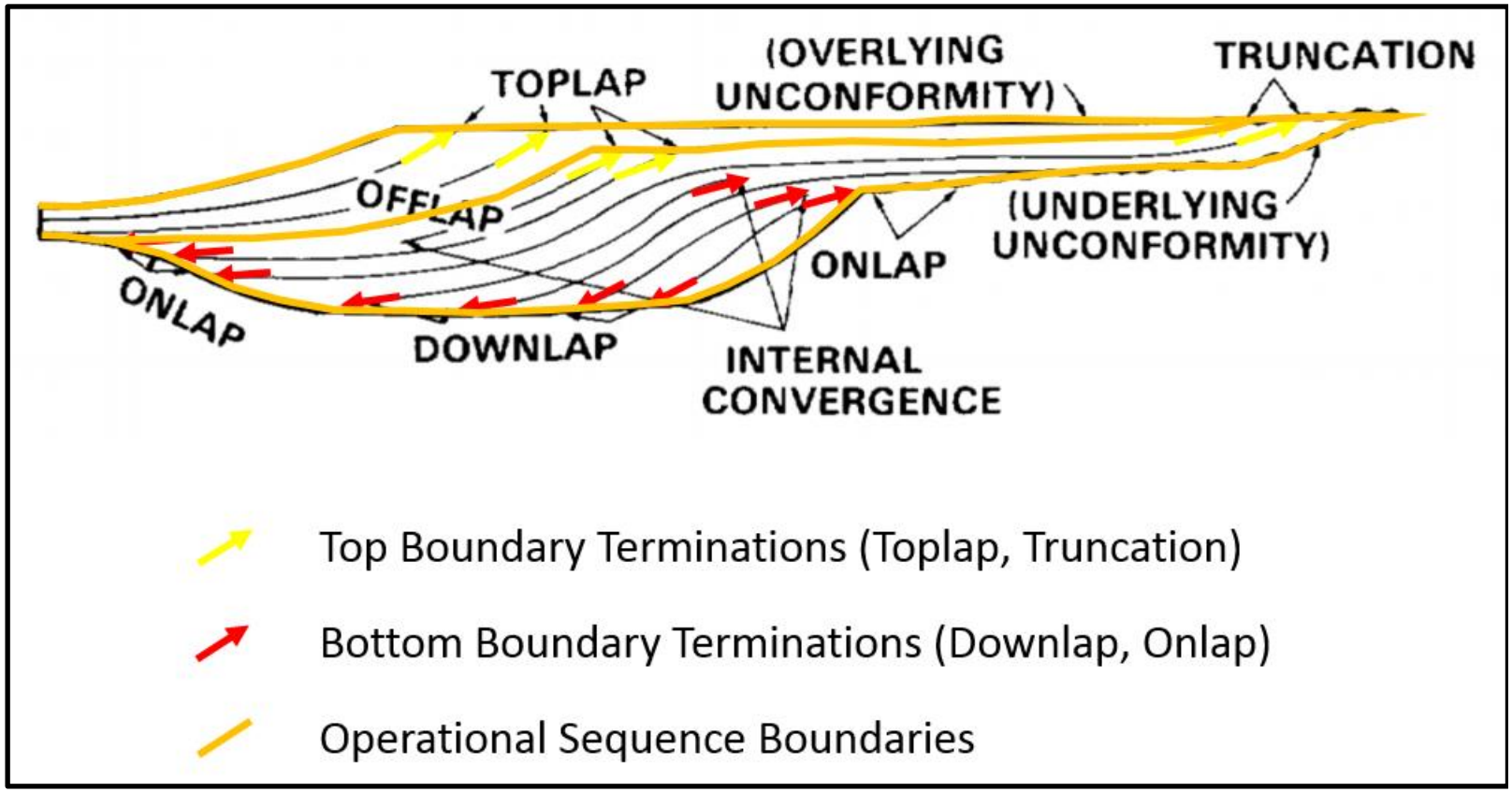

Figure 22: Diagram illustrating the symbols used to define terminations and operational sequence boundaries in this study (Vail, 1987).

Permian Sequence Stratigraphy

Sloss (1963) constitutes groundbreaking work on globally-correlated sequences places the Permian strata within the Absaroka Sequence, or Supercycle, of the North American Craton. In later work, Sloss' more detailed interpretation refines the placement of the Permian within the Lower Absaroka II (Sloss, 1988). The Absaroka II comprises a period of lower frequency and amplitude of eustatic fluctuation when compared with Absaroka I, and higher when compared with Absaroka III (Ross and Ross, 1995). Ross and Ross (1995) posit that the Permian is deposited as part of a 1st or 2nd order eustatic regression, and that the four stages within the Permian, the Wolfcampian, Leonardian, Guadalupian, and Ochoan, constitute cyclic sea level fluctuations within this overarching regression. In the fractal nature of eustacy, parasitic 3rd order and higher sea level fluctuations intrinsic to the overarching eustatic regression partially control deposition of the specific formations within those intervals. This investigation will focus on delineating 3rd, 4th, and possibly 5th order sequences and the control they exert upon Bone Spring Fm. deposition.

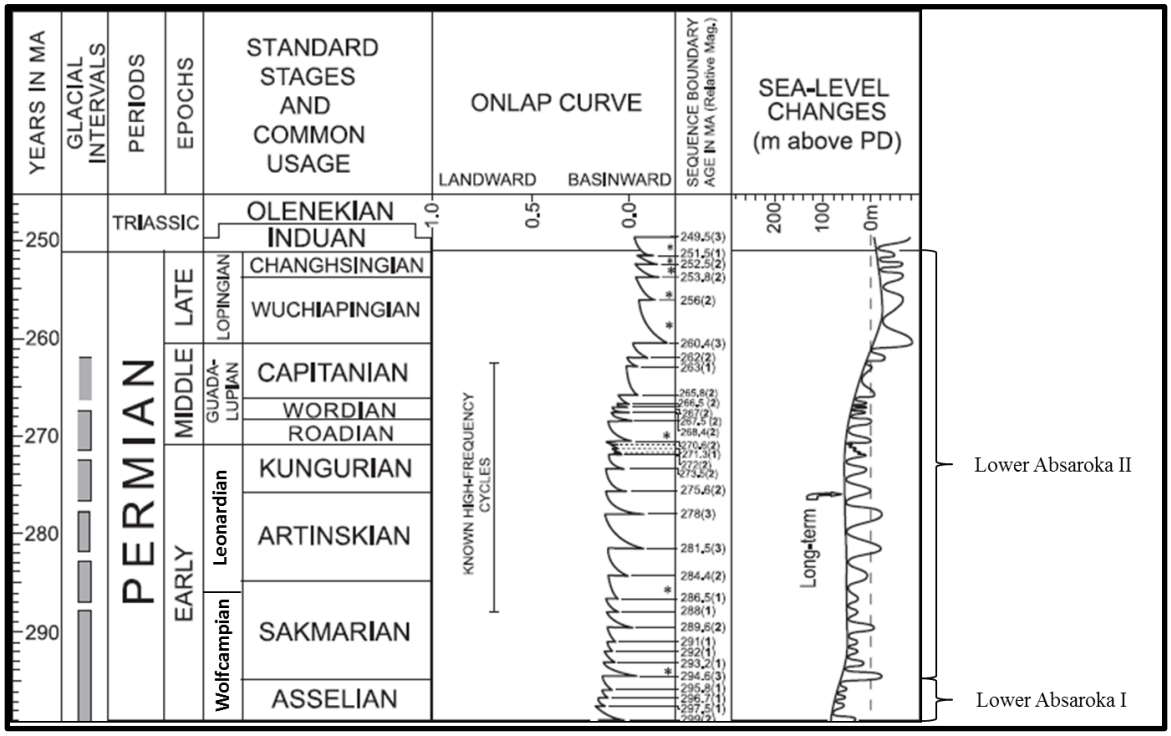

Figure 23: Geologic time scale highlighting the Leonardian location in the Lower Absaroka II with respect to supercycles on the North American Craton (Sloss, 1963). The onlap curve shows that there are multiple higher order cycles within the Leonardian (Haq and Schutter, 2008; Crosby, 2015).

According to Ross and Ross (1994), the Wolfcamp Fm. that unconformably underlies the Bone Spring Fm. is made up of four to five 3rd order sequence stratigraphic cycles. These 3rd order cycles in the Wolfcamp, as well as the later 3rd order cycles in the Bone Spring Fm., are attributed to glacio-eustacy, and more specifically ice sheet volumes on Gondwana (Veevers and Powell, 1987). Silver and Todd (1969) posit that a 2nd order unconformity caps the Wolfcamp on top of which the Bone Spring was deposited. The Wolfcampian 2nd order unconformity and that of the 2nd order unconformity at the top of the Bone Spring Fm. that underlies the deposition of the Brushy Canyon Formation represent 2nd order sequences boundaries that bound the Bone Spring Fm. (Silver and Todd, 1969).

Previous work by Ross and Ross (1994) and Montgomery (1998) places anywhere from four to eight 3rd order sequences within the Leonardian. This investigation identifies five 3rd order sequences within the Bone Spring formation. Ross and Ross (1995) and Crosby (2015) note that 3rd order sequences within the Bone Spring Fm. appear to last longer than in the Wolfcampian interval due to increased carbonate production during highstand relative sea level during the Leonardian. The 4th order and 5th order cycles identified in the well logs largely mirror those 3rd order cycles previously identified by way of their internal variation. This investigation identifies seven 4th order cycles, and sixteen 5th order cycles within the Bone Spring Fm. and correlates those cycles and their associated parasequences and systems tracts to the 3D seismic data. Figure 24 shows a gamma ray log with integrated Vail-Galloway interpretation methodologies applied, identifying the 3rd order highstands and lowstands associated with the Bone Spring Fm., and showing the formation tops included in the well logs and subsequently integrated with the seismic data. Of note, many of the provided formation tops in the well reports were considerably suspect, and as such, the formation tops presented in this investigation have been picked largely based on lithologic boundaries inferred from the adapted Galloway gamma ray motif analysis. These tops are imbued with stratigraphic significance when viewed through the lens of the reciprocal sedimentation model.

Chapter 4: Data Availability

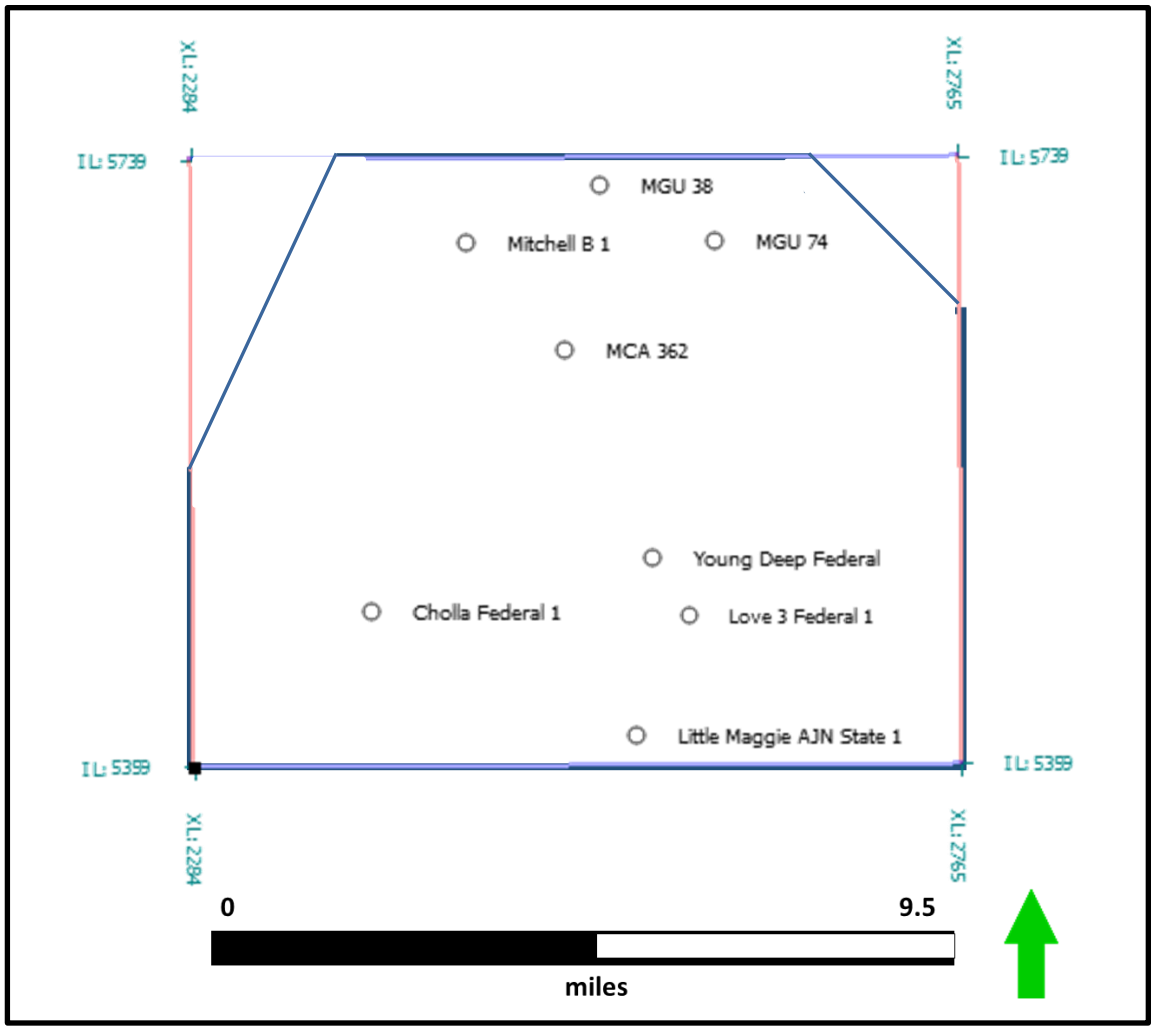

Figure 24: Data availability map showing the outline of the 3D survey provided for the study along with the relative positions of the wells that data was provided for within the survey.

The 3D seismic survey used in this investigation was generously provided by Schlumberger, who maintains an active interest in the Delaware Basin. The data from the eight wells within the bounds of the 3D seismic survey (Figure 24) were obtained from the public repository maintained by the New Mexico Oil Conservation Division

(NMOCD) and digitized by a third-party. The 3D seismic survey is in an area that is currently being explored and developed and remains proprietary to Schlumberger. Therefore, for the sake of confidentiality, the exact name and location of the 3D survey will be excluded from this study, and though the well names are public domain, their exact names and location will be likewise omitted to preserve the confidentiality of the seismic data. Figure 1 shows the approximate location of the study area in relation to the Delaware Basin's location and geometry. All subsequent maps will show the outline of the 3D survey and relative position of the well logs that were obtained for this investigation within the survey.

Log Data

Digital well logs were obtained from 72 wells within the study area and subsequently culled down eight according to log quality and available petrophysical curves. These selected well logs were then digitized by the author and 3rd parties using Neuralog software. The final set of criteria for filtering the well data were as follows: availability of gamma ray and sonic logs, with preference to those which also included either bulk density and/or neutron porosity logs that covered the Bone Spring. Due to the nature of public well log data, especially data spanning from as far back as two decades ago, petrophysical conditioning techniques were required to optimize the various logs for analysis (See Appendix I.1-3). Even with conditioning, the original array of petrophysical data from the 72 wells were found unsuitable for inclusion in this investigation for reasons ranging from failure to penetrate the Bone Spring Fm., insufficient depth intervals of petrophysical logs (highly constrained to certain target depths of as little as 150 feet), to poor data quality. Formation tops across the area were picked using these

well logs and patterns in log responses were used to identify stratigraphic trends. Regrettably, many of the wells situated on the portion of the seismic survey that overlies the subsurface shelf targeted shallow intervals and thus failed to penetrate to depths of use in this investigation. While these, as such, were insufficient for performing subsurface mapping of the Bone Spring Fm., their various petrophysical logs were useful in constraining important relationships between parameters including formation velocity and density (Appendix I.1).

Seismic Data

The Schlumberger 3D survey covers an area of ~100 square miles and was shot and processed in 2016 and 2017 respectively. Seismic data acquisition in the Delaware Basin is known to be difficult due to the shallow evaporitic sediments that inhibit seismic reflector data from accurately portraying underlying strata. The bin size and high CDP fold of this survey allow it to better image below the anhydrites than older vintage 3D surveys. High quality seismic data provides better imaging of reflector terminations empowering interpreters to more accurately make stratigraphic interpretations. Internal reflectors can also be identified within most of the major formations within the Bone Spring, but due to the nature of those deposits, i.e. sediment gravity flows and MTDs, these internal reflectors often appear chaotic. In order to improve interpretation, AASPI Acquisition Footprint Workflow was conducted, which markedly improved seismic data quality and afforded more interpretational accuracy (Appendix II).

Merging the sequence stratigraphic framework constructed from the well log with the seismic data afforded improved geologic interpretations to be made. Note that the polarity of the data is SEG Reverse Standard with peaks displayed in red (positive)

and troughs in blue (negative) (Brown, 2011). An example of the seismic data quality can be seen in Figure 25. Important acquisition parameters for the survey are as follows:

- Record Length: 4000 ms
- Sample Rate: 2 ms
- Bin Size: 110ft
- CDP fold up to 420
- Inlines: 5399 - 5799
- Xlines: 2284 – 2765
- Dominant Frequency: 60 Hz
- Tuning resolution: ~60ft

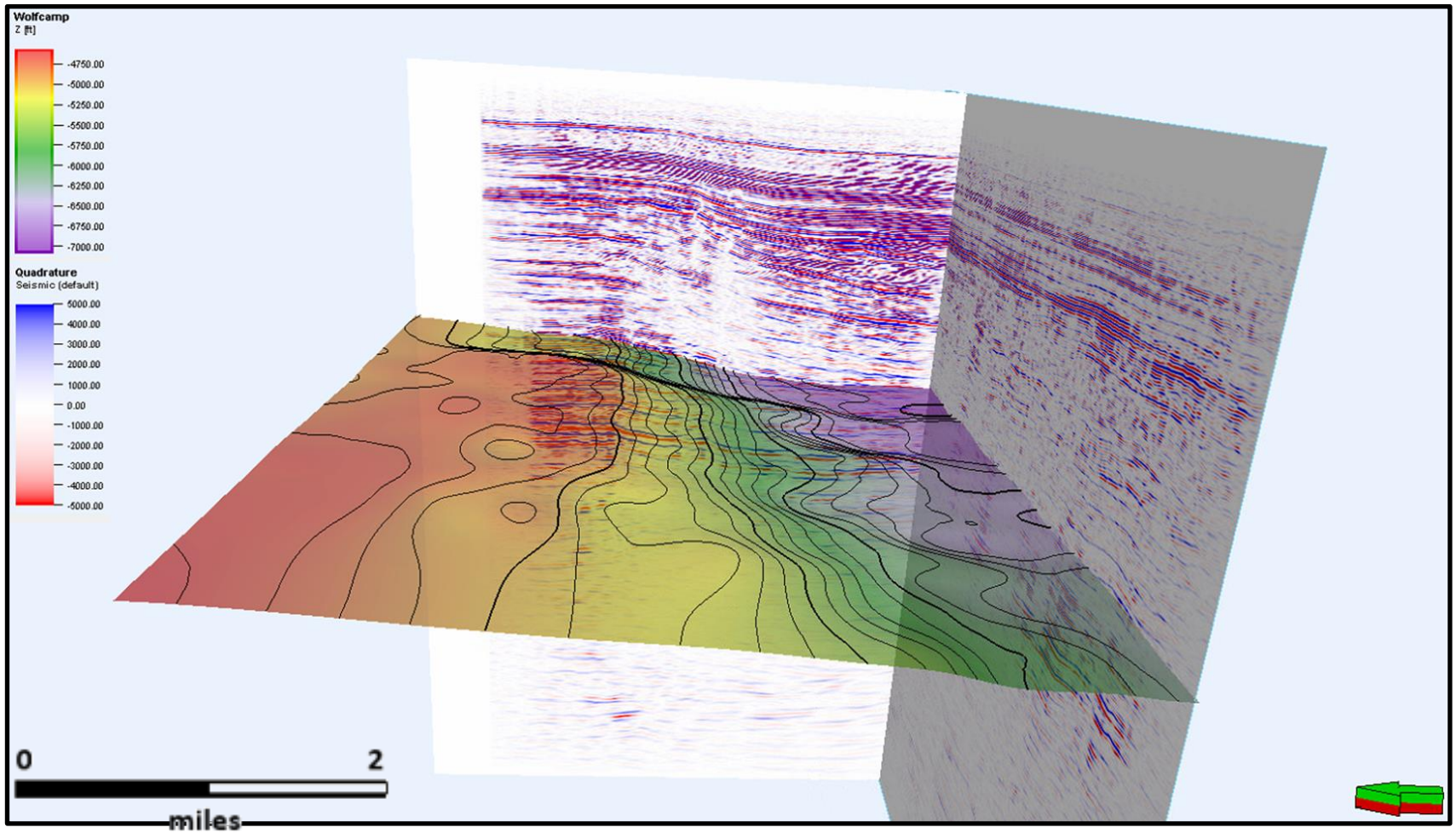

Figure 25: Example of the high-quality seismic data used in this study. The shown horizon is the top of the Wolfcamp Fm. that immediately underlies the Bone Spring and importantly provides inherited topography.

Chapter 5: Methods

This investigation was advanced initially through two mutually exclusive approaches – well log sequence stratigraphy and seismic stratigraphy – which were later integrated to great effect. Both approaches lent their respective strengths and displayed their respective shortcomings, though only through utilization of both was a final interpretation, derived from the integrated approaches, reached. The findings of this study confirm that the sum of these two approaches is indeed greater than the individual parts. Over the course of this chapter, the respective methods utilized in both approaches will be discussed before moving on to a discussion of the results. A methods map, linking methods with the concepts they encompass, may be found below (Appendix III).

Well Log Analysis

Analysis of the well logs utilized in this investigation (Chapter 4) began from a first order perspective. This was only in part aided by the well tops provided in the public domain well reports, as many of the utilized wells are decades old and tops reporting proved sporadic and sometimes very inaccurate. The major boundaries identified include the Wolfcamp, 3rd Bone Spring Sand, 3rd Bone Spring Limestone, 2nd Bone Spring Sand, 2nd Bone Spring Limestone, 1st Bone Spring Sand, 1st Bone Spring Limestone, Avalon, and Brushy Canyon.

A sequence stratigraphic framework was interpreted and correlated across a well transect that intercepted the Bone Spring Fm. through application of the adapted Galloway approach discussed above and with the objective of delineating sequence

boundaries and maximum flooding surfaces (see Chapter 3: Adapted Galloway Sequence Stratigraphy). The primary petrophysical log used to identify these sequences was the gamma ray (GR) curve, due to the insight it provides into process energy and lithology. Sonic, density, and neutron porosity logs were also valuable in both providing validation to lithologic trends interpreted via gamma response, and for later integration of well log data with the seismic data.

For example, increased carbonate content was observed to correlate with trends of increasing formation velocities and bulk density, and decreasing porosity. Though these interpretations often enjoyed validation from multiple logs, they were in no way taken by themselves as infallible. Geology is an imprecise science, as complete understanding of the true breadth, depth, and scope of the overarching, governing multivariate system is never possible; rather it is the job of the geoscientist to employ whatever data is available towards the best possible interpretation that is supported by that data. Nonetheless, in general terms, the log responses did afford delineation of carbonate and siliciclastic intervals that proved reasonable within a geologic context.

Seismic Analysis

To identify important horizons, and eventually compare the seismic stratigraphy to the well log sequence stratigraphy, the first step was to create synthetic well ties throughout the survey using the wells that had sonic and density logs. In some cases, the wells being utilized lack either sonic or density logs, and so a multi-well cross-plot between relating density and sonic to depth was performed in HampsonRussel^{TM} (HSR), and a Reverse Gardner function applied to back-calculate the missing parameter. Synthetic seismic logs were then created and used to perform a seismic well-tie in HSR.

With the well log petrophysical responses thus tied to the seismic reflection data, the seismic data, now converted into depth domain, was imported into Petrel^{TM}, wherein horizons of interest were mapped via the Autotracking function where possible, and manually picked where not. Mapped horizons include the Wolfcamp unconformity, Abo top, and internal interval tops within the Bone Spring Fm. These horizons were then used to make time structure and isochron maps. The resultant maps provide insights into structural trends, depositional architecture, and sediment stacking patterns and transport pathways within the Bone Spring Fm.

Next, crossline and inline (dip and strike, respectively) seismic slices intersecting wells were chosen for subsequent seismic sequence stratigraphic analysis via termination assignation according to the Vail approach. The resulting array of termination picks delineated sequence boundaries separating stratal packages into parasequence sets. 3rd order sequence boundaries were identified, breaking the Bone Spring into seven 3rd order sequences, which exceeded the framework constructed from 3rd order sequences identified within the adapted Galloway sequence stratigraphy, though not the 4th or 5th order. With this in mind, the study overlays 4th and 5th order adapted Galloway gamma ray motifs with the seismic reflection data in an attempt to reconcile the two stratigraphic frameworks. Convolution of seismic reflectors within the Bone Spring Fm, interval complicated this endeavor, as sequence boundary interpretation was at times quite difficult, especially when considering the preponderance of chaotic internal reflector signal arising from sediment gravity flows and MTDs characteristic to the formation. The challenge is compounded by the inherent challenge facing geophysical interpretation of carbonate seismic reflector data that arises from the natural propensity of carbonates

towards internal heterogeneity. Even so, sediment gravity flows were readily identified, and within this survey exhibit discrete flow times, and though many are captured in the seismic data, no doubt others fall below seismic resolution. In support of this notion, two sequence boundaries delineated in the Vail-derived seismic sequence stratigraphic framework that should define lowstand siliciclastic deposits appear instead as mere erosional surfaces, likely due to insufficient resolution.

Chapter 6: Results

Well Log Analysis

As described in the previous chapter, all the available logging tools (i.e. Petrel^{TM}, HampsonRussel^{TM}) were used to help to identify formation tops in the subsurface, create surfaces across the study area and delineate between the siliciclastic and carbonate internal divisions within the Bone Spring Carbonate Fm. Figure 24 shows the locations of all the well logs used in this study and identifies those wells that logged part of the Bone Spring Fm. and wells that logged the entire Bone Spring interval down to the Wolfcamp.

Though the entire Bone Spring Fm. was subjected to sequence stratigraphic investigation, the primary focus of this study and thus this discussion will be on the 1st, 2nd, and 3rd Bone Spring Sand intervals. Therefore, subsequent fence diagrams and seismic surfaces will display the 1st Bone Spring Lime as a combined interval, disregarding the subdividing Avalon Sand and other unknown sand interval(s) exposed in the integrated sequence stratigraphic framework. Subsequent sequence stratigraphic

analysis may break this out into multiple parasequences, and certainly there is much within the transition into the overlying Brushy Canyon formation that is deserving of more detailed study in the future.

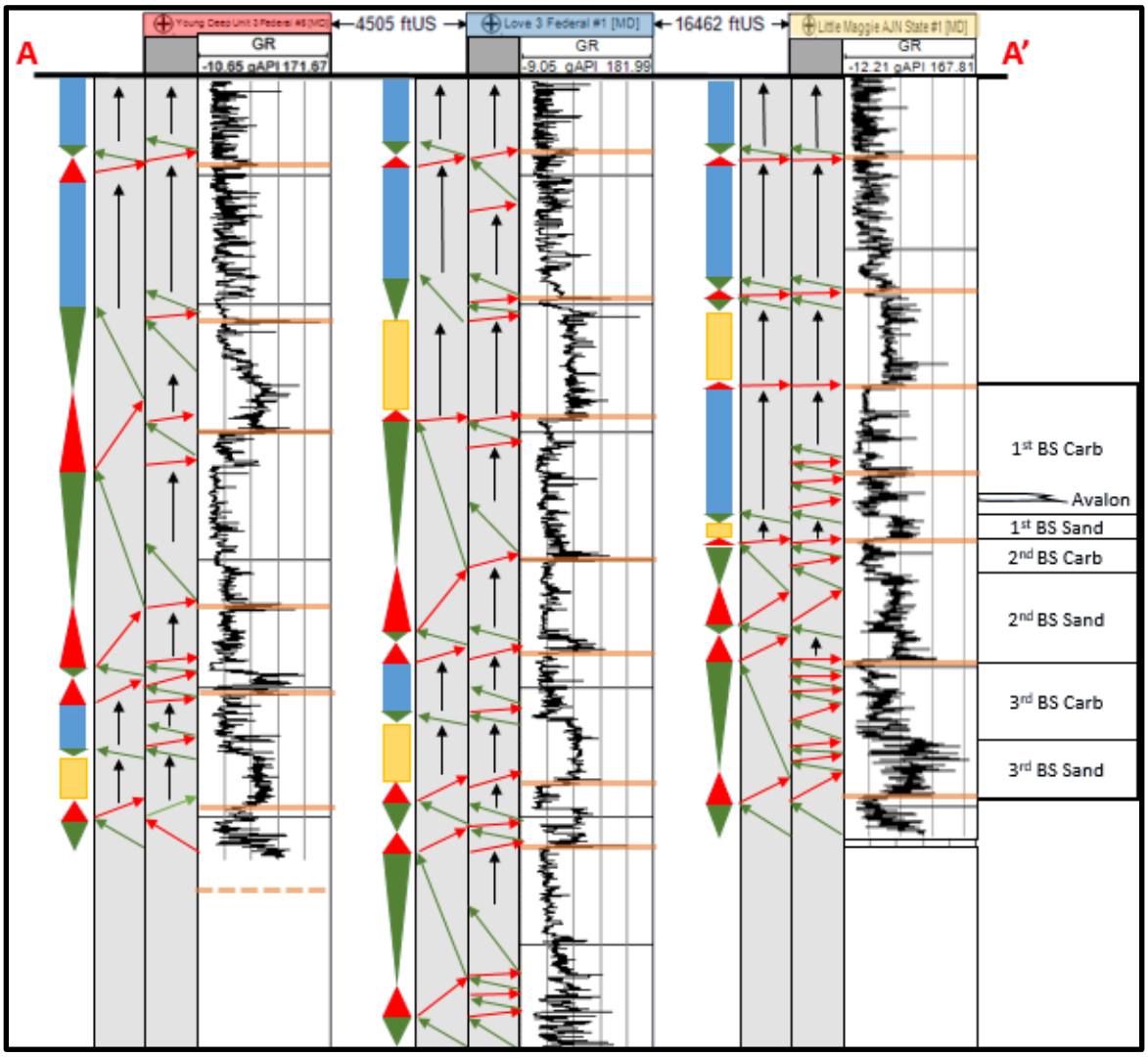

Figure 26: Cross section A – A' marking 3rd order sequence boundaries in orange. Five 3rd order sequences were identified using the adopted Galloway gamma ray motif technique.

Cross section A – A' (Figure 26) delineates sequence boundaries that were mapped which correlate to the tops of the four carbonate intervals within the Bone Spring. Maximum flooding surfaces (mfs) were identified as potential correlation

markers within the Bone Spring Sand intervals. The association of the mfs with the oscillation within the reciprocal sedimentation model from basinal siliciclastic deposition to shelf production of carbonates results in a prominent shift in the gamma ray signature that is easily recognized and easily correlated to other wells.

The 4th and 5th order sequence boundaries are delineated through the gamma ray log motif analysis, and as will be seen, add great value later in the study to the seismic sequence stratigraphy. For now, the 3rd order sequences as shown represent the skeletal inner construct of the consequent integrated sequence stratigraphic model that this study is building.

4th Order Sequence Stratigraphy

Galloway motifs were applied to 4th order cycles and mapped out over the selected wells in the study area through a recognition of the fractal nature of sea level fluctuations, especially in the context of sequence stratigraphic frameworks. With 3rd, 4th, and possibly 5th order cycles identified and mapped across the wells, it became clear that the overarching stratigraphy exhibited by the Bone Spring Fm. corresponds to 3rd order sea level fluctuations. The importance of the 4th and 5th order sea level fluctuations with respect to Bone Spring Fm. deposition did not become clear until after the seismic well tie was performed. Figure 27 also highlights the governing control over deposition that the fault zone that lies along the eastern portion of the study area exerts through the Bone Spring Fm. Though the most distally located with respect to the shelf-margin break, the Maggie well enjoys stratigraphic height over the other two wells as seen in Figure 27. This is in large part due to the other two wells situation within localized,

inherited topographic depressions associated with the major fault zone running through the survey. More on this fault zone will manifest in the chapters below that include seismic interpretation.

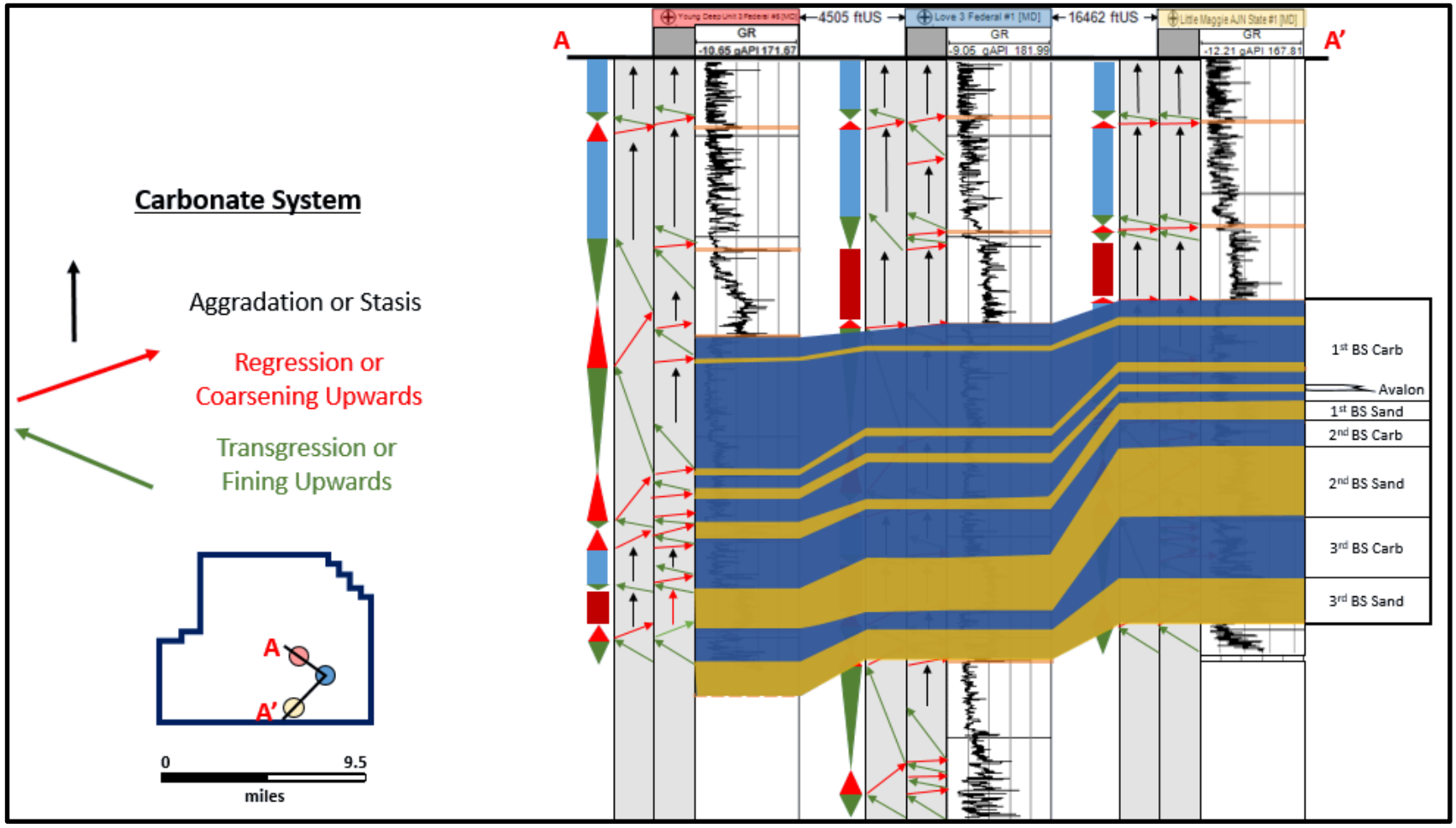

Figure 27: Fence diagram showing 3rd and 4th order adapted Galloway motifs interpretations. Blue shading on the GR curve corresponds to dominantly carbonate intervals while yellow shading corresponds to dominantly san intervals. Orange lines represent sequence boundaries and the respective Bone Spring fm. interval is marked to the right

The 4th order sequences correlate reasonably well between the wells, and as these wells lie within close proximity to one another. Within the 3rd Bone Spring Sand, two full 4th order sequences were mapped out. The sand was deposited on the top of the Wolfcamp as an unconformable surface as well as a 3rd order sequence boundary. The first sediments deposited within the 3rd Bone Spring Sand constitute lowstand deposits. Subsequent 4th order lowstands register as spikes in the gamma ray, likely from organic-rich shales.

The transition from predominately sand deposition to carbonate deposition at the 3rd Bone Spring Sand – 3rd Bone Spring Carbonate interface marks the first reversal in Galloway motif interpretation, such that low gamma intervals must needs be interpreted as cleaner carbonates deposited at highstands and higher gamma intervals thus interpreted as siliciclastics deposited during relative lowstands. Four complete 4th order cycles were interpreted in the 3rd Bone Spring Carbonate interval, though the overall signature suggests steadily increasing relative sea level. This follows logically, given the need for such conditions for sustained carbonate production and progradation to occur. The top of this interval corresponds to increasing gamma ray response and the onset of regression into the 2nd Bone Spring Sand.

The 2nd Bone Spring Sand is distinguished from its two counterparts by increased, sporadic carbonate input. All the same, from a 4th order cycles perspective, it appears simplistic, with only two full cycles. Perhaps the increased interval of relative sea level high proved sufficient to jumpstart carbonate production on the shelf, if short-lived in comparison to the Bone Spring Carbonate intervals. The top of this interval is marked by

transgression into high gamma silt and shale before giving way to lower gamma ray motifs equated with carbonates.

With the shift from siliciclastic to carbonate dominated deposition, the 2nd Bone Spring Carbonate develops a relatively thin transgressive carbonate highstand deposit before regressing into a more lowstand carbonate facies exhibiting increased gamma ray response. This is followed by another period of transgression before prominent regression initiates another period of siliciclastic deposition.

The 1st Bone Spring Stand is interpreted as being deposited entirely within one 4th order cycle. As such, it is unsurprising that this constitutes the thinnest Bone Spring Sand interval. The gamma ray response throughout remains blocky, suggestive of very little variation in the lowstand relative sea level. What spikes in the gamma ray response exist likely represent organic-rich shale drapes separating amalgamation surfaces caused by sediment gravity flows or channel migration.

The Avalon is a sand interval contained within the 1st Bone Spring Lime that has been interpreted as a 4th order lowstand deposit. After deposition of the Avalon sands, 3rd order transgression reinitiated carbonate deposition. The base of the upper 1st Bone Spring Lime enjoys a clean, blocky gamma ray response associated with highstand carbonate facies. This facies lies in the upper portion of the 1st Bone Spring Limestone interval before abrupt regression into the Brushy Canyon Fm. constituting a 3rd order unconformable sequence boundary.

Overall, application of the Galloway motifs from Pigott (2018) suggests that much of the internal character of the Bone Spring may be explained by 3rd order sequence stratigraphy, though remain best understood through the lens of 4th order cycles. These

4^{th} order sequences imprinted over the 3^{rd} order sequences highlight the patterns of reciprocal sedimentation that are visible throughout the Bone Spring Fm. Future studies that enjoy more robust well constraint should perform well correlation and subsequent mapping across the study area to better investigate trends in lithologic change that may be tied to 4^{th} order cycling in relative sea level.

Seismic Analysis

The final avenue of investigation for this study is the 3D seismic data that was provided by Schlumberger. Over the last two sections, a foundational conceptualization of Bone Spring Fm. deposition has been built using the adopted Galloway technique of analyzing gamma ray motifs. Through this analysis, excellent vertical resolution of sedimentation trends within the Bone Spring Fm. have been identified, and a sequence stratigraphic framework has been constructed. Now, the seismic data must be consulted and used to improve the lateral resolution of the investigation's interpretation. This section will discuss the picking of relevant horizons within the Bone Spring Fm., the creation of time structure and isochron maps, the seismic stratigraphic analysis conducted, and will conclude with an attempt to tie the adapted Galloway sequence stratigraphic motifs to the seismic.

Horizons, Time Structure Maps, and Isochrons

Before any horizons picking could be performed, the seismic well-tie had to be performed. This process served the dual purpose of allowing for domain conversion from two-way time (TWT) to depth (ft) and tying the petrophysical data contained within the well logs to the corresponding seismic reflectors. The paucity of synthetic ties ultimately

limits the accuracy of the interpretation of the horizons relevant to Bone Spring deposition and persists as an area which may be improved upon in future work. As is standard in the industry, horizon picking was postponed until major structural features within the seismic data that might affect that process were delineated. Small faults, apparently discrete fracture networks within the carbonate complex arising from syndepositional deformation (i.e. compaction), are observed throughout the survey, and remain too small to impact horizon picking. As such, the major fault zone that trends generally NE-SW along the eastern-most portion of the one major fault zone, though identified and mapped along the eastern side of the study area, does not manifest in Figure 38 below.

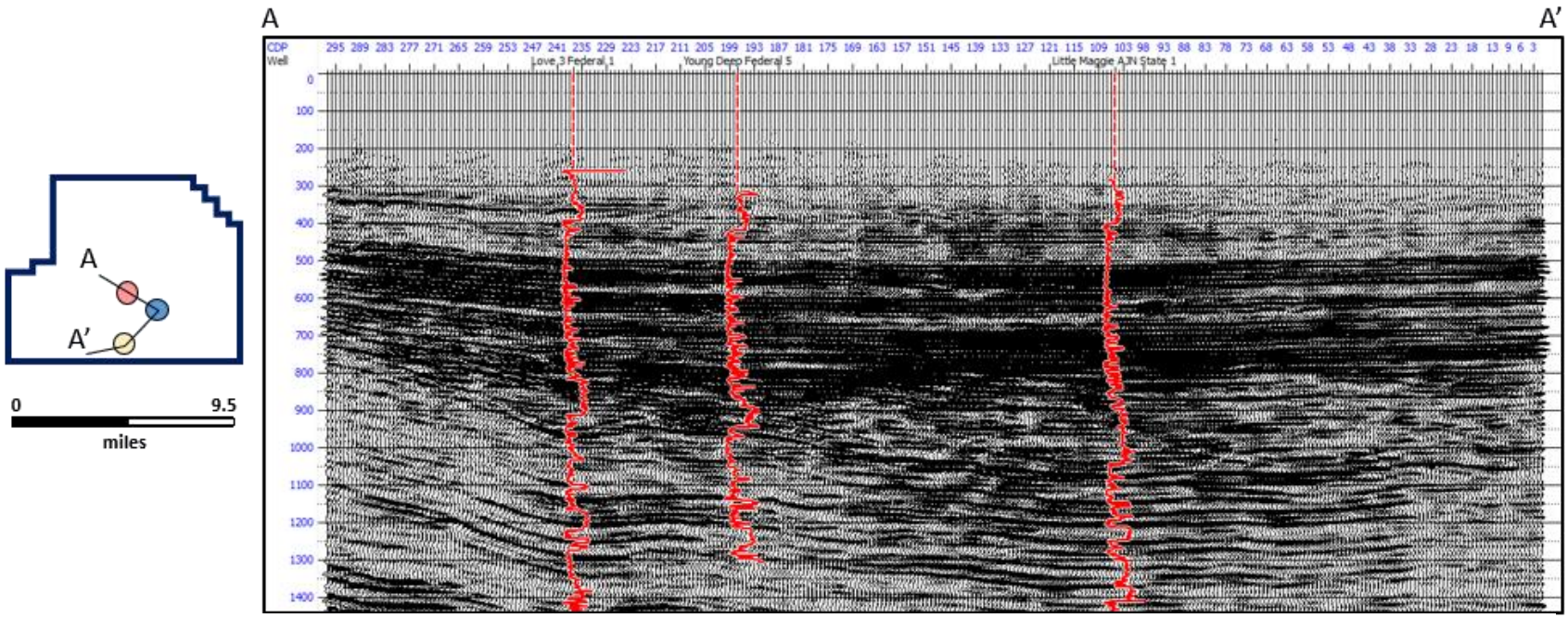

Figure 28: Arbitrary dip line A – A' through the study area, showing easily recognizable seismic reflector mirroring of prominent trends in the gamma ray response of the visible well logs (red).

Figure 28 highlights the utility of integrating petrophysical data, in this instance gamma ray response, with seismic data, as the trends seismic reflectors become much more readily accessible. Reflectors marking the top of the Wolfcamp Fm., the Bone Spring Fm., and the Brushy Canyon Fm. stand out prominently. Within the Bone Spring reflectors marking the top of each change in dominant lithology can be picked out with relative ease.

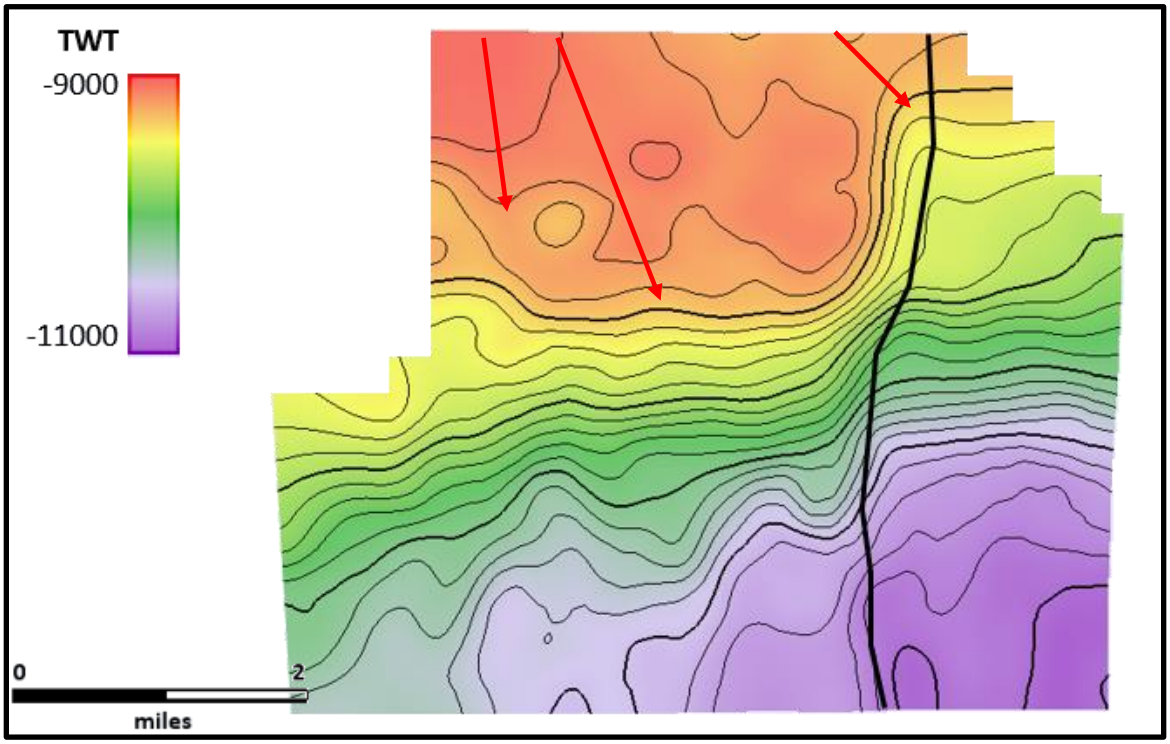

Figure 29: Time structure map in two-way time in ms (TWT) on the top of the Wolfcamp. This surface represents the base, or inherited topography, of the Bone Spring Fm. and therefore exerts a control on its subsequent deposition. The red arrows represent potential sediment transport pathways that could have acted as incised canyons feeding sediment into the basin. The black line to the right illustrates the picked fault zone.

Figure 29 shows a time structure map on the top of the Wolfcamp. The major fault zone running through the study area is highlighted in black and valley like structures running perpendicular to depositional dip are highlighted with red arrows. Structure mapping via well log and seismic stratigraphy previously showed far less detail than what is shown above. It was postulated that sediment transport pathways, likely incised valleys, would be seen running perpendicular to depositional dip. The Wolfcamp time structure map shows some evidence of these valleys. Three potential valleys may be seen on the structure map separated by ridges. This inherited topographic imprint upon sedimentation patterns will continue to be evidenced in isochron maps of younger Bone Spring Fm. intervals, and their full impact may be observed below via annotated horizon probes, co-rendering dip magnitude and seismic dip (Appendix IV.1-4). Though the valleys observed at the Wolfcamp level vary from those observed in subsequent, shallower structure maps, the shelf morphology mirrors closely that exhibited above though with marked progradation seen, and with evolving accommodation space upon the shelf, some migration of the incised valleys is to be expected. Crosby (2015) and Bickley (2019) contend that these valleys were likely influenced by the natural spur and grove topography of the shelf carbonates with incised valleys preferentially forming in the carbonate groves, and this study offers further validation to that assertion. Preferential deposition resulting from structurally derived topographic lows may also be seen on the structure maps. Two prevailing structurally high trends dominate the study, the E-W trend of the shelf to the north, and the N-S trend following dendritic patterns mirroring those seen in river systems or reef spur and groove geomorphologies. The highest topographic gradient occurs along the fault zone, which appears to exert decreasing, yet

persistent, control on Bone Spring Fm. deposition over time. Generally, sediments thin over the structural highs and thicken southward in the basin, though subsequent isochron maps show that sediment accumulation upon the shelf in topographic lows does occur.

3rd Bone Spring Sand

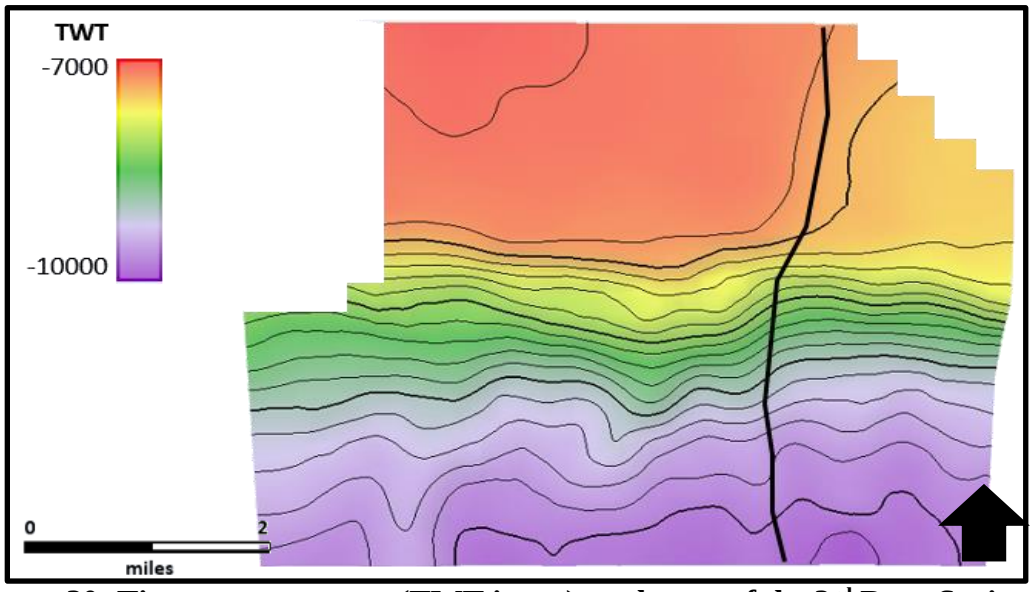

Figure 30: Time structure map (TWT in ms) on the top of the 3rd Bone Spring Sand

2nd Bone Spring Sand

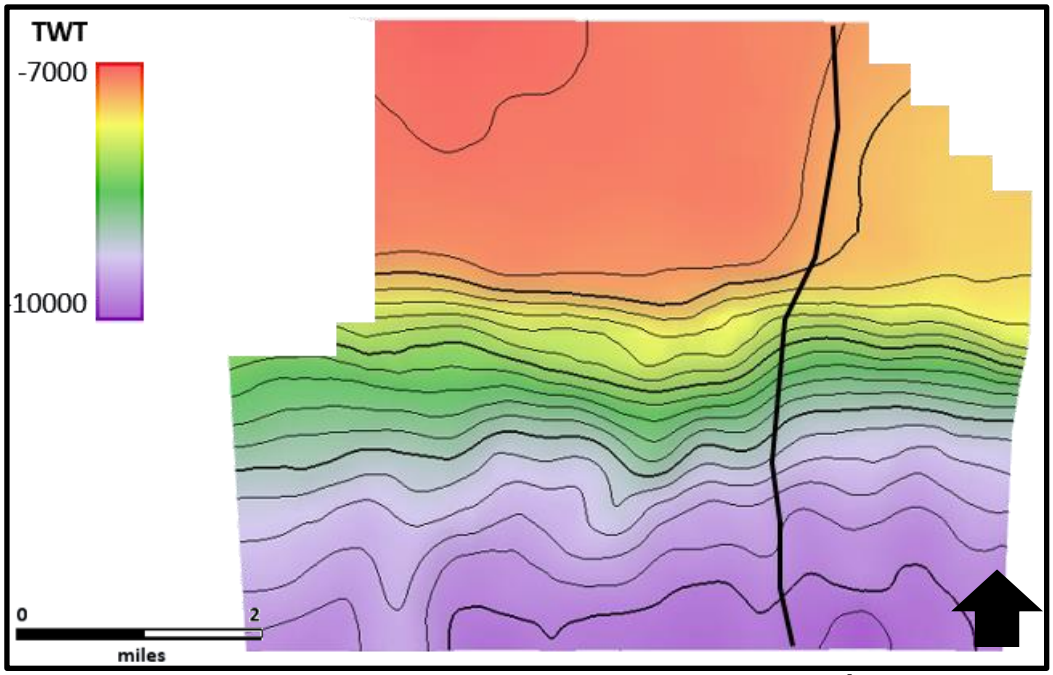

Figure 31: Time structure map (TWT in ms) on the top of the 2nd Bone Spring Sand.

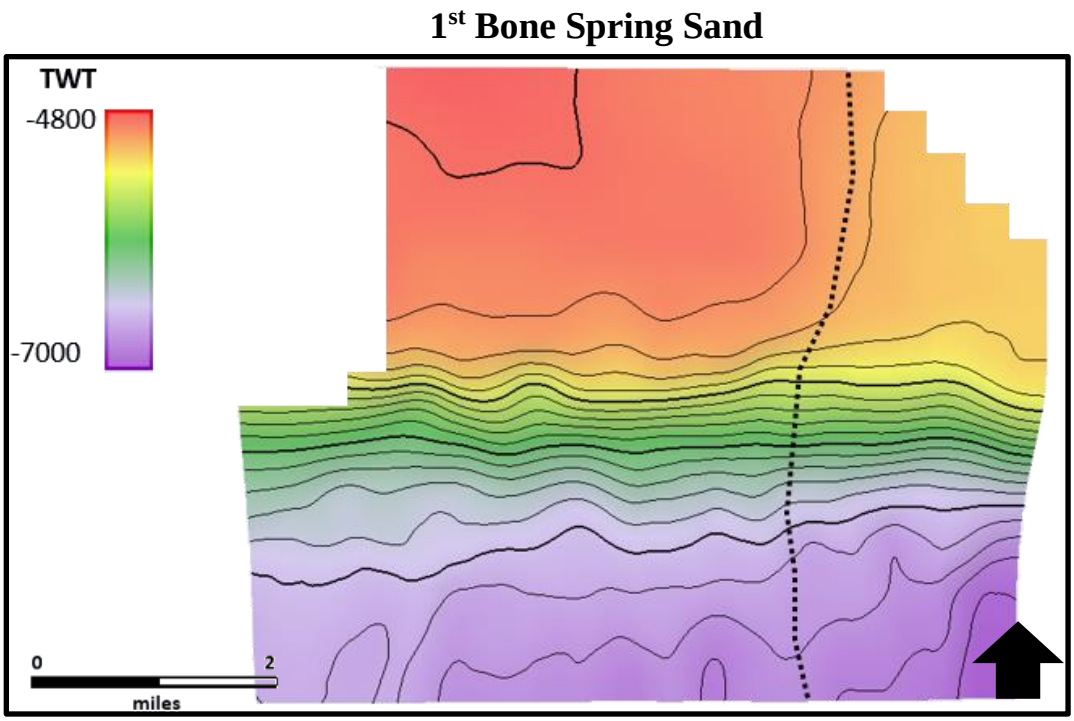

Figure 32: Time Structure map (TWT in ms) on the top of the 1st Bone Spring Sand.

Figures 30-32 show the time structure maps on the tops of the prominent sand intervals of the Bone Spring Fm. that were picked. The incised valleys mentioned above may be somewhat inferred from contour lines. Additionally, the major fault system on the eastern side of the survey continues to influence topography, though decreasingly though time, up into the 1st Bone Spring 3rd order sequence.

Figures 33-35 show the isochron maps made from these internal Bone Spring horizons. The isochrons represent the same intervals as the isopach maps shown earlier in the time structure maps. Interestingly, all of the isochron maps show significant lowstand deposition and sediment bypass. Depositional trends within the basin, though, conform to expected patterns of sedimentation according to accommodation space

afforded by spur and groove topography, with southward thinning away from the shelf-slope margin.

3rd Bone Spring Sand

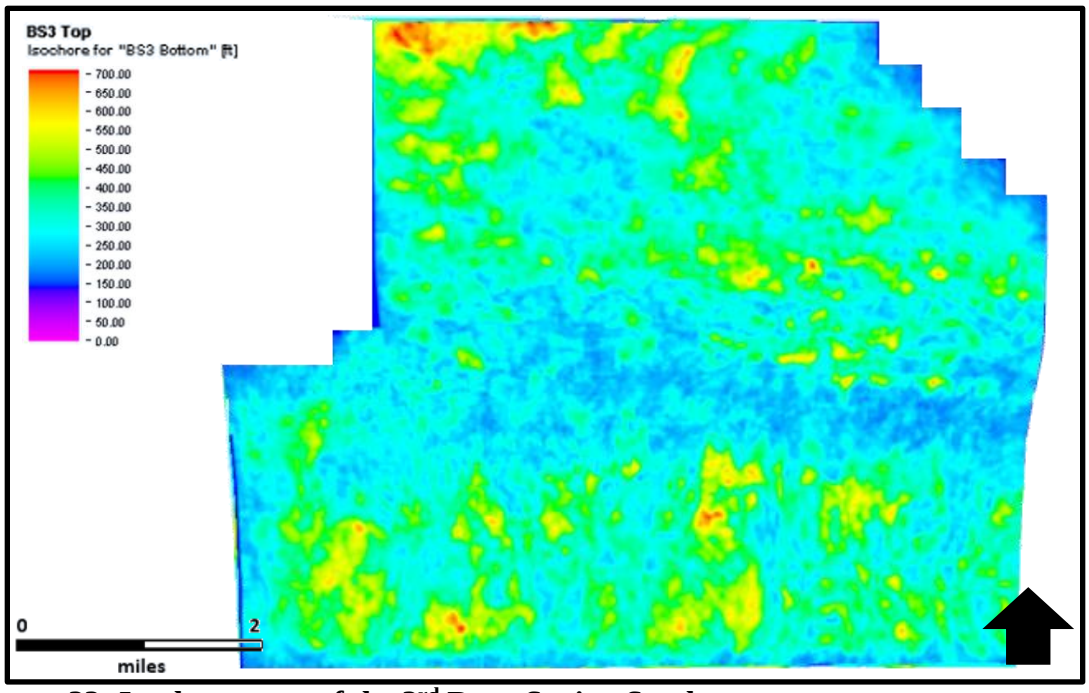

Figure 33: Isochron map of the 3rd Bone Spring Sand.

2rd Bone Spring Sand

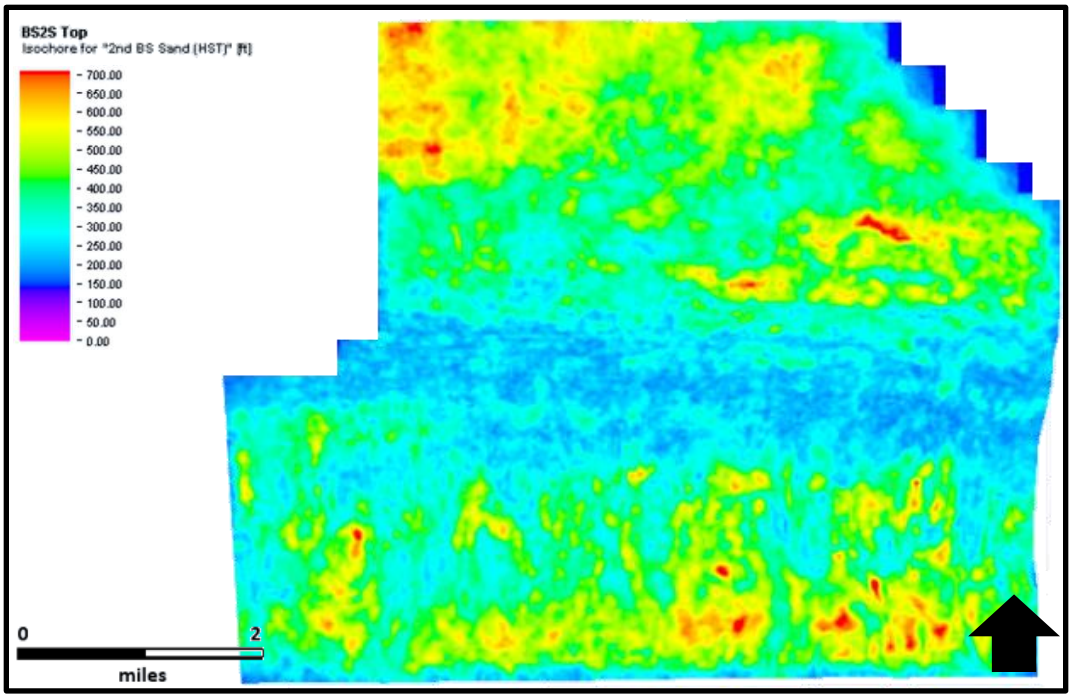

Figure 34: Isochron map of the 2nd Bone Spring Sand.

1st Bone Spring Sand

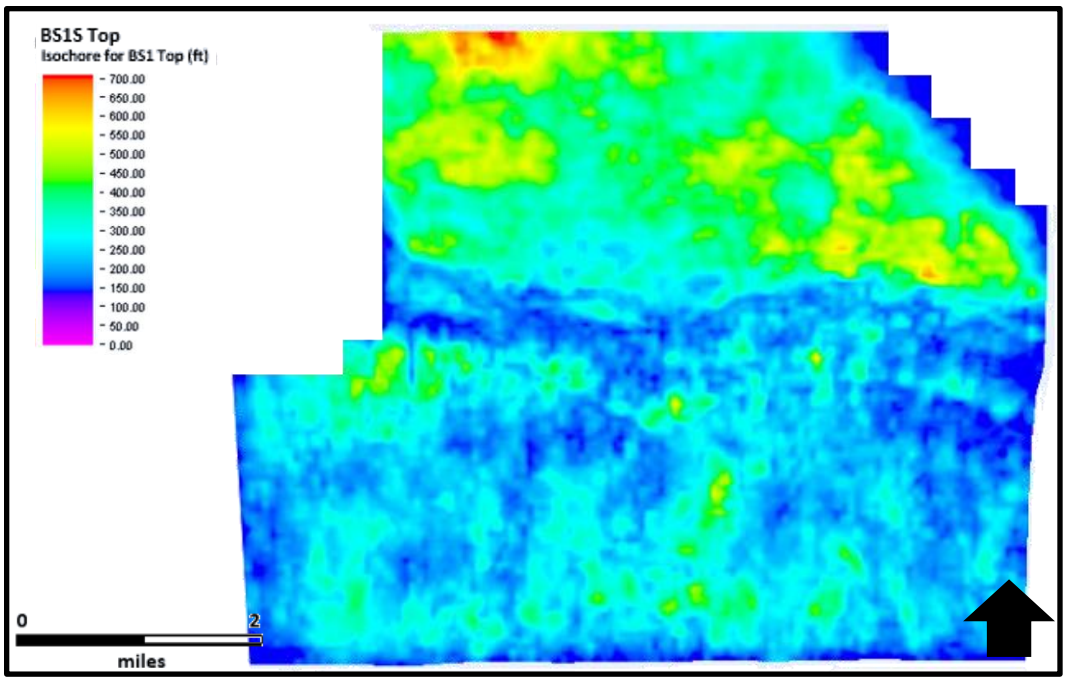

Figure 35: Isochron map of the 1st Bone Spring Sand.

Figure 36 below shows the 3rd Bone Spring Sand isochron map alongside a time slice from the survey at a corresponding depth. Note the similarities between the spur and groove patterns visible in the coherence volume (top) and the sedimentary packages of the basinal Bone Spring Fm. visible in the isochron map (below). Apparently, deposition of the Bone Spring Fm. in the basinal setting is largely by accommodation space created by the ridge-valley topography characteristic of carbonate spur and groove architecture. In general, the valleys or grooves align with trends of greater thickness in the 3rd Bone Spring Sand, and in the other intervals, suggesting that spur and groove architecture doubled as sediment transport pathways during Bone Spring Fm. deposition.

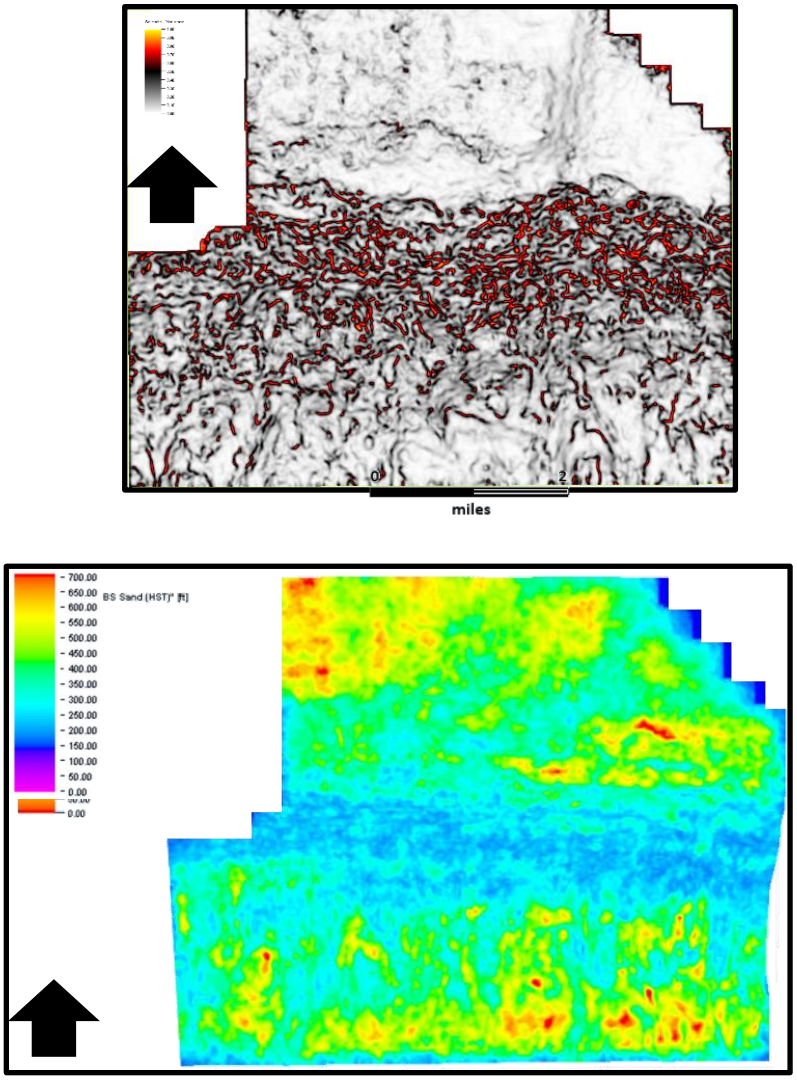

Figure 36: Comparison of time slice (-7050ms TWT) showing variance attribute (top) to the isochron of the 2nd Bone Spring Sand (bottom) to highlight the mirroring of compensational sedimentation according to available accommodation space with the topographic profile created by spur and groove architecture.

The depositional model discussed above constitutes a departure from that expected to be on display in this study area. That is, the conventional lowstand, bypass of siliciclastic sediments into the basin and eventual deposition into lobate, turbidite deposits or apron fans as modeled by Li et al. (2015) in Figure 37 and confirmed by

Crosby (2015) and Bickley (2019). Therein, valley incision occurring through carbonate reef structures results in sediment transport from across the shelf and into basin floor aprons via sediment flows or MTDs, wherein sediment remains thickest proximal to the toe of slope and thins rapidly in the basinward direction. Such a model is widely accepted, and has been proven across many basins worldwide, yet this author believes that it fails to account for the ultimate depositional result of such gravity-driven, submarine flows across highly scoured basal surfaces rife well-defined depositional highs

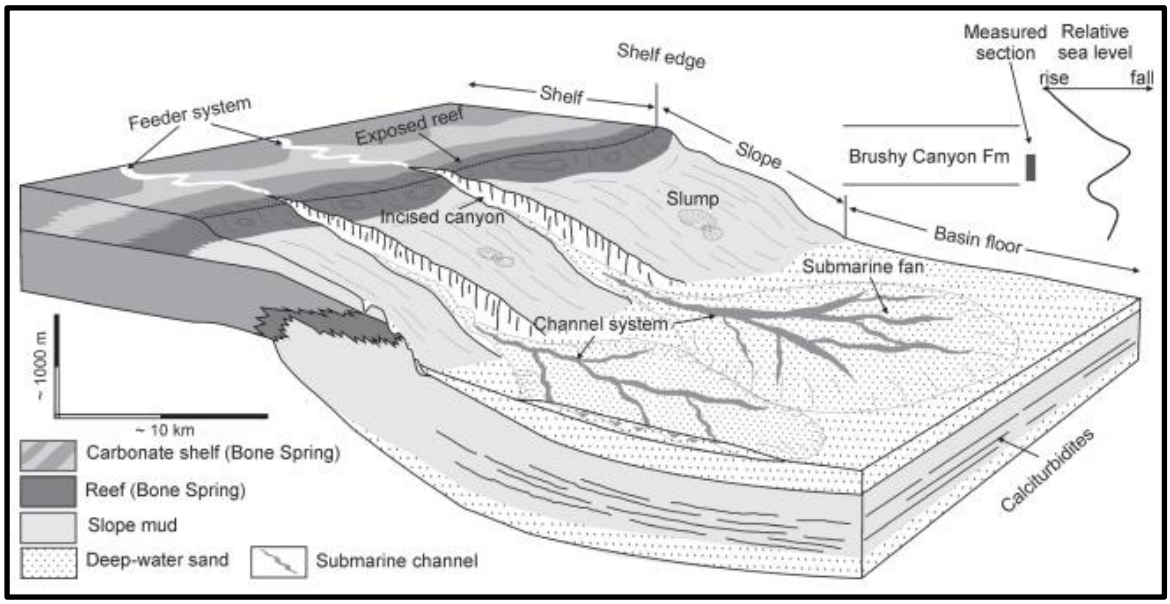

and lows.

Figure 37: Illustrative model done by Li et al. (2015) representing expected depositional processes for sedimentation occurring during the Bone Spring Fm.

Another interesting aspect of sedimentation within the survey is the response shown with respect to the fault zone that cuts through the eastern portion of the study along a general NE-SW trend. The 3rd Bone Spring Sand isochron shows active sedimentation across the margin of the fault zone derived depression and thick deposition in the depositional low therein on the shelf. The 2nd Bone Spring Sand isochron shows

no active sediment pathways crossing the fault zone, but with sediment thickness still present in the depression. This suggests possible sediment sourcing from the east-northeast. By the time of the 1st Bone Spring Sand, expression of the fault zone is minimal, and appears to exert no control over sediment deposition. Building upon this realization, horizon probes displaying RMS Amplitude as an indicator of porosity, and subsequently dolomitization, after Pereira (2009) and Sarhan (2012) were generated and used to interpret facies distribution. The resultant interpretation matches closely with the classical facies distribution model established by Wilson (1975), and may be seen below (Appendix V.1-2).

Considering the time-structure maps and the isochrons of the 3rd, 2nd and 1st Bone Spring Sand intervals, the depositional model proposed by Li et al. (2015) and championed by both Crosby (2015) and Bickley (2019) fails to satisfactorily account for the observed trends in deposition. The marked difference in proximity of the activel prograding carbonate complex in this study as when compared to those of Crosby and Bickley perhaps plays a fundamental part in this departure. Active reef complexes develop spur and groove architecture, most pronounced proximal to the slope margin, as is visible in this study. Proximity to the carbonate complex may equate to more carbonate material in this case, which might provide a mechanism by which the spur and groove architecture in this study might enjoy more pronounced gradients in its topographic profile. Higher highs and lower lows, topographically speaking, would have a greater impact on the accommodation space available, and thus heighten the role of such architecture in basinal depositional processes. A proposed depositional mechanism providing further insights into the cyclic, alternating carbonate – siliciclastic

sedimentation observed in the Bone Spring Fm., as well as the compensational stacking patterns, may be found below (Appendix VI.1-5).

Seismic Stratigraphy

With the depositional model reasonably validated using seismic time structure maps and isochron maps, seismic stratigraphic analysis was performed using the integrated well log and seismic reflection data. Terminations were picked across seismic crosslines that intersected well locations where gamma ray logs might be overlain onto the reflection data so as to provide some interpretational constraint. These terminations are shown on the seismic in Figures 38-40 below.

Figure 38: Seismic sequence stratigraphic terminations delineated on Xline slice shown on survey map. Yellow arrows represent top terminations while red arrows represent bottom terminations.

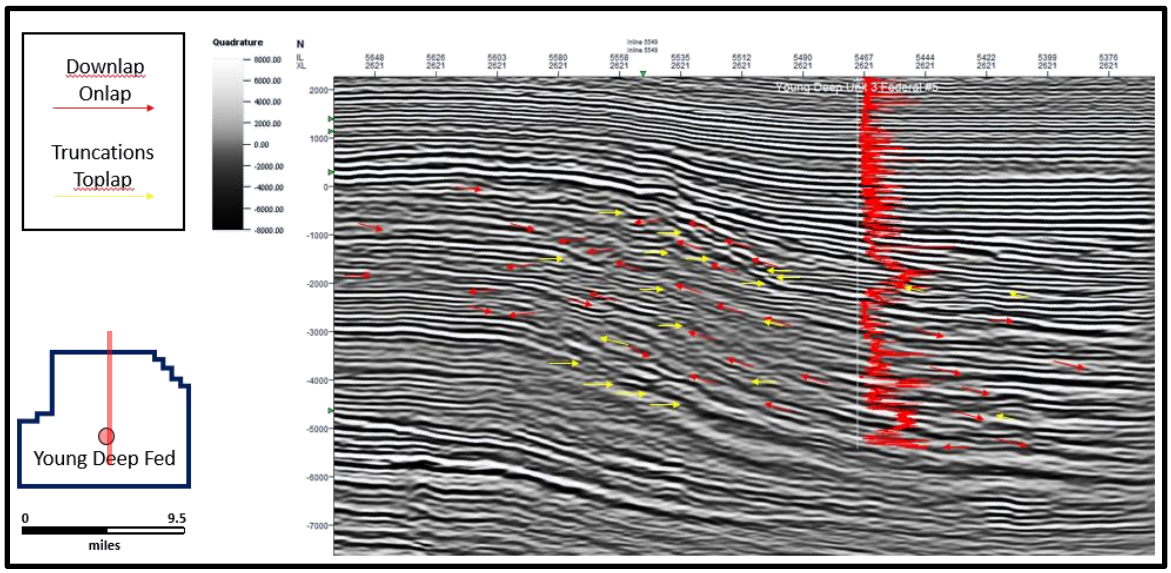

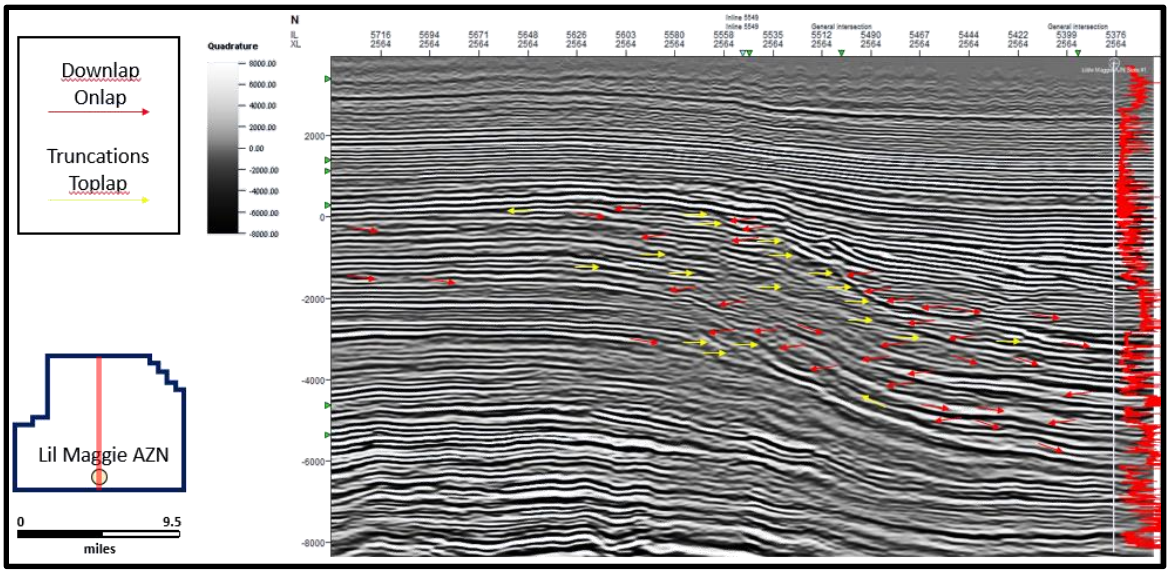

Figure 39: Seismic sequence stratigraphic terminations delineated on Xline slice shown on survey map. Yellow arrows represent top terminations while red arrows represent bottom terminations.

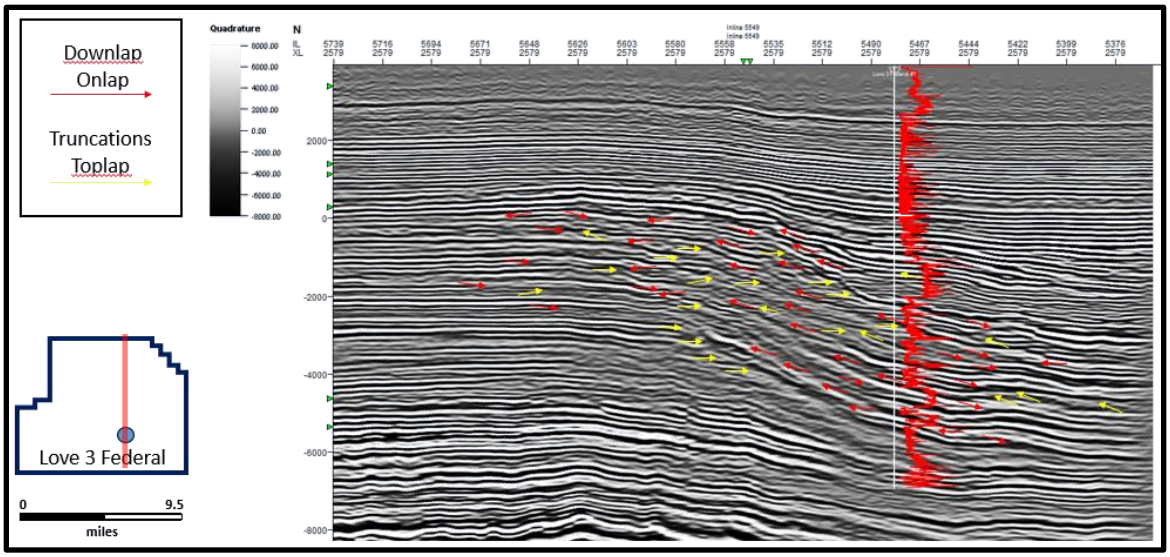

Figure 40: Seismic sequence stratigraphic terminations delineated on Xline slice shown on survey map. Yellow arrows represent top terminations while red arrows represent bottom terminations

Due to the nature of onshore seismic data, both the higher complexity of strata geometries that may be found there as well as the tendency towards compromised seismic acquisition quality, terminations can be much more difficult to pick with onshore data than offshore data. Still, upper and lower terminations can be picked identifying the four 3rd order sequences of the Bone Spring Fm. and are recognized as those boundaries that host two or more termination types. As expected, the sequence boundaries within the Bone Spring interval line up with the tops of highstand carbonates, with most terminations throughout the Bone Spring Fm. being either toplap or downlap in nature, though along onlap surfaces truncations are also in evidence.

Toplap terminations associated with erosional truncation are observed at both the top of the Wolfcamp-Bone Spring sequence boundary as well as at the Bone Spring – Brushy Canyon boundary. Complicating the recognition of termination patterns somewhat is the pattern of downlap and onlap terminations that have been recognized scouring surfaces caused by mass transport deposition, and which highlight the highly scoured basin floor that allowed for amalgamation of lowstand sand intervals. With this analysis not only confirming but exceeding the four third order sequences within the Bone Spring observed using well log sequence stratigraphy, an attempt to compare higher order sequence stratigraphy was carried out.

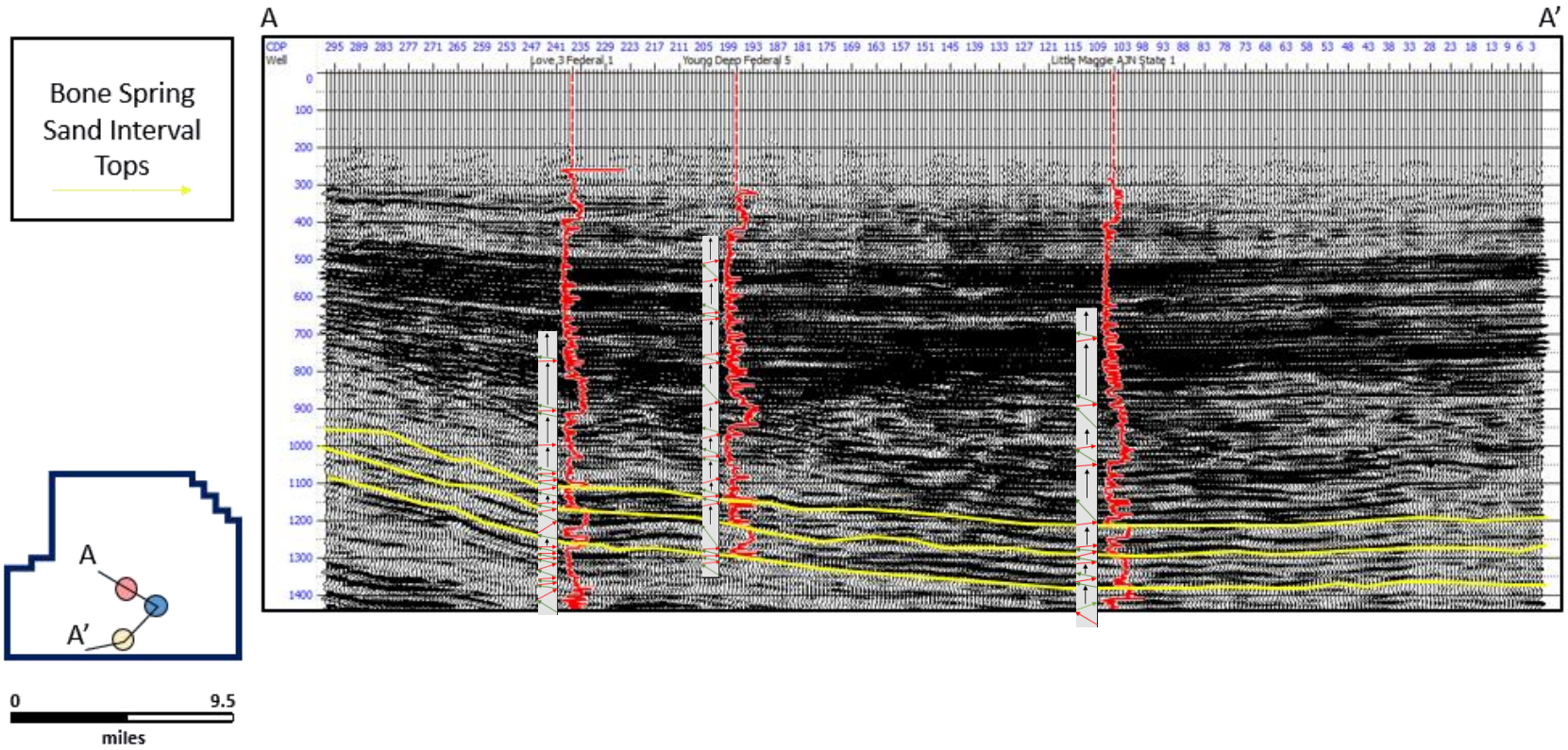

Figure 41: Arbitrary line A–A ‘ . Yellow lines represent the picked sand horizons within the Bone Spring interval. Overlain arrows are the adapted Galloway motifs determined from well logs. Red logs are GR logs. From this initial sequence stratigraphic framework, the seismic sequence stratigraphic framework was built.

Figure 41 illustrates an attempt to overlay the adapted Galloway sequence stratigraphic motifs with the seismic. Yellow lines on the seismic represent the major internal Bone Spring horizons picked across the survey. The overlay was created manually by correlating the adapted Galloway motifs from gamma ray response in the well logs with synthetic seismic logs that were then tied to the actual reflection data of the 3D survey. The red logs shown here are gamma ray response, which allow an accurate translation of these motifs to the seismic given the adopted Galloway approach of this study. Overall, these overlain motifs heighten the accuracy in interpretation of the reflectors within the Bone Spring intervals, which are characteristically chaotic. While these reflectors generally look fairly chaotic due to the matt transport complexes, the overlain Galloway provide some constraint to the interpretation of the seismic reflectors.

Many of these 4^{th} and 5^{th} order parasequences can only be seen through overlay of the adopted Galloway motifs, as they often fall beneath seismic resolution. Most readily accessible for interpretation are the carbonate highstand deposits and the onlap surfaces that developed with the rapid carbonate deposition on the shelf. Within the sand intervals, the maximum flooding surfaces provide the best correlation, and offer some welcome slide-to-slide validation to the seismic sequence stratigraphic surfaces given the chaotic nature of the seismic data. Recognizing this, it seems good practice to reverse engineer the seismic stratigraphic framework by building out from the well bore, and its gamma ray log, as a means of the QC'ing the interpreted stratal packages delineated by reflector terminations.

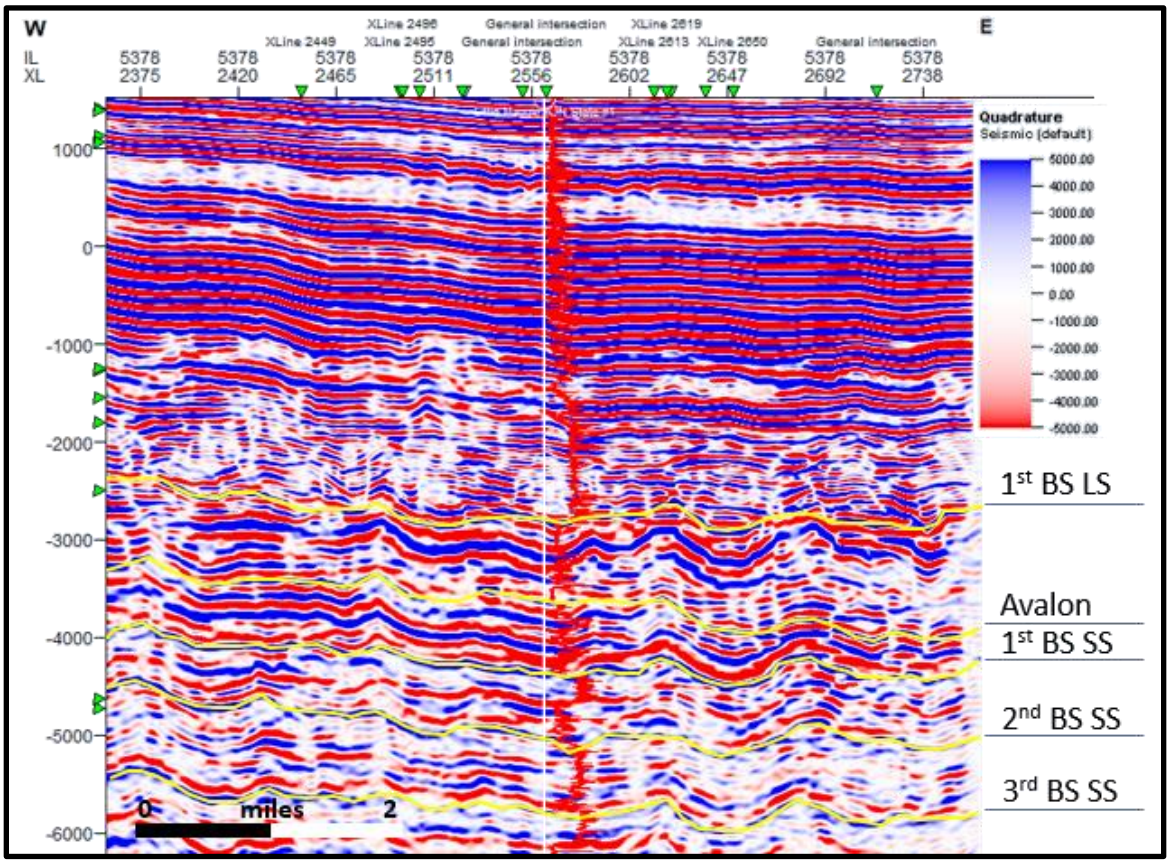

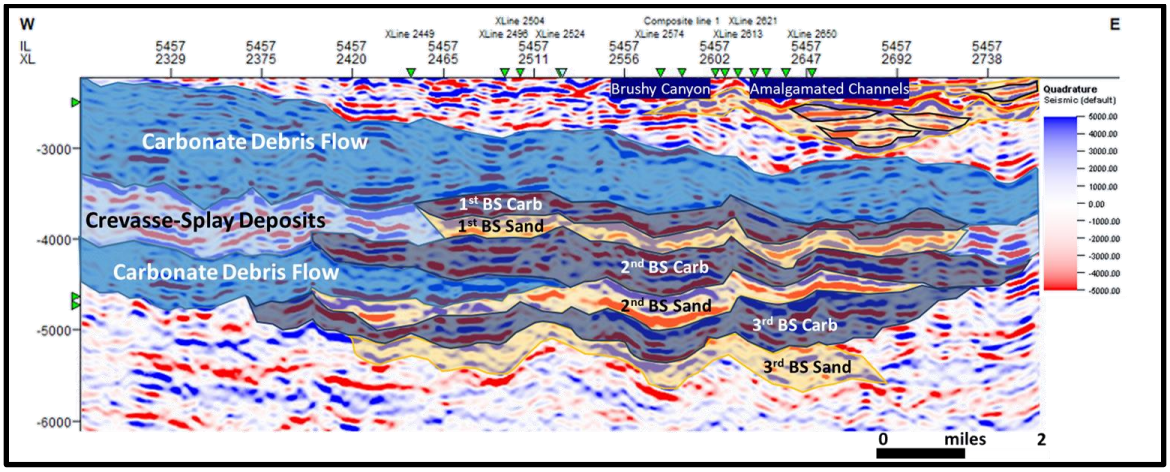

Figures 42 (above) and 43 (below): Zoomed in view of Inline seismic slices that show seismic facies interpretation of depositional architecture, including MTDs, channel-fill, and crevasse-splay deposits within the Bone Spring Fm. interval. Figure 43 is included in the Appendix, Appendix VII, in enlarged fashion.

Figures 42 and 43 above show a zoomed in Inline seismic slice, providing insights into the depositional architecture on display within the Bone Spring Fm. interval. The Bone Spring Fm. sand intervals are highly channelized within grooves created by topographic ridges that apparently constitute spur-carbonate buildups. To the flanks, chaotic reflectors, with sporadic strong reflector packages, constitute carbonate MTDs and detrital boundstone blocks contained therein. The erosional surfaces of these carbonate MTDs correspond with red peaks, as is expected given the polarity scheme, and also are marked by toplapping terminations along their bottom. The channelized sands pinch-out laterally at the meeting of amalgamation surfaces which developed in response to compensational stacking.

Overall, the seismic analysis done in this study refined the depositional model of the Bone Spring largely because of the excellent resolution, horizontal and vertical, afforded by the integrated Vail-Galloway approach utilized in this study. More specifically, this investigation proposes a mechanism by which MTDs and sediment gravity flows act as a vehicle by which the alternating cycles and compensational stacking patterns inherent to reciprocal sedimentation models is achieved (Appendix VI.1-5) The structure and isochron maps highlighted sedimentation pathways during Bone Spring Fm. deposition and provided evidence for basinal depositional processes by exposing the dendritic, spur and groove patterning. In addition, seismic stratigraphic analysis helped to confirm the 3rd order sequence boundaries observed within the Bone Spring, while 4th and 5th order sequence boundaries exposed areas where seismic

resolution alone failed to capture the full stratigraphic picture of Bone Spring Fm. deposition. As such, comparison of the seismic data to these 4^{th} and 5^{th} order adapted Galloway motifs allows for a more detailed interpretation of depositional features shown on the seismic.

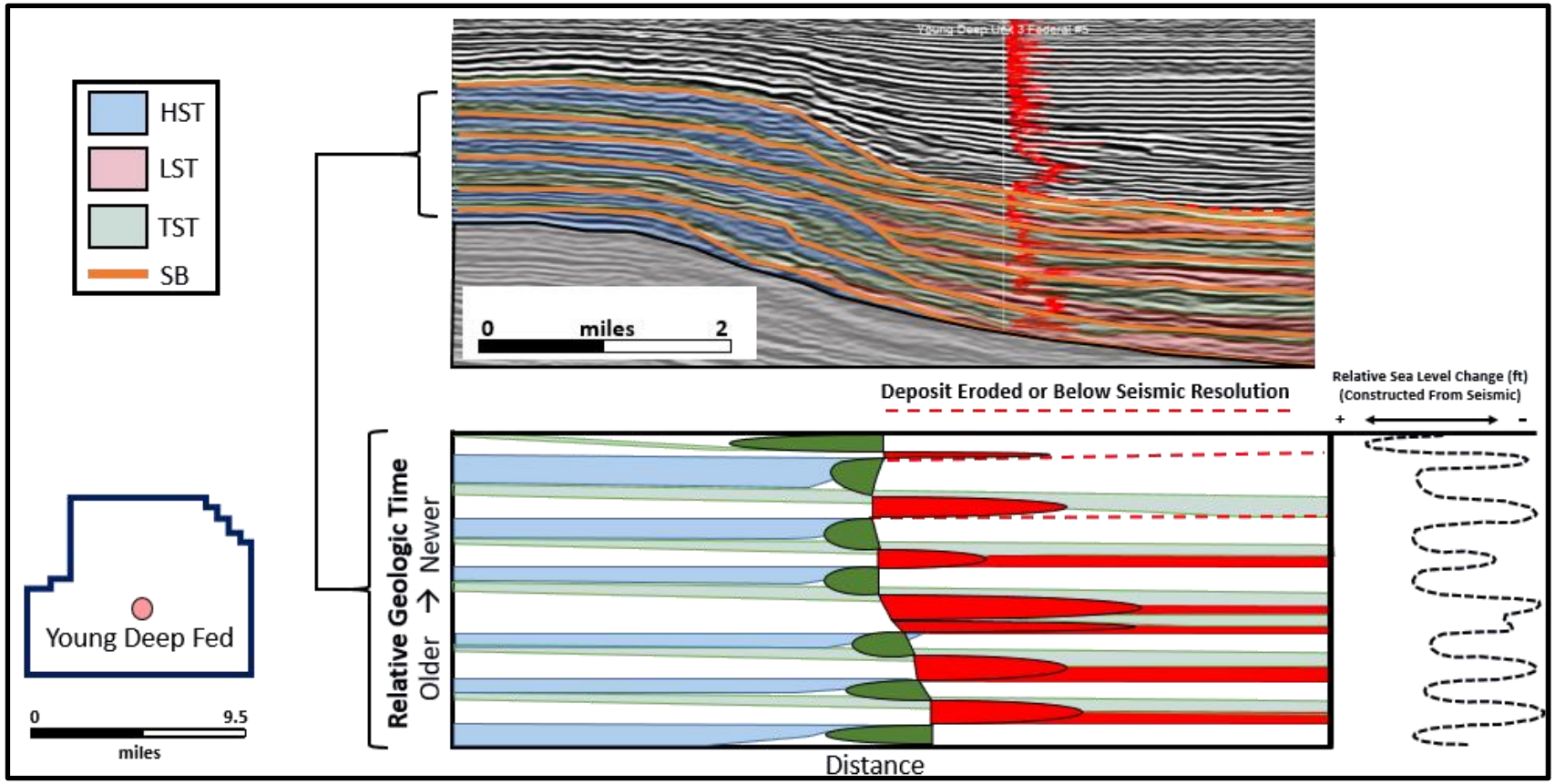

Figure 44: Chronostratigraphic model and reconstructed relative sea level curve derived from the sequence stratigraphic framework.

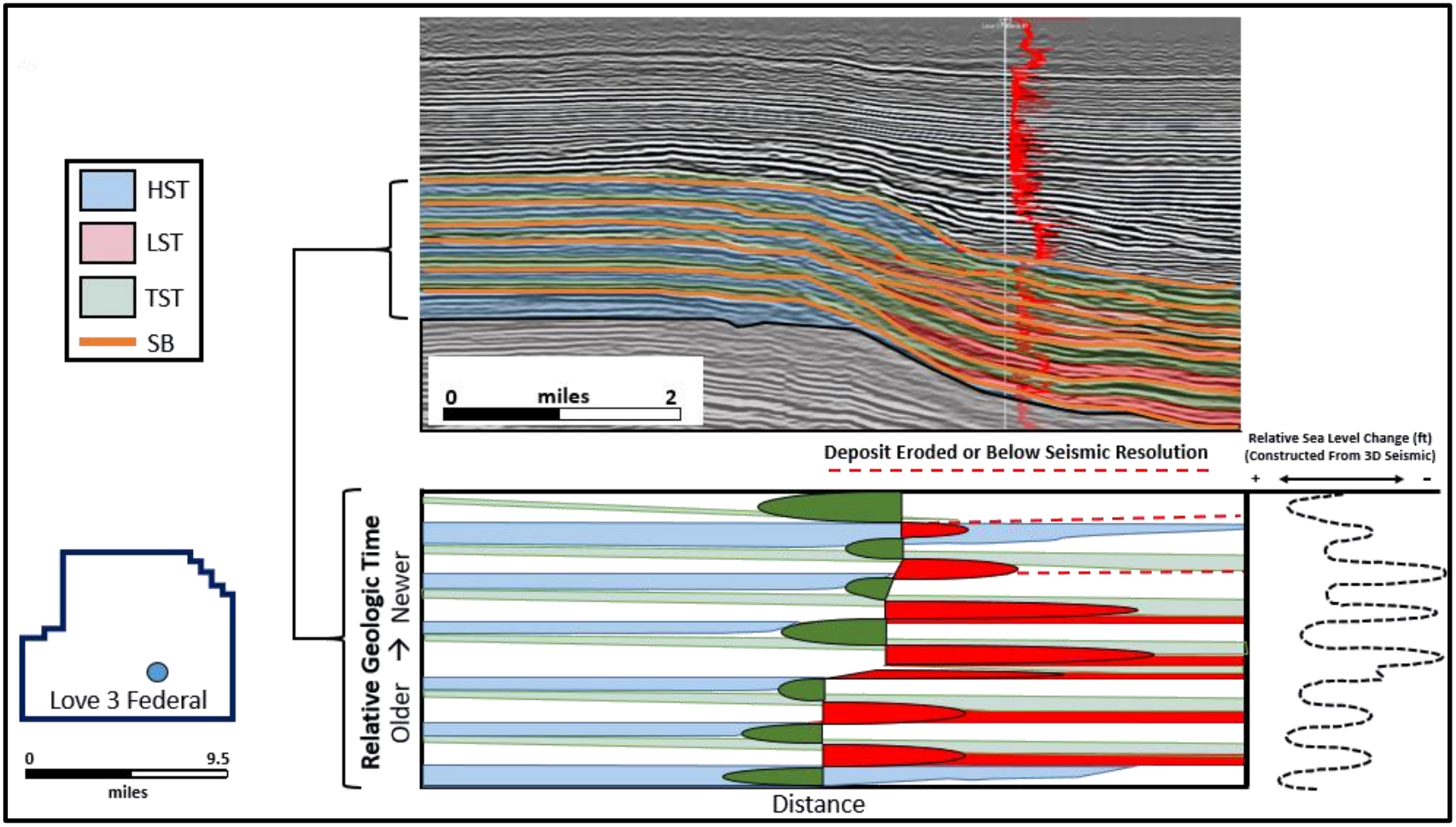

Figure 45: Chronostratigraphic model and reconstructed relative sea level curve derived from the sequence stratigraphic framework.

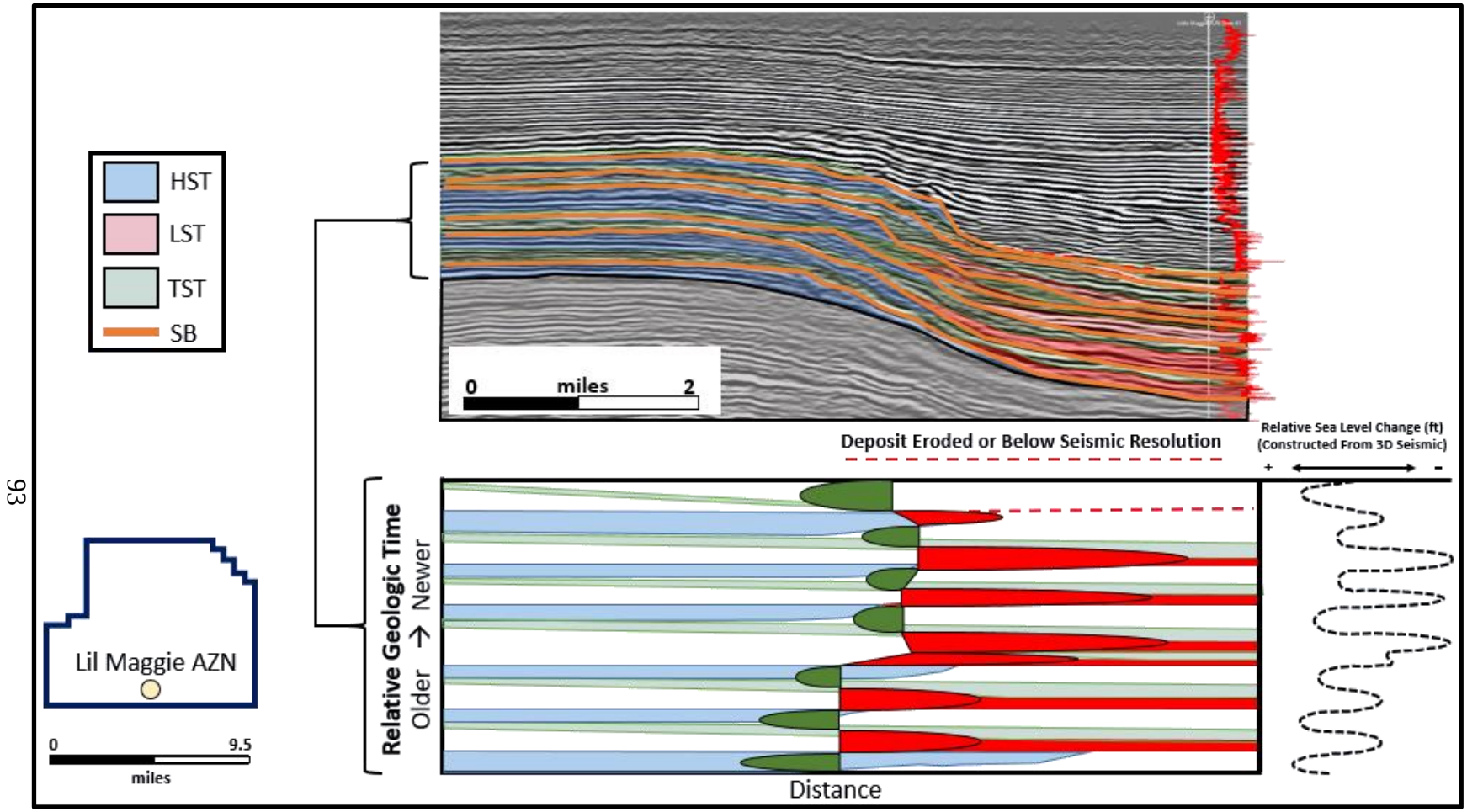

Figure 46: Chronostratigraphic model and reconstructed relative sea level curve derived from the sequence stratigraphic framework.

The chronostratigraphic models (Figure 44-46) above were constructed from the seismic sequence stratigraphic framework according to the methods of Radivojevic and Pigott (2010) and afforded the reconstruction of relative sea level curves according to the relationships between sequence boundary surfaces within. As seen in Figure 57, the Haq et al. (2008) eustatic curve shares notable similarities to the relative sea level curves generated in this study, such as an overall 6 highstand-lowstand cycles during Bone Spring Fm. deposition. The differences between the two curves may be understood as the difference between autochthonous and allochthonous processes unique to the Northwestern Shelf and N. Delaware Basin during this specific time period; processes that governed over depositional processes, and thus reflect in the relative sea level curve derived from the sequence stratigraphic model of which those depositional processes lie at the very heart. That is to say, at least some autochthonous, or extra-basinal process control on sedimentation is observed due to the similarities in the relative and eustatic sea level curves, but the differences highlight, too, the apparent role of allochthonous controls on sedimentation.

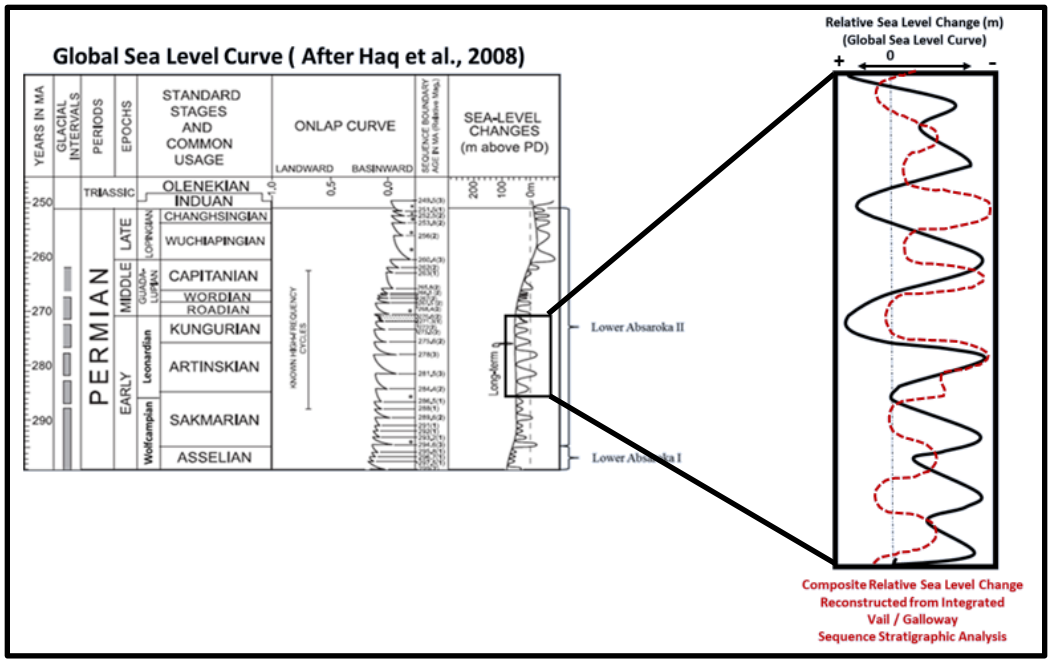

Figure 47: Comparison of the Haq et al. (2008) eustatic curve during the Leonardian and Bone Spring Fm. deposition to the reconstructed composite relative sea level curve from this study. Similarities and differences suggest interplay between auto- and allochthonous control over depositional processes. Solid black line represents the Haq et al. curve and the dashed red line represents the relative sea level curve inferred from the chronostratigraphic interpretation.

Chapter 7: Conclusions

Conclusions

Using well logs and seismic data this study investigated depositional processes of the Bone Spring Fm. towards the end of constructing a high-resolution (vertical and lateral) integrated Vail-Galloway sequence stratigraphic framework. Once constructed, that sequence stratigraphic framework provided penetrating insights into the governing controls on sedimentation, which in turn allowed validation or contradiction of

depositional models as responsible for the observed Bone Spring Fm. Only by using all of the available data in an integrated manner was the full potential of both this investigation and the sequence stratigraphic framework realized. Sequence stratigraphy from well logs allowed for the identification of 3rd and 4th order sequences within the Bone Spring at excellent vertical resolution. The orders were determined using an adapted Galloway technique that accounted for the reciprocal sedimentation model wherein carbonate-siliciclastic deposition cycles according to both relative sea level and accommodation space. Finally, seismic analysis confirmed the 3rd order sequences and even some of the 4th order sequences identified from the well logs. Seismic structure maps and isochrons further refined the depositional model by identifying sediment supply pathways, i.e. spur and groove topography, and structural controls, i.e. inherited topography heavily influenced Laramidian extensional deformation, on deposition as well as identifying trends in sedimentation. Positive correlation of 3rd and 4th order sequences identified exclusively from well logs and then subsequently tied to and confirmed in the seismic data proves the concept of integrated Vail-Galloway sequence stratigraphic interpretation as both valid and worthy, capable of providing means towards achieving a more accurate and higher resolution interpretation combination of these tools allows for a more detailed interpretation of the seismic data. Below is a summary of some of the major findings of this study.

- 3rd order sequences in the study area were mapped across the survey and confirmed as exerting primary control over highstand carbonate and lowstand siliciclastic deposition.

- More detailed analysis using adapted Galloway motifs determined that 4th order within the Bone Spring interval also exert levels of control that help explain the complex changes observed within 3rd order sequences. Explaining these complex changes will have impacts on well planning and development of the Bone Spring because it helps to identify minute vehicles within the sequence stratigraphic framework for facies distributions within the Bone Spring.
- Integrating the interpreted 4th order sequences with the seismic data vastly improved interpretation of the reflector terminations.
- Seismic time structure and isochron maps proved valuable resources for identifying major structural features, depositional architecture, and providing penetrating insights into the importance of inherited topography as an overarching control on deposition within the Bone Spring Fm.

Overall, this investigation provides a refined sequence stratigraphic depositional model of the Bone Spring with immediate pertinence to the ongoing development of this unit in this study area as well as in other locations. The depositional model created through this investigation may serve as tool for implementing more efficacious well planning and drilling operations, while also laying the groundwork for future study of the Bone Spring Fm. Even more, a previously undocumented LST deposit was identified in the integrated sequence stratigraphic model, designated as 4.5 (shown in red) in the modified stratigraphic model (Appendix VIII). More thorough investigation of this potential LST deposit is in order, ideally aided by the

addition of not only greater well control (both greater well density and more robust array of petrophysical logs), but also through analysis of core and/or cuttings data.

Recommendations for Future Work

The biggest constraint to this investigation was the paucity of suitable well log data. Given the excellence of the 3D seismic available through Schlumberger for this study area, it remains imperative that more in-depth investigations that are not so constrained take place in the future. Some recommendations are:

- Higher resolution sequence stratigraphic analysis for each individual Bone Spring formation, as this study took a broader approach with the intent to construct an overarching sequence stratigraphic framework for the Bone Spring Fm. in its entirety.
- Seismic facies analysis and inversion may be done in order to realize the ultimate potential of the seismic data, especially if integrated with well data and subjected to machine learning techniques so as to gain insights into trends in minerology, diagenetic evolution, porosity construction/destruction as well as other important reservoir parameters.
- Analysis of the evolution of carbonate highstand reef slopes and investigation of correlations between onlap surface angles and observed trends in sedimentation and depositional architecture within the basin.
- Further investigation into the efficacy of RMS Amplitude as a predictor of dolomitization within carbonate intervals, as proposed by Azevedo and Perez (2009) and Sarhan (2012).

References

Adams, J. E., 1944, "Upper Permian Ochoa Series of Delaware Basin, West Texas and Southeastern New Mexico: *AAPG Bulletin*, 28.11, p. 1596-1625.

Adams, J. E., 1951, Starved Pennsylvanian Midland basin: AAPG Bulletin, v. 35, p. 2600-2607.

Adams, J.E., 1965, Stratigraphic-Tectonic Development of Delaware Basin: Bulletin of the American Association of Petroleum Geologists, v. 49.11, p. 2140-2148.

Bachmann, Joseph, Philip Stuart, Brian Corales, Blake Fernandez, Peter Kissel, Holly Stewart, David Amoss, Blaise Angelico, Alonso Guerra-Garcia, K. Blake Hancock, Richard Roberts, and Bill Sanchez, 2014, The "New" Horizontal Permian Basin. < *https://docplayer.net/15628065-The-new-horizontal-permian-basin.html*> Accessed October, 2019

Bickley, 2019, High resolution sequence stratigraphy and seismic stratigraphy of the Leonardian Bone Spring Formation Delaware Basin, Southeast New Mexico. University of Oklahoma Master's Thesis

Brown, A. R., 2011, Interpretation of Three-Dimensional Seismic Data Seventh Edition: AAPG Memoir 42, p. 48

Catuneanu, O., W.E. Galloway, C.G.St.C Kendall, A.D. Miall, H.W. Posamentier, A. Strasser, and M.E. Tucker, 2011, Sequence Stratigraphy: Methodology and Nomenclature: Newletters on Stratigraphy, v. 44/3, p. 173-245.

Catuneanu, O., V. Abreu, J.P. Bhattacharya, M.D. Blum, R.W. Dalrymple, P.G. Eriksson, C.R. Fielding, W.L. Fisher, W.E. Galloway, M.R. Gibling, K.A. Giles, J.M. Holbrook, R. Jordan, C.G.St.C. Kendall, B. Macurda, O.J. Martinsen, A.D. Miall, J.E. Neal, D. Nummedal, L. Pomar, H.W. Posamentier, B.R. Pratt, J.F. Sarg, K.W. Shanley, R.J. Steel, A. Strasser, M.E. Tucker, and C. Winker, 2009, Towards the Standardization of Sequence Stratigraphy: Earth-Science Reviews, v. 92.1-2, p. 1-33.

Crosby, C. B., 2015, Depositional History and High Resolution Sequence Stratigraphy of the Leonardian Bone Spring Formation, Northern Delaware Basin, Eddy and Lea Counties, New Mexico. University of Oklahoma Master's Thesis

Crosby, Charles B., John D. Pigott, and Kulwadee L. Pigott, 2017, Bone Spring Formation High Resolution Sequence Stratigraphy, Northern Delaware Basin, Eddy and Lea Counties, New Mexico, AAPG Annual Convention & Exhibition, Houston, TX.

DrillingInfo, 2019, Permian Basin Production and Development for the E&P Insider: <https://www.drillinginfo.com/production/permian-basin/article?EPinsider> Accessed October, 2019

EIA, 2017, U.S. Crude Oil and Natural Gas Proved Reserves, 2017: *<http://www.eia.gov/naturalgas/crudeoilreserves/?src=home-b1>* Accessed September, 2019.

Ellison, S. P. Jr., 1941, Revision of Pennsylvanian Conodonts: Jour, Paleontology, v. 15, p. 107-143.

Galley, John E, 1958, Oil and geology in the Permian basin of Texas and New Mexico: North America: Habitat of Oil, v. 18, p. 395-446.

Galloway, W., E., 1989, Genetic stratigraphic sequences in basin analysis; 1, Architecture and genesis of flooding-surface bounded depositional units, AAPG bulletin, 73,125-142.

Hamlin, H. S., and Baumgardner, R. W., 2012, Wolfberry (Wolfcampian-Leonardian) Deep-Water Depositional Systems in the Midland Basin: Stratigraphy, Lithofacies, Reservoirs, and Source Rocks, Bureau of Economic Geology, University of Texas at Austin, 2012.

Haq, B. U., and S. R. Schutter, 2008, A Chronology of Paleozoic Sea-Level Changes: Science, v. 322, p. 64-68

Hardage, B. A., J. L. Simmons, V. M. Pendleton, B. A. Stubbs, and B. J. Uszynski, 1998, 3-D Seismic Imaging and Interpretation of Brushy Canyon Slope and Basin Thin-bed Reservoirs: Geophysics, v. 63.5, p. 1507.

Hardenbol et al., 1998, Mesozoic and Cenozoic sequence chronostratigraphic framework of European basins: SEPM Special Publication, v. 60.

Harris, P.M.M. and Saller, A.H., 1999, Subsurface expression of the Capitan depositional system and implications for hydrocarbon reservoirs, northeastern Delaware Basin, AAPG Annual Convention & Exhibition, Houston, TX.

Hart, B.S., 1997, New Targets in the Bone Spring Formation, Permian Basin: Oil & Gas Journal, p. 85-88.

Henderson, C. M., V. I. Davydov, B. R. Wardlaw, and O. M. Hammer, 2012, Chapter 24: The Permian Period, in F.M. Gradstein, ed., The Geologic Time Scale 2012: 1st ed. Oxford: Elsevier, 2012. P. 654-677

Hickman, R. G., Varga R. J., and Altany, R. M., 2009, Structural style of the Marathon thrust belt, west Texas: Journal of Structural Geology, *v.* 31.9, p. 900-909.

Hill, C.A., 1996, Geology of the Delaware Basin, Guadalupe, Apache, and Glass Mountains, New Mexico and West Texas: Society for Sedimentary Geology, Albuquerque, New Mexico, v. 96-39.

Hills, J. M., 1970, Late Paleozoic structural directions in southern Permian basin, west Texas and southeastern New Mexico: AAPG Bulletin, v. 54.1, p. 1809-1827.

Hills, J.M., 1984, Sedimentation, Tectonism, and Hydrocarbon Generation in Delaware Basin, West Texas and Southeastern New Mexico: AAPG Bulletin, v. 68.3, p. 250-267.

Keller, G.R., J.M. Hills, and R. Djeddi, 1980, A Regional Geological and Geophysical Study of the Delaware Basin, New Mexico and West Texas: New Mexico Geological Society Guidebook, p. 105-111.

Kocurek, G. and B.L. Kirkland, 1998, Getting to the Source: Aaeolian Influx to the Permian Delaware Basin Region: Sedimentary Geology, v. 117.3-4, p. 143-149.

Li, Shunli, 2015, The role of sea level change in deep water deposition along a carbonate shelf margin, Early and Middle Permian, Delaware Basin: Geologica Carpathica, p. 99-116.

Maley, V. C., and Huffington, R. M., 1953, Cenozoic fill and evaporate solution in the Delaware Basin, Texas and New Mexico: Geological Society of America Bulletin, v. 64.5, p. 539-546.

May, Jeff, 2018, Well Log Sequence Stratigraphy: Applications to Exploration and Production. 2018. Unpublished Nautilus Lecture Notes.

Mazzullo, S. J., 1981, Facies and burial diagenesis of a carbonate reservoir: Chapman Deep (Atoka) field, Delaware Basin, Texas: AAPG Bulletin, v. 65.5, p. 850-865.

Mazzullo, S.J., 1995, Permian Stratigraphy and Facies, Permian Basin (Texas-New Mexico) and Adjoining Areas in the Midcontinent United States *in* P.A. Scholle, T.M. Peryt, and D.S. Ulmer-Scholle, eds., The Permian of Northern Pangea, Berlin: Springer-Verlag, v. 2, p. 41 58.

Mccullough, B.J., 2014, Sequence-Stratigraphic Framework and Characterization of the Woodford Shale on the Southern Cherokee Platform of Central Oklahoma: Master's thesis, University of Oklahoma, Norman, Oklahoma, 210 p.

McGowen, J. H., Granata, G. E. and Seni, S. J., 1979, Depositional framework of the lower Dockum Group (Triassic) Texas panhandle: Bureau of Economic Geology, University of Texas, Report of Investigations 97-1979, p. 60

Mitchum, R. M., 1977, Seismic Stratigraphy and Global Changes of Sea Level: Part 11. Glossary of Terms used in Seismic Stratigraphy: Section 2. Application of Seismic Reflection Configuration to Stratigraphic Interpretation: Seismic Stratigraphy – Applications to Hydrocarbon Exploration, p. 205-212.

Montgomery, S.L., 1998, The Permian Bone Spring Formation, Delaware Basin: Petroleum Frontiers, v. 14.3, p. 1-89.

Mullins, H.T., and H.E. Cook, 1986, Carbonate Apron Models: Alternatives to the Submarine Fan Model for Paleoenvironmental Analysis and Hydrocarbon Exploration: Sedimentary Geology, v. 48.1-2, p. 37-79.

Pereira, L.A.G.R., 2009, Seismic attributes in hydrocarbon reservoirs characterization. Universidade de Aveiro Doctoral dissertation.

Pigott, J.D., and D. Radivojevic, 2010, Seismic stratigraphy based chronostratigraphy (SSBC) of the Serbian Banat region of the Pannonian Basin, *Open Geosciences*, Vol. *2*.4, p. 481-500.

Pigott, J.D., 2017, GEOL 5363: Carbonate Geology. Fall 2017. Unpublished Lecture Notes.

Pigott, J.D., 2018, GPHY 5613: Introduction to Seismic Stratigraphy. Fall 2018. Unpublished Lecture Notes.

Pigott, J.D., 2018, GPHY 5613: Introduction to Sequence Stratigraphy. Spring 2018. Unpublished Lecture Notes.

Pigott, J.D., Esra Yalcin, Kulwadee L. Pigott, and Michael Williams, 2015, 3D Delaware basin model: Insight into its heterogeneous petroleum system evolution as a guide to new exploration, West Texas Geological Society Convention, Midland, Tx.

Saller, A.H., J.W. Barton, and R.E. Barton, 1989, Slope Sedimentation Associated with a Vertically Building Shelf, Bone Spring Formation, Mescalero Escarpe Field, Southeastern New Mexico: SEPM Special Publication, v. 44, p. 275-288.

Sarhan, M.A., 2017, The efficiency of seismic attributes to differentiate between massive and non-massive carbonate successions for hydrocarbon exploration activity. NRIAG Journal of Astronomy and Geophysics, v. 6.2, pp.311-325.

ShaleExperts, 2019, Permian Basin: <https://www.shaleexperts.com/plays/permian-basin/Overview?menu> Accessed October, 2019

Shumaker, R.C., 1992, Paleozoic Structure of the Central Basin Uplift and Adjacent Delaware Basin, West Texas: AAPG Bulletin, v. 76.11, p. 1804-1824.

Slatt, R.M., 2013 GEOL 5970: Reservoir Characterization I. Fall 2016. Unpublished Lecture Notes.

Slatt, R. M., 2006, Stratigraphic Reservoir Characterization for Petroleum Geologists, Geophysicists, and Engineers, v. 10, Elsevier.

Sloss, L.L., 1963, Sequences in the Cratonic Interior of North America: Geological Society of America Bulletin, v. 74.2, p. 93-113.

Sloss, L.L., 1988, Chapter 3: Tectonic Evolution of the Craton in Phaerozoic Time, in L.L. Sloss, ed., Sedimentary Cover – North American Craton: U.S.: The Geology of North America: The Geological Society of America, p. 25-41.

Ross, C.A. and J.R.P. Ross, 1995, Permian Sequence Stratigraphy in P.A. Scholle, T.M. Peryt, and D.S. Ulmer-Scholle, eds., The Permian of Northern Pangea: Berlin: Springer-Verlag, v. 1, p. 98-113.

Ruppel, Stephen C., and W. Bruce Ward, 2013, Outcrop-based Characterization of the Leonardian Carbonate Platform in West Texas: Implications for Sequence-stratigraphic Styles in the Lower Permian: AAPG Bulletin, v. 97.2, p. 223-250.

Silver, B.A. and R.G. Todd, 1969, Permian Cyclic Strata, Northern Midland and Delaware Basins, West Texas and Southeastern New Mexico: AAPG Bulletin, v. 53.11, p. 2223-2251.

Thore, Pierre D., and Corrine Juliard, 1999, Fresnel zone effect on seismic velocity resolution: *Geophysics* v. 64.2, p 593-603.

USGS, 2018, USGS Announces Larges Continuous Oil Assessment in Texas and New Mexico: <https://www.usgs.gov/news/usgs-announces-largest-continuous-oil-assessment-texas-and-new-mexico> Accessed June 21, 2019.

Vail, P. R., 1987, Seismic Stratigraphy Interpretation Using Sequence Stratigraphy: AAPG Studies in Geology 27, volume 1:Atlas of Seismic Stratigraphy.

Van Wagoner, J. C., 1998, Sequence stratigraphy and marine to nonmarine facies architecture of foreland basin strata, Book Cliffs, Utah, USA: *AAPG Bulletin, v.* 82.8, p. 1607-1618.

Veevers, J. J., and C.M. Powell, 1987, Late Paleozoic Glacial Episodes in Gondwanaland Reflected in Transgressive-regressive Depositional Sequences in Euramerica: Geological Society of America Bulletin, v. 98.4, p. 475-487.

Walper, J. L., 1977, Paleozoic tectonics of the southern margin of North America: Gulf Coast Association of Geological Societies Transactions, v. 27, p. 230-241

Williams, Michael T., John D. Pigott, and Kulwadee L. Pigott, 2014, Delaware Basin Evolution: Preliminary Integrated 1D,2D, And 3D Basin Model for Petroleum System Analysis, 2014, AAPG Annual Convention & Exhibition, Houston, Tx.

Wilson, J. L., 1975, Carbonate facies in geologic history: New York, Springer-Verlag, 470 p

Yang, K.M. and S.L. Dorobek, 1995, The Permian Basin of West Texas and New Mexico: Tectonic History of a "Composite" Foreland Basin and Its Effects on Stratigraphic Development: SEPM Special Publication, v. 52, p. 149-174

Zhou, Y., 2014, High Resolution Spectral Gamma Ray Sequence Stratigraphy of Shelf Edge to Basin Floor Upper Capitan Permian Carbonates, Guadalupe Mountains, Texas and Delaware Basin, New Mexico: Master's thesis, University of Oklahoma, Norman, Oklahoma, 131 p.112

Appendix

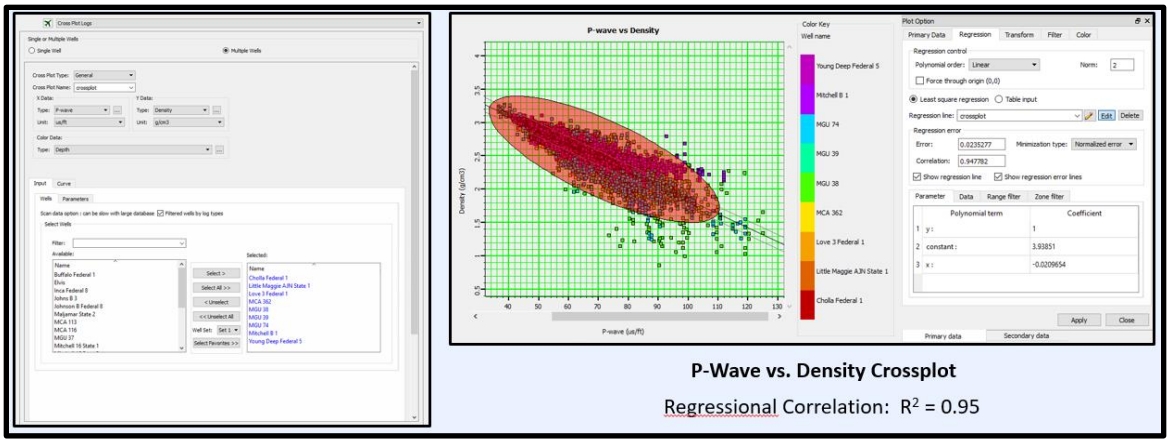

Appendix I.1: Petrophysical conditioning performed on well logs included P-wave vs. Density cross plotting in order to establish regressional correlation ($R^2 = 0.95$) for later pseudo-sonic log generation.

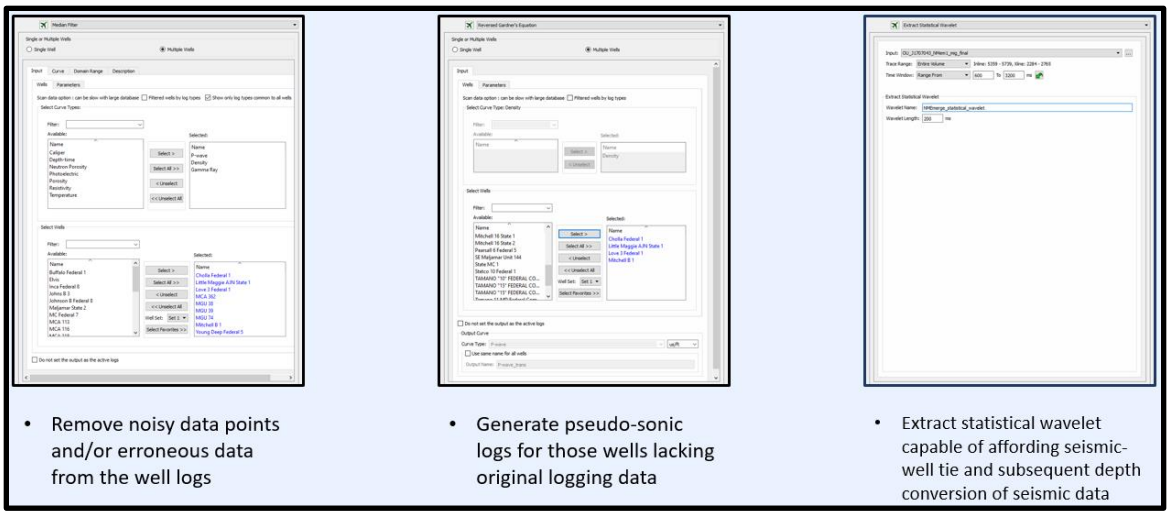

Appendix I.2: Petrophysical conditioning performed on well logs also included application of Median Filter and Reverse Gardner Equation. Finally, a statistical wavelet was generated.

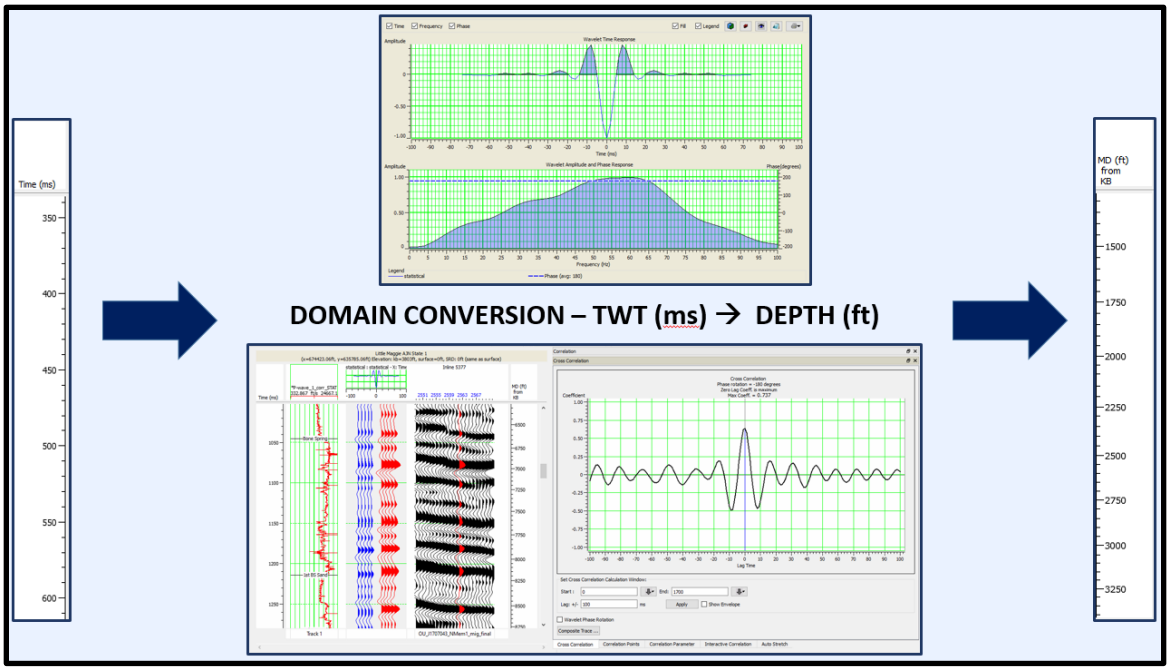

Appendix I.3: Petrophysical conditioning enhanced and improved the eventual process by which seismic data was converted from TWT domain (ms) into Depth domain (ft) via seismic well-tie.

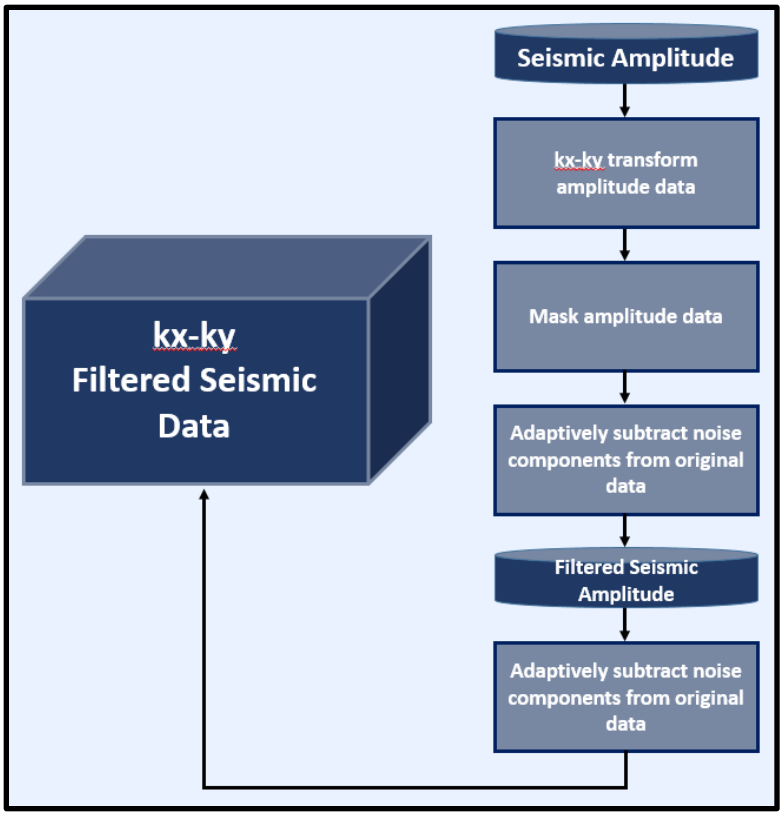

Appendix 2: AASPI Footprint Acquisition Removal Workflow utilized in this thesis investigation.

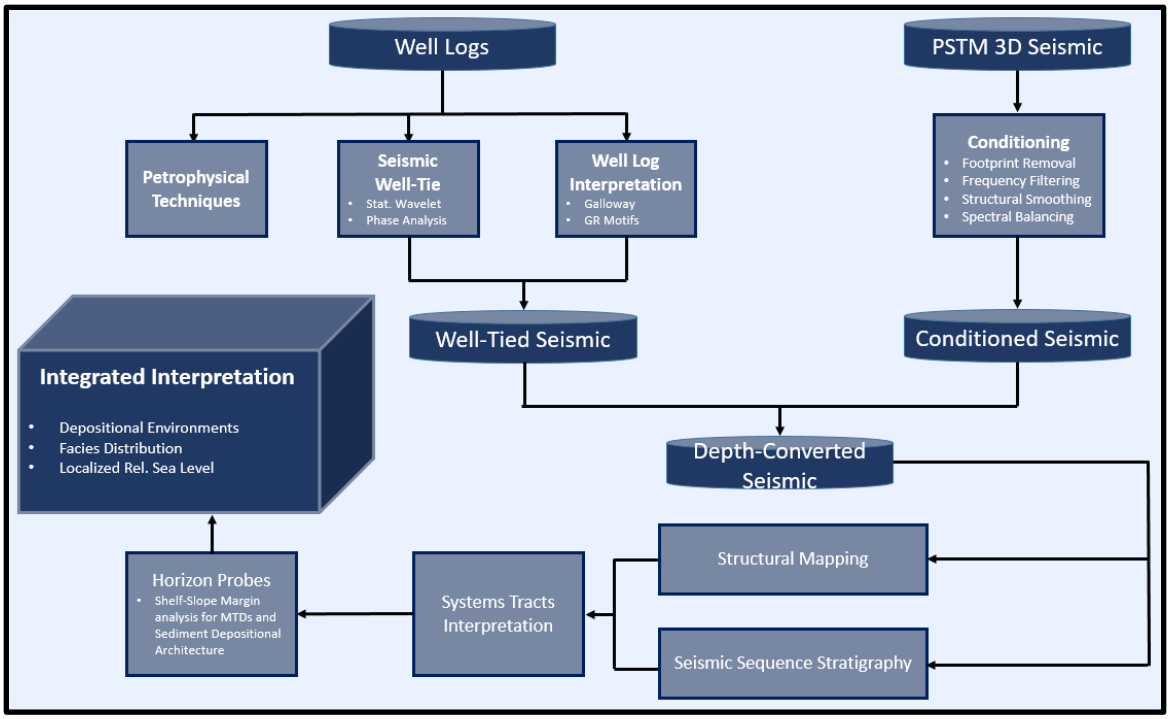

Appendix III: Methods map linking the methods utilized in this seismic investigation to the to the concepts they encompass.

Appendix IV.1-4 (top to bottom): Horizon probes corendered with dip magnitude and seismic dip highlighting interpreted major fault zones that play a governing role over Bone Spring Fm. deposition, as well as shelf progradation over time.

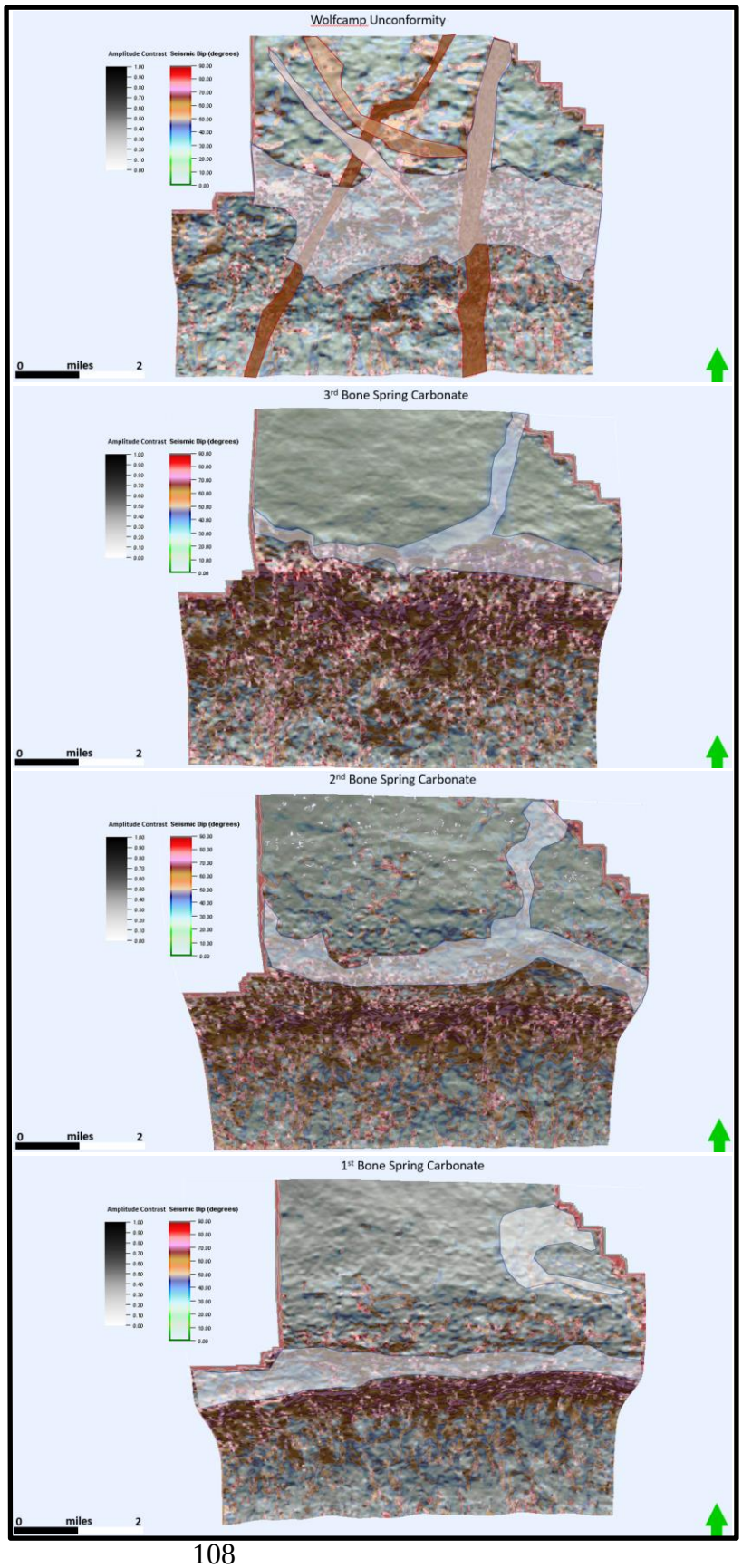

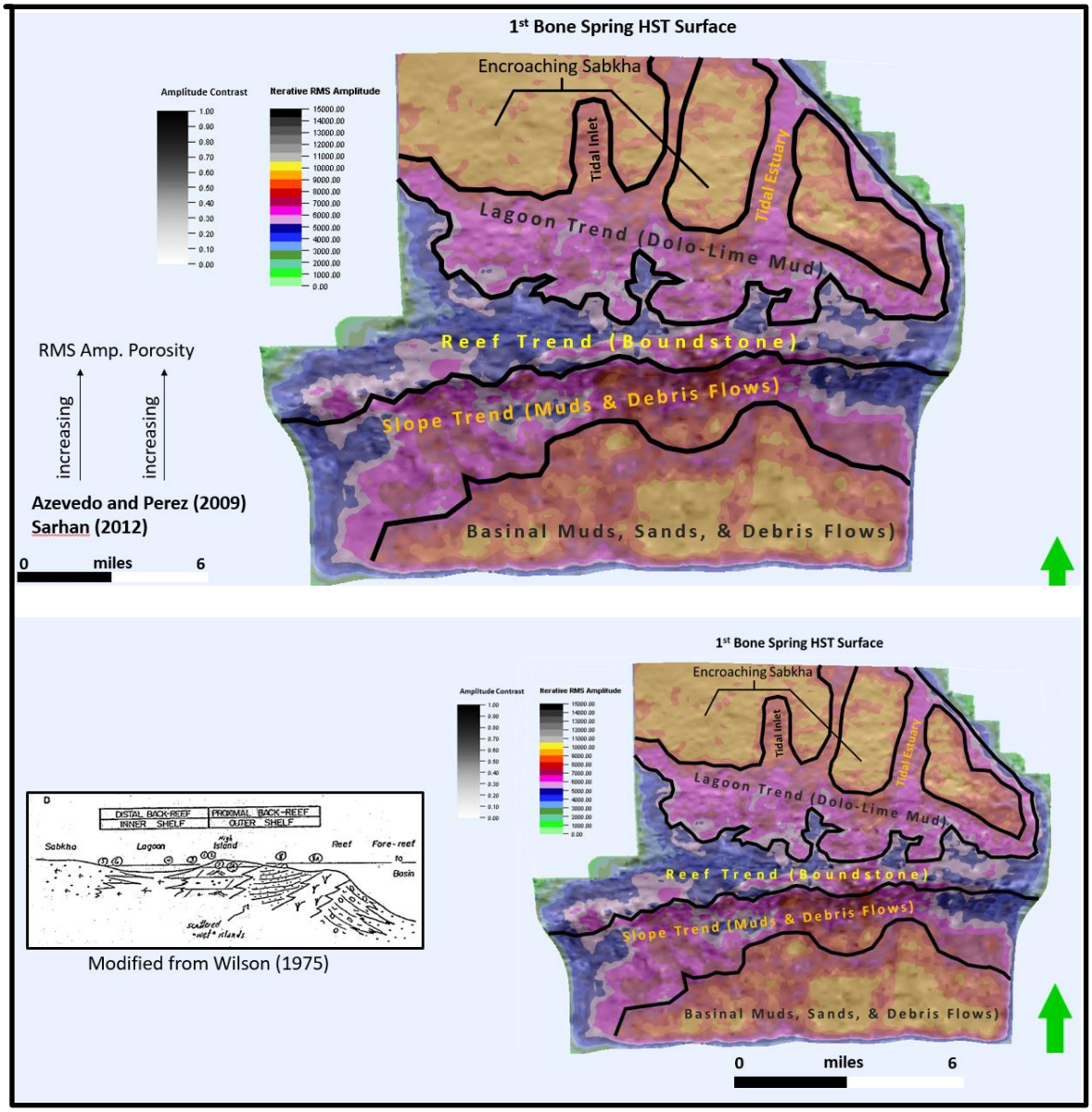

Appendix V.1-2 (top to bottom): Horizon probes corendered with dip magnitude and Iterative RMS Amplitude highlighting lithologic trends according to the correlation outlined by Azevedo and Perez (2009) and Sarhan (2012) between increasing RMS Amplitude and increasing porosity. Below, interpreted facies distributions are compared to Wilson's classical 1975 facies model for carbonate systems, and marked similarities are present.

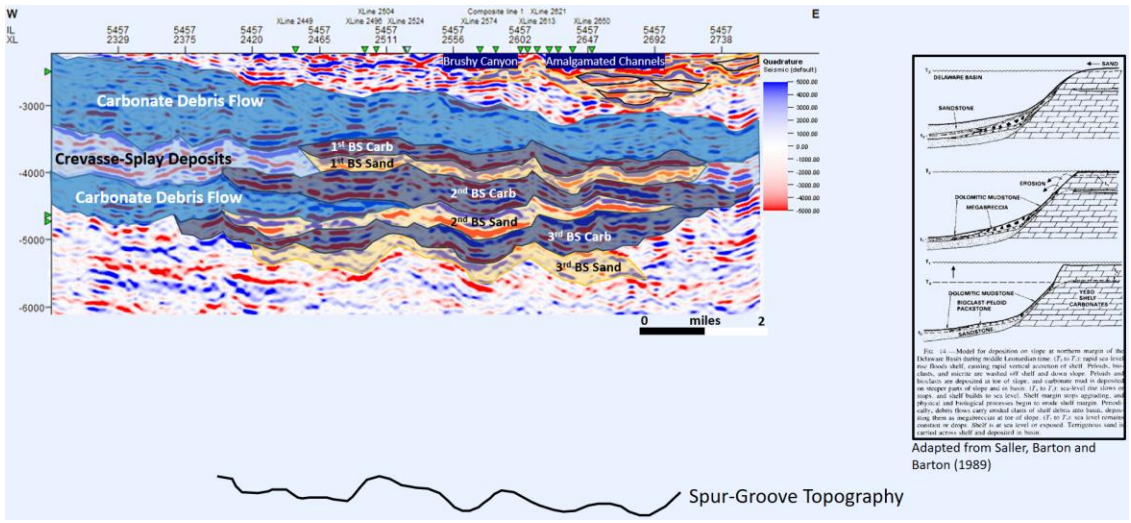

Adapted from Saller, Barton and Barton (1989)

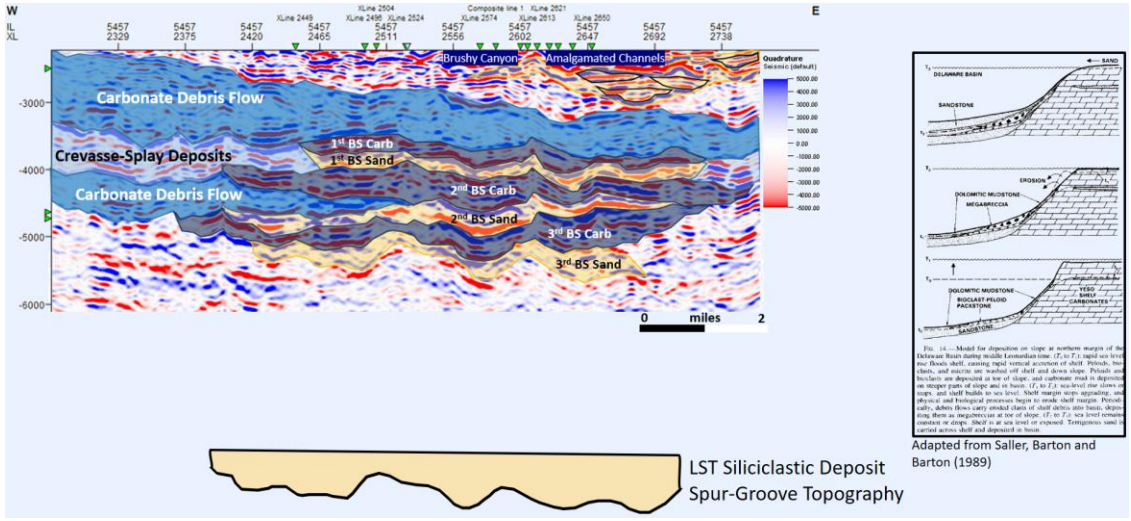

Adapted from Saller, Barton and Barton (1989)

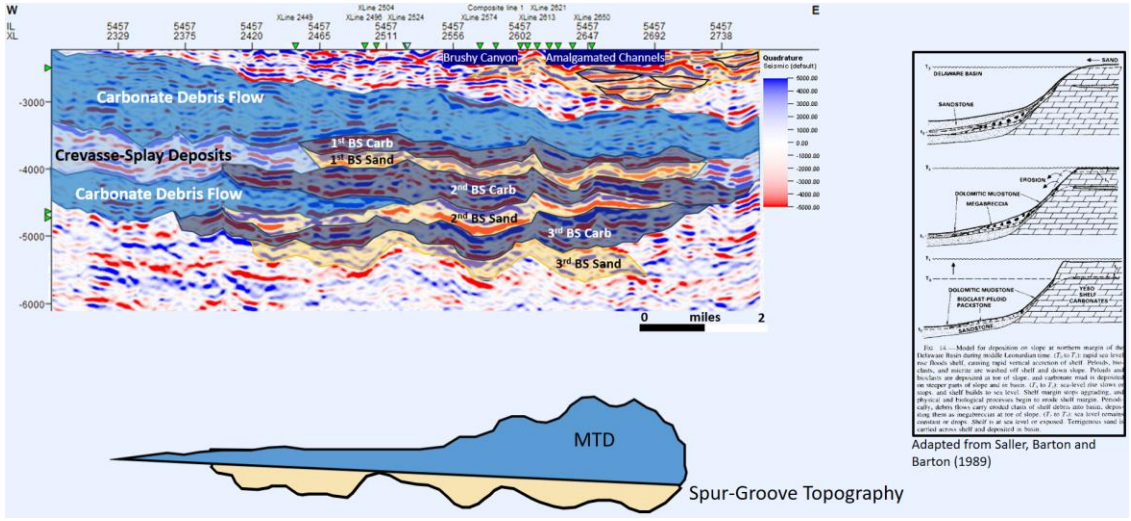

Adapted from Saller, Barton and Barton (1989)

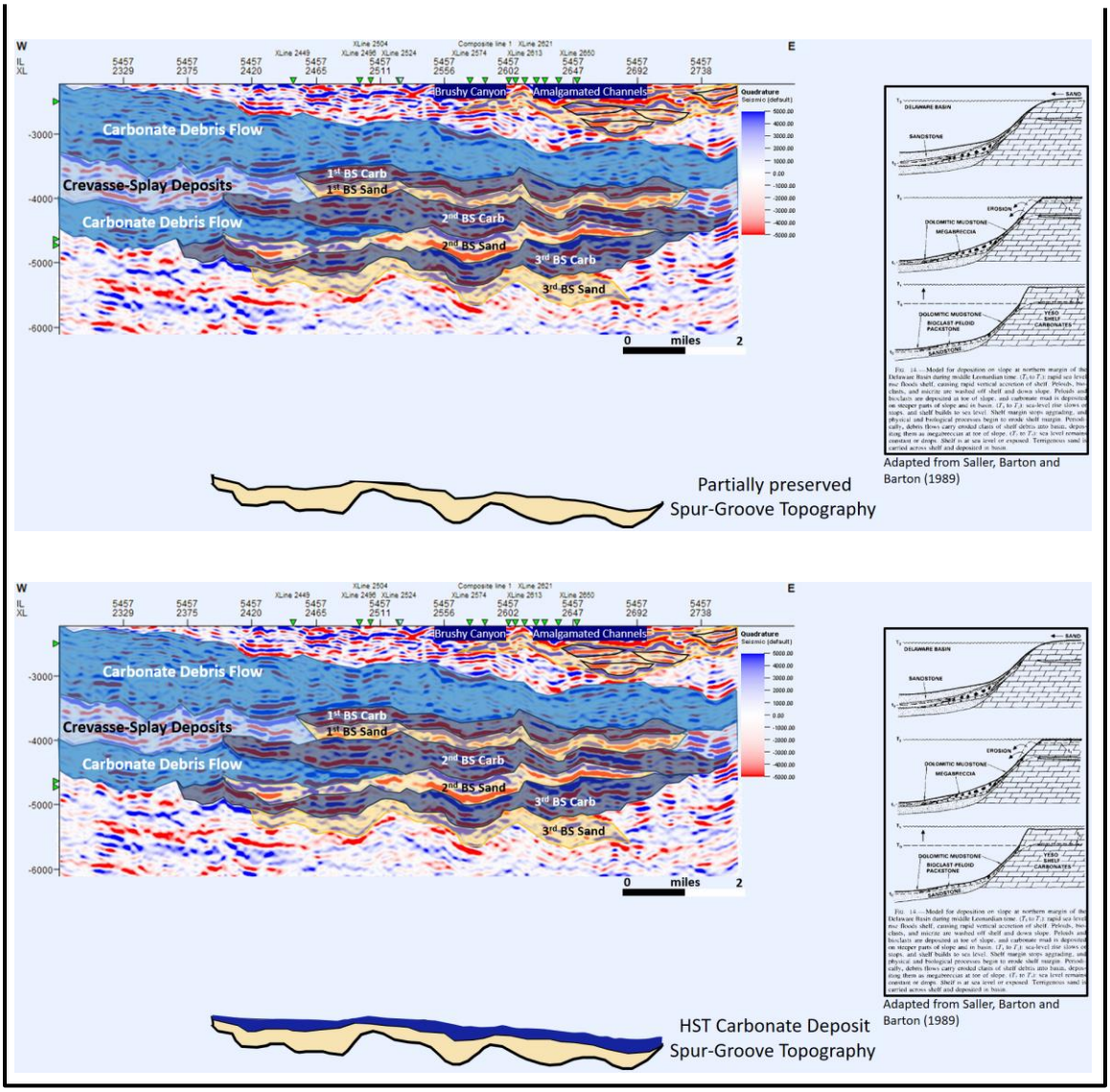

Appendix VI.1-5 (top to bottom): Strike line with sediment pathways and depositional architecture interpreted; step-by-step progression of proposed depositional mechanism by which reciprocal sedimentation and compensational stacking patterns observed in the Bone Spring Fm. may be explained, building upon previous work by Saller, Barton and Barton (1989). carbonate systems, and marked similarities are present.

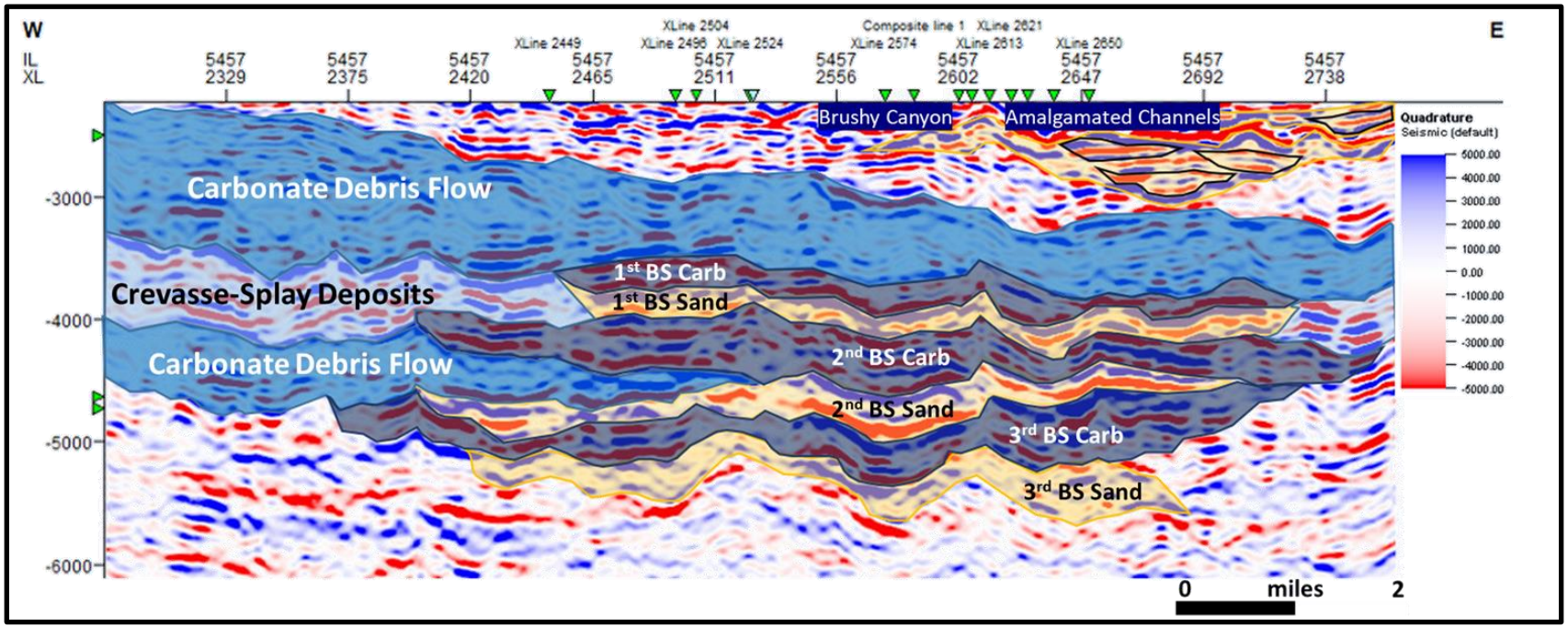

Appendix VII: Seismic strike line showing interpreted depositional architecture along with well-tie correlated intraformational boundaries within Bone Spring Formation.

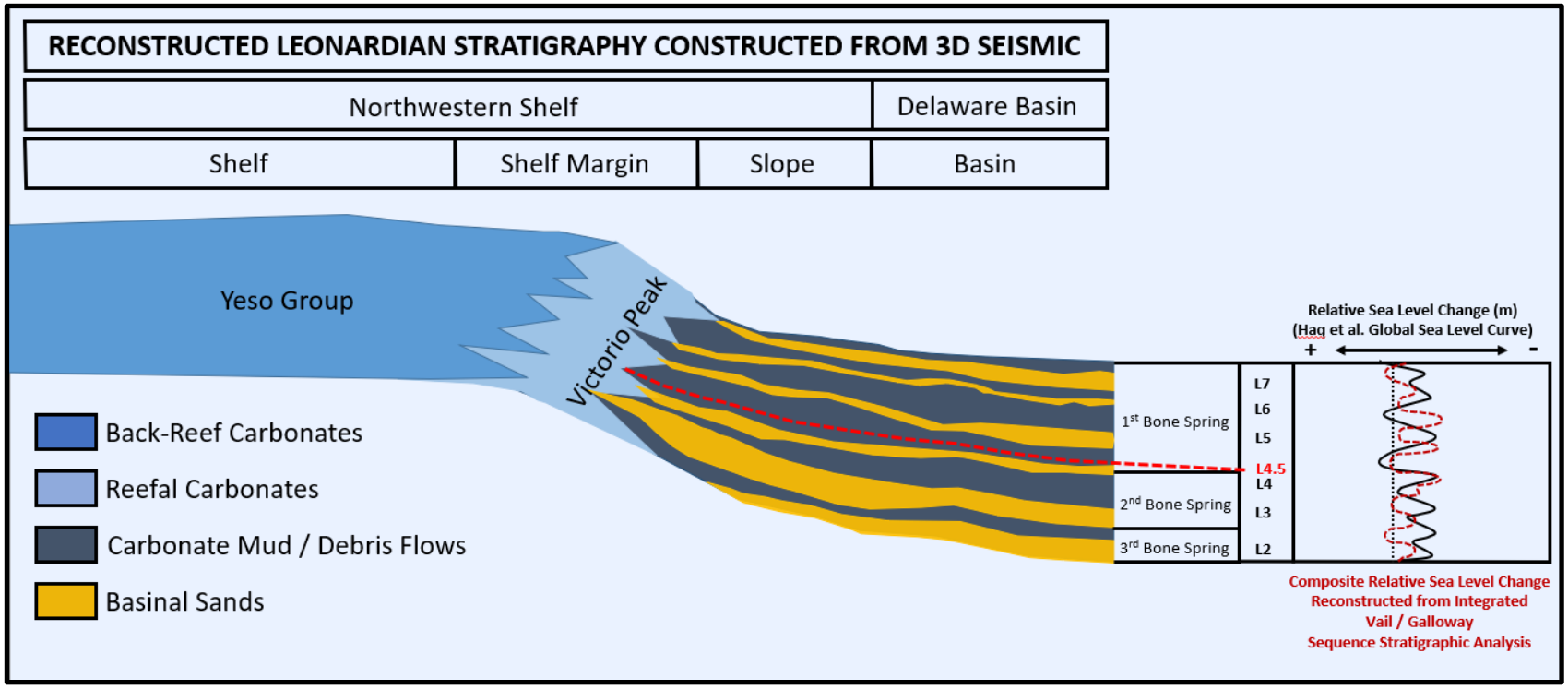

Appendix VIII: Modified subsurface stratigraphic model of the Leonardian formations studied in this investigation, with hitherto undocumented LST deposit highlighted (red dashed line, red text).